The

Philosophical Magazine

FIRST PUBLISHED IN 1798

A Journal of Theoretical Experimental and Applied Physics

UNIVERSITY OF HAWAII LIBRARY
NOV 10 '59

Vol. 4 July 1959 No. 43
Eighth Series

£1 5s. 0d., plus postage
Annual Subscription £13 10s. 0d., payable in advance

ALERE FLAMMAM

Printed and Published by
TAYLOR & FRANCIS LTD
RED LION COURT, FLEET STREET, LONDON, E.C.4

THE PHILOSOPHICAL MAGAZINE

Editor
Professor N. F. Mott, M.A., D.Sc., F.R.S.

Editorial Board
Sir Lawrence Bragg, O.B.E., M.C., M.A., D.Sc., F.R.S.
Sir George Thomson, M.A., D.Sc., F.R.S.
Professor A. M. Tyndall, C.B.E., D.Sc., F.R.S.

Authors wishing to submit papers for publication in the Journal should send manuscripts directly to the Publishers.

Manuscripts should be typed in *double* spacing on one side of quarto (8 × 10 in.) paper, and authors are urged to aim at absolute clarity of meaning and an attractive presentation of their texts.

References should be listed at the end in alphabetical order of authors and should be cited in the text in terms of author's name and date. Diagrams should normally be in Indian ink on white card, with lettering in soft pencil, the captions being typed on a separate sheet.

A leaflet giving detailed instructions to authors on the preparation of papers is available on request from the Publishers.

Authors are entitled to receive 25 offprints of a paper in the Journal free of charge, and additional offprints can be obtained from the Publishers.

The *Philosophical Magazine* and its companion journal, *Advances in Physics*, will accept papers for publication in experimental and theoretical physics. The *Philosophical Magazine* publishes contributions describing new results, letters to the editor and book reviews. *Advances in Physics* publishes articles surveying the present state of knowledge in any branch of the science in which recent progress has been made. The editors welcome contributions from overseas as well as from the United Kingdom, and papers may be published in English, French and German.

61-05082

Q1
P5
v. 4
pt 2

A new International Journal

ERGONOMICS

HUMAN FACTORS IN WORK, MACHINE CONTROL AND EQUIPMENT DESIGN

General Editor
A. T. WELFORD
University of Cambridge, Psychological Laboratory, Downing Place, Cambridge

Associate Editor (Anatomy and Physiology)
W. F. FLOYD

Assistant Editor
Miss H. M. CLAY

Editorial Board
H. Bastenier, *Belgium*; R. B. Bromiley, *Canada*; R. Bonnardel, Bernard Metz, *France*; E. A. Müller, *Germany*; M. G. Bennett, W. E. Hick, Sir Charles Lovatt Evans, L. G. Norman, *Great Britain*; F. H. Bonjer, *Netherlands*; S. P. M. Forssman, *Sweden*; E. Grandjean, *Switzerland*; H. S. Belding, P. M. Fitts, *U.S.A.*

Contents of February, 1959

Symposium on Training

Introductory Address. By P. H. St. J. Wilson, C.B., C.B.E., Chief Industrial Commissioner, Ministry of Labour and National Service
Physiological Bases of Training. By Albert Hemingway, Department of Physiology, School of Medicine, University of Leeds
Training Operatives in Industry. By W. Douglas Seymour, Clent, Worcestershire
The Training of Shoe-Machinists. By W. T. Singleton, The British Boot, Shoe and Allied Trades Research Association, Kettering
A Theory of the Acquisition of Speed-Skill. By E. R. F. W. Crossman, Department of Psychology, Reading University, England
Practice and Knack : Some Comments on Learning and Training in Industry. By Isabel Blain, National Institute of Industrial Psychology
The Operator as a Self-Regulating System: A Factory Experiment. By S. David M. King, Organization & Training (Consultants) Limited, 19 Bolton Street, London, W.1
Note on Current Trends in Literature on Training. By Ezra V. Saul, Institute for Applied Experimental Psychology, Tufts University, Medford, Massachusetts
Circuit Training. By G. T. Adamson, Department of Physical Education, The University, Leeds
The Limitations of a ' Procrustean ' Approach to the Optimization of Man–Machine Systems. By F. V. Taylor and W. D. Garvey, U.S. Naval Research Laboratory, Washington, D.C.
Physical Training in Relation to the Energy Expenditure of Walking and to Factors Controlling Respiration During Exercise. By J. E. Cotes and F. Meade, Medical Research Council, Pneumoconiosis Research Unit, Llandough Hospital, Penarth, Glamorgan, Wales
Problems of Training of the Cardiovascular System. By M. J. Karvonen, Institute of Occupational Health, Helsinki, Finland
Training Muscle Strength. By E. A. Müller, Max-Planck-Institut für Arbeitsphysiologie, Dortmund, Germany
Abstracts of other Papers Delivered at the Symposium

Price £1 5s. 0d. per part plus postage
Subscription price per volume £4 15s. 0d. post free, payable in advance

Printed and Published by
TAYLOR & FRANCIS LTD
RED LION COURT, FLEET STREET, LONDON, E.C.4

Orders originating in U.S.A. and Canada should be sent to the Academic Press Inc., 111 Fifth Avenue, New York, 3, N.Y., U.S.A.

INTERNATIONAL JOURNAL OF RADIATION BIOLOGY

and related studies in Physics, Chemistry and Medicine

Editor
W. M. Dale, M.D., D.SC.
Dept. of Biochemistry, Christie Hospital & Holt Radium Institute, Withington, Manchester, 20

Assistant Editor
John Wakefield, B.A., F.Z.S.

Editorial Board
Charlotte Auerbach, *U.K.;* J. H. Baxendale, *U.K.;* D. W. van Bekkum, *Holland;* E. H. Betz, *Belgium;* H. A. S. van den Brenk, *Australia;* A. A. Buzzatti-Traverso, *Italy;* J. Coursaget, *France;* F. Devik, *Norway;* M. Haissinsky, *France;* A. Hollaender, *U.S.A.;* B. F. Kaufmann, *U.S.A.;* G. Klein, *Sweden;* H. Langendorff, *Germany;* M. Magat, *France;* M. Nakaidzumi, *Japan;* E. Paterson, *U.K.;* H. Ulrich, *Switzerland;* M. Westergaard, *Denmark.*

Contents of April, 1959

Impairment of Fertility by Whole-body Irradiation of Female Mice. By R. H. Mole, Medical Research Council, Radiobiological Research Unit, Atomic Energy Research Establishment, Harwell, Berks, England

Some Effects of X-rays on Dividing Cells in the Testis and Bone Marrow of the Marsupial *Potorous Tridactylus*. By G. B. Sharman, M.R.C. Radiobiological Research Unit, A.E.R.E., Harwell, Berks, England

The Effect of Cysteamine on the Survival of Spermatogonia after X-irradiation. By Anita M. Mandl, Department of Anatomy, University of Birmingham

Identification and Follow-up of Homologous and Heterologous Bone-marrow Transplants in Radiation-chimeras. By W. Welling, O. Vos, W. W. H. Weyzen and D. W. van Bekkum, Medical Biological Laboratory of the National Defence Research Council TNO, Rijswijk (Z.H.), Netherlands

The Effect of Colloidal ^{198}Au on the Bone Marrow and its Replacement in Rabbits. By J. M. Garvan, E. P. George, F. A. Rocke, St. Vincent's Hospital, Darlinghurst, N.S.W., Australia, and S. Vince, Institute of Child Health, Royal Alexandra Hospital for Children, Camperdown, N.S.W., Australia

The Viability of Near-normal Irradiated Chromosomes. By A. J. Bateman, Christie Hospital and Holt Radium Institute, Manchester, England

Response of Megakaryocytes on the ' August ' Rat of X-irradiation. By Shirley M. Simpson, Physics Department (Downs Branch), Institute of Cancer Research, Royal Cancer Hospital, Fulham Road, London, S.W.3

Further Observations on the Radiation Chemistry of Aqueous Solutions of Thiourea. By W. M. Dale and J. V. Davies, Department of Biochemistry, Christie Hospital, Manchester 20

Price per part £1 0s. 0d. plus postage
Subscription per volume (4 issues) £3 15s. 0d. post free, payable in advance

Printed and Published by
TAYLOR & FRANCIS LTD
RED LION COURT, FLEET STREET, LONDON, E.C.4

Orders originating in U.S.A. and Canada should be sent to the
Academic Press Inc., 111 Fifth Avenue, New York 3, N.Y., U.S.A.

Journal of Electronics and Control

A Philosophical Magazine Associated Journal

Editor:
J. THOMSON, M.A., D.Sc., M.I.E.E., F.Inst.P.
Consultant Editor:
Professor N. F. MOTT, F.R.S.
Editorial Board:
Professor P. AIGRAIN (France)
Professor H. B. G. CASIMIR (Holland)
J. F. COALES (U.K.)
Professor K. G. EMELEUS (U.K.)
D. W. FRY (U.K.)
Dr. W. KLEIN (Germany)
Dr. R. KOMPFNER (U.S.A.)

Contents of March, 1959

Electronics Section

New Experimental Results for Plasma Electron Oscillations. By D. W. Mahaffey, Physics Department, Queen's University of Belfast
The Measurement of the Temperature Dependence of the Mobility and Effective Lifetime of Minority Carriers in the Base Region of Silicon Transistors. By D. M. Evans, Official communication from the D.S.I.R. Radio Research Station, Slough
Kinetic Theory of Space-Charge II: Electron Collisional Damping in the Magnetron (and Diode). By Louis Gold, Lincoln Laboratory, Massachusetts Institute of Technology, Lexington, Massachusetts
The Space Charge Field Emission Hypothesis Applied to Hayashi Data on Discharges through Gases. By Herman Ritow, Highland Park, Illinois
The Effect of Trigger Pulse Polarity on the Anode Breakdown Time of the Cold Cathode Arc Conduction Tetrode. By R. Feinberg, Ferranti Ltd., seconded to The Manchester College of Science and Technology

Control Section

Measurement of Magnetic Flux Density by Paramagnetic Resonance. By C. P. Allen and M. Sherry, Communication from the Staff of the Research Laboratories of The General Electric Company Limited, Wembley, England
The Faraday Effect in Anisotropic Semiconductors. By I. G. Austin, Communication from the Staff of the Research Laboratories of The General Electric Company Limited, Wembley, England
The Differential Transformer (Displacement Pick-Up) in Polymer Testing. By A. R. Payne and A. E. Eagles, Research Association of British Rubber Manufacturers Shawbury, Shrewsbury, Shropshire

Price per part £1 5s. plus postage
Price per volume £7 post free, payable in advance
6 monthly issues per volume

Printed and Published by

TAYLOR & FRANCIS LTD
RED LION COURT, FLEET STREET, LONDON, E.C.4

Orders originating in U.S.A. and Canada should be sent to the
Academic Press Inc., 111 Fifth Avenue, New York, 3, N.Y., U.S.A.

Advances in Physics

A Quarterly Supplement of the Philosophical Magazine

Editor:
PROFESSOR N. F. MOTT, M.A., D.Sc., F.R.S.

Editorial Board:
SIR LAWRENCE BRAGG, O.B.E., M.C., M.A., D.Sc., F.R.S.
SIR GEORGE THOMSON, M.A., D.Sc., F.R.S.
PROFESSOR A. M. TYNDALL, C.B.E., D.Sc., F.R.S.

Contents of January, 1959

The Theory of Superconductivity. By C. G. Kuper, Department of Natural Philosophy, St. Salvator's College, St. Andrews

The Modern Theory of Superconductivity. By I. M. Khalatnikov and A. A. Abrikosov, Institute of Physical Problems, Kaluzhskove Shosse, 32 Moscow, U.S.S.R.

Price per part £1 plus postage

Price per annum £3 15s. post free

Printed and Published by

TAYLOR & FRANCIS LTD

RED LION COURT, FLEET STREET, LONDON, E.C.4

A new International Journal

Molecular Physics

Editor: H. C. LONGUET-HIGGINS, F.R.S.
Associate Editor: J. H. VAN DER WAALS

Editorial Board:

J. Bjerrum, *Copenhagen*; G. Careri, *Padua*; C. A. Coulson, *Oxford*; F. H. C. Crick, *Cambridge*; P. J. W. Debye, *Cornell*; D. Hadži, *Ljubljana*; O. Hassel, *Oslo*; W. Heitler, *Zürich*; J. O. Hirschfelder, *Wisconsin*; D. F. Hornig, *Princeton*; J. A. A. Ketelaar, *Amsterdam*; J. G. Kirkwood, *Yale*; R. Kronig, *Delft*; J. W. Linnett, *Oxford*; A. Liquori, *Rome*; Dame Kathleen Lonsdale, *London*; P-O. Löwdin, *Uppsala*; M. Magat, *Paris*; R. S. Mulliken, *Chicago*; A. Münster, *Frankfurt*; L. J. Oosterhoff, *Leiden*; L. E. Orgel, *Cambridge*; J. A. Pople, *Teddington*; I. Prigogine, *Brussels*; R. E. Richards, *Oxford*; J. S. Rowlinson, *Manchester*; G. S. Rushbrooke, *Newcastle upon Tyne*; L. E. Sutton, *Oxford*; H. W. Thompson, *Oxford*; B. Vodar, *Bellevue, Paris.*

Contents of April, 1959

The Colours of Transition Metal Hexafluorides. By the late W. Moffitt, G. L. Goodman, Chemistry Department, Harvard University, M. Fred and B. Weinstock, Argonne National Laboratory, Lemont, Illinois

Intensities in Inorganic Complexes. III. Octahedral Complexes of Ni(II) and V(III). By C. J. Ballhausen and Andrew D. Liehr, Bell Telephone Laboratories, Incorporated, Murray Hill, New Jersey

Theory of Anisotropic Hyperfine Interactions in π-electron Radicals. By Harden M. McConnell, Gates and Crellin Laboratories of Chemistry, California Institute of Technology, Pasadena, California and John Strathdee, Shell Development Company, Emeryville, California

The Electronic Structure of Hydrogen Fluoride. By R. A. Ballinger, National Physical Laboratory, Teddington, Middlesex

Molecular-orbital Treatment of a New Type of Heteroaromatic Compound. By R. D. Brown and B. A. W. Coller, Chemical Laboratories, University of Melbourne, Carlton, N.3, Victoria, Australia

Statistical Mechanics of Solid and Liquid Mixtures of Ortho- and Para-hydrogen. By A. Bellemans and Agnessa Babloyantz, Faculty of Sciences, Université Libre de Bruxelles, Belgium

On the Motion of a Particle Coupled to Lattice Vibrations. By Thor A. Bak, M. Goche and F. Henin, Faculté des Sciences, Université Libre de Bruxelles, Belgium

The Singularities of the Integrals in Mayer's Ionic Solution Theory. By Harold L. Friedman, Faculté des Sciences, Université Libre de Bruxelles

Calculation of Vibrational Relaxation Times in Gaseous Cyanogen. By P. G. Dickens, Inorganic Chemistry Laboratory, Oxford

Thermodynamic Properties of Clathrates. I. The Heat Capacity and Entropy of Argon in the Argon Quinol Clathrates. By N. G. Parsonage and L. A. K. Staveley, Inorganic Chemistry Laboratory, Oxford

Price per part £1 5s. 0d. plus postage
Subscription per volume (4 issues) £4 15s. 0d. post free, payable in advance

Printed and Published by
TAYLOR & FRANCIS LTD
RED LION COURT, FLEET STREET, LONDON, E.C.4

Orders originating in U.S.A. and Canada should be sent to the
Academic Press Inc., 111 Fifth Avenue, New York, 3, N.Y., U.S.A.

Physics in Medicine and Biology

**A Taylor & Francis Journal published in association
with The Hospital Physicists' Association**

Editor: J. E. Roberts, D.Sc.
Consultant Editor: Professor N. F. Mott, F.R.S.

Editorial Board

R. Bonet-Maury, *Paris*; J. Dainty, *Edinburgh*; H. E. Johns, *Toronto*; W. A. Langmead. *London*; D. A. McDonald, *London*; J. S. Mitchell, *Cambridge*; G. J. Neary, *Harwell*; B. Rajewsky, *Frankfurt*; J. Rotblat, *London*; S. Rowlands, *London*; H. P. Schwan, *Philadelphia*: R. Sievert, *Stockholm*; F. W. Spiers, *Leeds*; J. F. Tait, *Massachusetts*; A. J. H. Vendrik, *Nijmegen*.

Contents of January, 1959

The Measurement of Exposure Dose for High Energy Radiation with Cavity Ionization Chambers. By T. E. Burlin, B.Sc., Physics Department, Hammersmith Hospital, London, W.12

The Energy Response of a Victoreen Condenser Ionization Chamber. By A. J. D. Szilvasi, Ph.D. and G. N. Whyte, Ph.D., National Research Council, Ottawa, Canada

An Analysis of Clasp Design in Partial Dentures. By J. A. Warr, M.A.(Cantab.), B.Sc. (London), B.D.S.(London), L.D.S.R.C.S.Eng., Department of Prosthetics, The London Hospital Medical College, Turner Street, London, E.1

A Study of the External Gamma-ray Field Arising from a Radioactive Source Situated in Air and in a Scattering Medium. By H. A. B. Simons, M.A., Ph.D. and S. Chomet, M.Sc., Physics Department, The Royal Free Hospital School of Medicine, 8 Hunter Street, London, W.C.1

A Wide Range Direct Reading X-Ray Dosemeter. By S. Stuart, Electronic Instruments Ltd., Richmond, Surrey and S. B. Osborn, B.Sc., A.Inst. P., University College Hospital, London, W.C.1

Pulmonary Diffusion of Oxygen. By B. F. Visser, Ph.D. and A. H. J. Maas, M.Sc., Pulmonary Function Laboratory, State University Hospital, Utrecht, Netherlands

The Influence of the Anomalous Viscosity of Blood upon its Oscillatory Flow. By M. G. Taylor, M.D., Physiology Department, Medical College of St. Bartholomew's Hospital, London

Subscription price per volume £3 10s. post free, payable in advance
4 parts per volume—£1 per part plus postage

Printed and Published by

TAYLOR & FRANCIS, LTD
RED LION COURT, FLEET STREET, LONDON, E.C.4
Orders originating in U.S.A. and Canada should be sent to the
Academic Press Inc., 111 Fifth Avenue, New York, 3, N.Y., U.S.A.

INTERNATIONAL JOURNAL

OPTICA ACTA

European Journal of Optics **Journal Européen d'Optique** **Europäische Zeitschrift für Optik**

English Editor: C. G. Wynne, 13 Elwill Way, Beckenham, Kent, U.K.

Rédacteur Français: A. Maréchal, 3 Boulevard Pasteur, Paris, France

Deutscher Herausgeber: G. Franke, Laufdorfer Weg 2, Wetzlar, Germany

Editorial Board

J. M. Otero y Navascues, *Madrid;* R. W. Ditchburn, *Reading;* A. Arnulf, *Paris;* A. Biot, *Gand;* J. Cabannes, *Paris;* P. Fleury, *Paris;* F. Gabler, *Vienna;* G. Hansen, *Oberkochen;* E. Ingelstam, *Stockholm;* H. Korte, *Braunschweig;* W. S. Stiles, *London;* G. Toraldo di Francia, *Florence;* A. C. S. van Heel, *Delft.*

Contents of April, 1959

Correction Approchée de l'Effet de Lobe en Radioastronomie. Par J. Arsac, Observatoire de Meudon

Colour Perception with the Peripheral Retina. By J. D. Moreland and A. Cruz, Technical Optics Section, Imperial College, London

A Fourier Analyser for Optical Frequency Response Determinations. By J. M. Naish, Royal Aircraft Establishment, Hampshire England

Photo-sensitive Reactions in Foveae of Normal and Cone-monochromatic Observers. By R. A. Weale, Visual Research Division, Ophthalmological Research Unit, (Medical Research Council), Institute of Ophthalmology, Judd Street, London, W.C.1

Contrast Transfer in the Grating Spectrograph. By A. Lohmann, Institute of Optical Research, Stockholm 70, Sweden

Doppelbrechungs-interferenzfarben sehr dünner Plättchen. Von S. Rösch, Wetzlar

Price per part £1 (1375 fr.), (DM 11.75), ($2.80), plus postage

Subscription price per volume (4 parts) £3 15s. (5155 fr.), (DM 44), ($10.50), post free, payable in advance

Printed and Published by

TAYLOR & FRANCIS LTD

RED LION COURT, FLEET STREET, LONDON, E.C.4

A HISTORY OF MATHEMATICS

from antiquity to the early nineteenth century

by J. F. SCOTT, B.A., D.Sc., Ph.D.
Vice-Principal of St. Mary's College,
Strawberry Hill, Twickenham,
Middlesex

Author of *The Scientific Work of René Descartes* (1596–1650), *Mathematical Work of John Wallis, D.D., F.R.S.* (1616–1703), and other works.

CONTENTS: Mathematics in Antiquity—Greek Mathematics—The Invention of Trigonometry—Decline of Alexandrian Science and the Revival in Europe—Mathematics in the Orient—Progress of Mathematics during the Renaissance—New Methods in Geometry—The Rise of Mechanics—The Invention of Decimal Fractions and of Logarithms—Newton and the Calculus—Taylor and Maclaurin, the Bernoullis and Euler, Related Advances—The Calculus of Variations, Probability, Projective Geometry, Non-Euclidean Geometry—Theory of Numbers—Lagrange, Legendre, Laplace, Gauss.

This volume is intended primarily to help students who desire to have a knowledge of the development of the subject but who have too little leisure to consult original works and documents. The author has availed himself of the facilities afforded by the Royal Society and other learned Societies to reproduce extracts from manuscripts and many scarce works.

$9\frac{3}{4} \times 6\frac{3}{4}$ Price 3 guineas

Printed and Published by
TAYLOR & FRANCIS LTD.
Red Lion Court, Fleet Street,
London, E.C.4

THE SCIENTIFIC WORK OF RENÉ DESCARTES 1596-1650

BY

J. F. SCOTT, B.A., M.SC., PH.D.

With a Foreword by

H. W. Turnbull, M.A., F.R.S.

This book puts the chief mathematical and physical discoveries of Descartes in an accessible form and fills an outstanding gap upon the shelf devoted to the history of philosophy and science. There is to be found in this volume the considerable contribution that Descartes made to the physical sciences, which involved much accurate work in geometrical optics and its bearing upon the practical problem of fashioning lenses, as also the deeper problems of light and sight and colour. The careful treatment that Dr. Scott has accorded to the work of Descartes is very welcome. The book is well worth reading and will be an asset to all libraries. This publication is recommended and approved by the Publication Fund Committee of the University of London.

212 *pp.* 7 × 10 *amply illustrated*

PRICE £1–0–0 NET

Printed and Published by
TAYLOR & FRANCIS LTD.
Red Lion Court, Fleet Street,
London, E.C.4

The Lattice Specific Heats of Solid Hydrogen and Deuterium[†]

By R. W. Hill and O. V. Lounasmaa[‡]
Clarendon Laboratory, Oxford

[Received February 16, 1959]

Abstract

Measurements of the specific heats of solid parahydrogen and orthodeuterium in the temperature range from 2 to 18°K are described. Anomalous contributions arising from orthohydrogen and paradeuterium impurities were minimized by converting the specimens catalytically in the liquid state, but could only be made negligible for hydrogen. The specific heat at constant volume is deduced for each substance, and its temperature variation discussed in terms of a reduced Debye temperature. It is shown that the behaviour of both substances is very similar to that calculated by Leighton (1948) for crystals of f.c.c. structure.

§ 1. Introduction

The lattice specific heats of solids of low melting point are of interest in connection with the reduced equation of state of solids and lattice dynamics in general, but the available experimental data are rather scanty. In particular, measurements are needed at liquid helium temperatures to establish the behaviour of the specific heat in the low-temperature limit. Although both hydrogen and deuterium have anomalous contributions to their low-temperature specific heats, the lattice contributions can nevertheless be measured for parahydrogen and orthodeuterium respectively, since the anomalous behaviour is confined to orthohydrogen and paradeuterium molecules. Neither parahydrogen nor orthodeuterium can be prepared in an ideally pure state, and it is desirable that the concentration of the unwanted molecular species be sufficiently low for anomalous effects to be negligible.

Efficient ortho : para conversion requires the use of a catalyst, and is therefore limited to the gas and liquid phases. The purest specimens which can be prepared with reasonable ease are therefore those which are in thermal equilibrium at the triple point temperature; for hydrogen the 'impurity' concentration is then only 0·02%, but for deuterium it is 1·5%. Anomalous effects can thus be made negligible for hydrogen, but for deuterium they are always appreciable, so that it is necessary to analyse the specific heat into contributions. This analysis can be made with reasonable certainty from measurements on a number of specimens having low, but different, paradeuterium concentrations. In existing measurements, these conditions have not been satisfied (§ 2).

[†] Communicated by the Authors.

[‡] Now at the Wihuri Physical Laboratory, University of Turku, Finland.

§ 2. PREVIOUS MEASUREMENTS

Many investigations of the specific heats of solid hydrogen and deuterium have been made in the past, mostly to provide data for thermodynamic studies. For that purpose, the precise behaviour of the specific heat at the lower temperatures is of little importance. These measurements can be divided into two classes: those made in the vicinity of the triple point only, where small concentrations of the unwanted molecular species are unimportant, and those extending to liquid helium temperatures where the criteria given in § 1 need to be satisfied before analysis of the specific heat is possible. The field covered by existing measurements of C_p is shown in the following table:

	Authors	Temp. Range	Specimen
p–H_2	Johnston *et al.* (1950)	12·7–14°K	Satisfactory
	Hill and Ricketson (1954)	2–14°K	0·5% ortho
	Mendelssohn *et al.* (1931)	3–14°K	Doubtful
	Clusius and Hiller (1929)	11–14°K	Satisfactory
o–D_2	Gonzales *et al.* (1957)	0·3–13°K	3% para
	Kerr *et al.* (1951)	11–18°K	Satisfactory
	Clusius and Bartholomé (1935)	11–18°K	Satisfactory

It can be seen that there is a good deal of satisfactory data for the higher temperatures, but that at the lower temperatures there is none which permits a proper analysis of the lattice specific heat. All the above work refers strictly to the saturation specific heat C_s which should approximate closely to the value at constant pressure C_p. From the theoretical point of view, however, it is the specific heat at constant volume, C_v, which is of interest. Measurements of this quantity have been made by Bartholomé and Eucken (1936) at temperatures above 11°K, but its measurement at lower temperatures would present grave difficulty. Their work is used here to provide a basis for calculating the C_p–C_v correction at lower temperatures (§ 5).

§ 3. EXPERIMENTAL

3.1. *Specimen Preparation*

The raw materials used for this investigation were the gases produced by the electrolysis of ordinary and heavy water (99·7%D_2O). All impurities other than isotopic ones are effectively removed during the conversion to the appropriate molecular species; this conversion was accomplished in two stages. First, the gas was adsorbed on activated charcoal cooled with liquid hydrogen in a vessel external to the main cryostat. After about an hour, some of the gas was desorbed and this sample was condensed into the calorimeter which contained about 1 g of ferric hydroxide catalyst. To complete the conversion, the calorimeter and specimen were cooled to a temperature a little above the triple point and held there for about two hours by pumping over a separate supply of liquid hydrogen in a second compartment of the calorimeter. The reason for carrying out the preparation in two stages was that the heat evolved in the complete conversion of normal hydrogen is very considerable ($\sim 250\,\mathrm{cal\,mole^{-1}}$) and it was found much easier to remove the greater part of this heat outside the cryostat. Even with the dilute specimens used, the conversion in the calorimeter was readily observed from the rapid warming when pumping was stopped. Periodic observations on this warming rate gave a rough measure of the time required for complete equilibrium; a large additional safety factor was allowed in reaching the figure of two hours quoted above.

Fig. 1

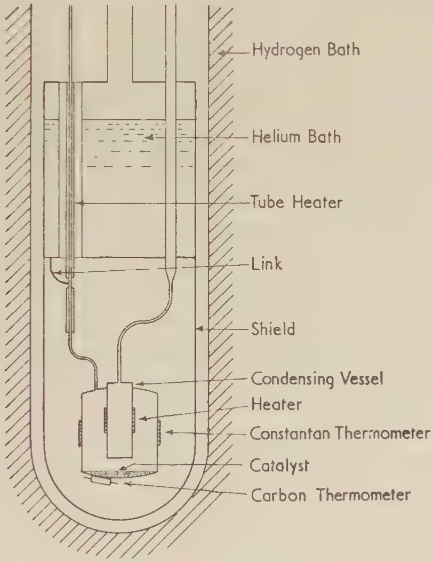

The cryostat.

3.2. *Calorimetric Apparatus*

The cryostat used for these experiments has been described in detail elsewhere (Hill 1954). For the present experiments, one modification was made; a thermal link was introduced between the calorimeter tube and the helium bath as shown in fig. 1. The original reason for insulating the tube was to prevent sublimation of the sample to this point when measurements were made at the higher temperatures. For low-temperature measurements of small heat capacities, however, the heat leak down this tube would be excessive. The procedure adopted was therefore to make the measurements at high and low temperatures in separate experiments, the link being introduced or omitted as required. A heating coil wound on the calorimeter tube was used to prevent sublimation during the initial cooling of the apparatus. The design of the calorimeter differed somewhat from that previously described, the condensing vessel being located inside the calorimeter. With this design, better thermal coupling between coolant, specimen, and heater is achieved, which greatly facilitates the experimental procedure.

The thermometers used were a carbon resistor ('Lab' 47 ohm, $\frac{1}{4}$ watt size) for liquid helium temperatures, and a constantan resistance thermometer for higher temperatures. Both thermometers were calibrated against the vapour pressure of liquid helium on the T55E scale. The constantan thermometer was also calibrated against the vapour pressure of solid and liquid hydrogen, and a gas thermometer calibration was used for interpolation.

§ 4. RESULTS

4.1. *Parahydrogen*

In view of the adequacy of existing data at the higher temperatures, measurements were confined to the temperature range below 9°K so that all the results could be obtained with the thermal link in position. Two runs were made with different specimens to check the reproducibility of the measurements. The numerical data are given in table 1, and are displayed in a graph of C_pT^{-3} against T^2 (fig. 2). This plot gives a convenient display of the data, and also demonstrates deviations from the T^3 law. Within the experimental uncertainty, there is no indication that anomalous effects are appreciable, and it is assumed that these data represent the behaviour of pure parahydrogen. The equation of the line fitted to the data is

$$C_p = 1{\cdot}21 \times 10^{-3}T^3 + 8{\cdot}5 \times 10^{-6}T^5 \text{ joules mole}^{-1}\text{ deg}^{-1}.$$

4.2. *Orthodeuterium*

Four runs were made on deuterium specimens having nominal paradeuterium concentrations of 1·5 or 2·15%, these figures being inferred from the temperature at which the conversion was allowed to take place. In addition, three runs were made on similar specimens in the temperature range above 10°K, and some further runs on 31·5 and 17% mixtures.

4.2.1. *Orthodeuterium at low temperatures*

The data obtained below 9°K are shown in fig. 3 using the same plot as for parahydrogen; the effect of the anomalous contribution is clearly

Table 1. The Specific Heat of Parahydrogen; Measured Values

The unit of C_p is millijoules deg^{-1} mole^{-1}

Expt. 1		Expt. 2	
T°K	C_p	T°K	C_p
2·531	19·9	2·053	11·6
2·625	23·4	2·218	14·2
2·752	27·9	2·414	18·0
2·765	28·9	2·632	22·9
2·788	28·5	2·865	30·1
2·977	35·9	3·115	38·7
3·009	37·3	3·504	55·7
3·278	47·3	4·12	91·2
3·423	53·6	4·56	131
3·586	63·2	5·00	169
3·695	68·6	5·49	232
4·20	94·2	5·98	324
4·72	151	6·52	432
5·55	257	7·18	590
6·33	400	7·90	862
6·78	481	8·47	1113
7·24	624		
7·83	812		
8·45	1155		
9·25	1530		

Fig. 2

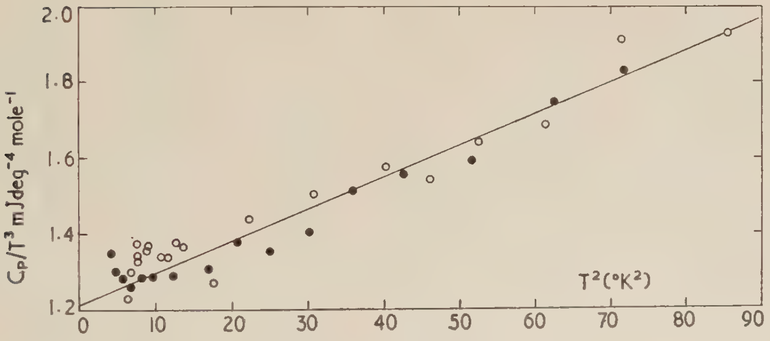

The specific heat of parahydrogen.
○ Expt. 1. ● Expt. 2.

seen. Numerical values are given in table 2. In order to separate the lattice contribution, the data were fitted to an expression

$$C_p = AT^3 + BT^5 + CT^{-2}.$$

The first two terms should represent the lattice specific heat, and the

Fig. 3

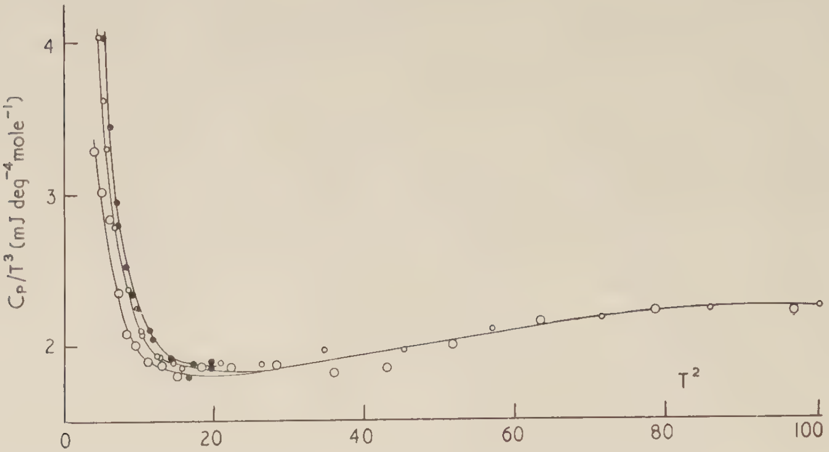

The specific heat of nominal orthodeuterium
○ Expt. 3. ○ Expt. 4. ● Expt. 5.

Table 2. The Specific Heat of Nominal Orthodeuterium; Measured Values

The unit of C_p is millijoules deg^{-1} mole^{-1}

Expt. 3		Expt. 4		Expt. 5	
T°K	C_p	T°K	C_p	T°K	C_p
1·984	41·3	2·012	26·8	1·690	29·4
2·168	41·1	2·252	34·5	1·874	38·6
2·280	42·9	2·488	43·6	2·080	44·5
2·418	46·8	2·694	46·0	2·274	47·3
2·628	50·5	2·904	53·0	2·460	51·2
2·632	50·2	3·106	59·9	2·657	55·3
2·895	58·2	3·343	70·5	2·675	54·5
2·932	59·7	3·610	85·6	2·886	60·6
3·211	69·5	3·901	106	3·032	65·2
3·232	69·8	4·28	146	3·140	69·4
3·519	84·7	4·74	197	3·387	81·6
3·583	88·3	5·34	284	3·442	83·4
3·832	106	6·00	394	3·765	103
3·978	116	6·56	521	3·788	104
4·58	181	7·19	741	4·088	128
5·15	255	7·95	1075	4·150	134
5·90	403	8·87	1540	4·429	164
6·72	593	9·84	2100	4·452	167
7·55	904	10·67	2750		
8·47	1315	11·36	3240		
9·27	1770				
10·01	2240				

last term the 'tail' of the paradeuterium anomaly. This expression is admittedly approximate, but may be considered adequate if all the runs can be represented using the same values of A and B, but different values of C since this depends on concentration. Figure 4 contains the same data as fig. 3 except that at term CT^{-2} has been subtracted from each run, the values of C adopted for runs 3, 4 and 5 being 0·14, 0·10 and 0·16 joule deg mole^{-1} respectively. At the lowest temperatures the correction varies as T^{-5}; below 2·5°K it is so large that interpretation of the data in this simple way is meaningless. Such data have therefore been excluded from fig. 4. A single line now represents all the data, and it is assumed that it equally represents the behaviour of the lattice specific heat; the equation to the line is $C_p = 1{\cdot}60 \times 10^{-3} T^3 + 8{\cdot}3 \times 10^{-6} T^5$ joules mole^{-1} deg^{-1}. For comparison, the data of Gonzales, White and Johnston for 97% orthodeuterium are included. Data below 6°K have been omitted because of the difficulty in treating the anomalous contribution; above 6°K this contribution should be negligible.

Fig. 4

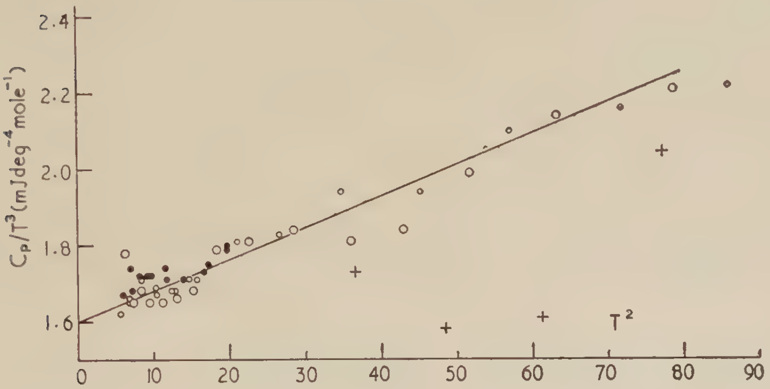

The specific heat of orthodeuterium (data of fig. 3 corrected for anomalous contributions)
○ Expt. 3. ○ Expt. 4. ● Expt. 5.
+ Gonzales *et al.* (1957)

4.2.2. *Orthodeuterium at higher temperatures*

At the higher temperatures, the vapour pressure of the solid becomes appreciable, and a vaporization correction is required. If the volume accessible to the vapour is entirely at the temperature of the calorimeter, the relation between C_s and the measured heat capacity C_m is given by:

$$nC_s = C_m - T\frac{d}{dT}\left\{\frac{dp}{dT}(V - nV_s)\right\}$$

where n is the total number of moles of specimen, V and V_s are the calorimeter volume and the molar volume of the solid respectively, and p is the saturation vapour pressure. In the present experiment part of the volume accessible to the vapour was at temperatures other than that of the calorimeter, and the equation for this case becomes more involved. However, if two runs are made with different values of n, all other parameters being unchanged, then it is easily shown that

$$(n_1-n_2)C_s=C_{m1}-C_{m2}+T\frac{d}{dT}\left\{\frac{dp}{dT}(n_1-n_2)V_s\right\}.$$

In this formula, n_1-n_2 is a constant, and the temperature variation of V_s is small; thus

$$(n_1-n_2)C_s=C_{m1}-C_{m2}+(n_1-n_2)V_sT\frac{d^2p}{dT^2}. \quad . \quad . \quad . \quad (1)$$

This is the relation actually used; since two runs are needed to obtain one set of values of C_s, it is not possible to give the results in the form of individual measured points and values are therefore calculated at integral temperatures only. Three pairs of experiments were performed using different values of n_1 and n_2; the results are compared in table 3.

Table 3. Deuterium Specific Heats at Higher Temperatures from eqn. (1)

The unit of C_p is joules deg^{-1} mole^{-1}

T°K	Expt. 6 C_p	Expt. 7 C_p	Expt. 8 C_p
10	—	—	2·23
11	—	—	2·87
12	—	—	3·75
13	4·67	4·52	4·55
14	5·68	5·59	5·59
15	6·84	6·72	6·73
16	8·14	8·04	7·93
17	9·64	9·57	9·35
18			11·62

4.2.3. *Ortho:paradeuterium mixtures*

These measurements essentially confirmed the data of Gonzales, White and Johnston; in particular, no evidence was found of a λ-type anomaly such as is found in hydrogen of sufficiently high ortho concentration. As these measurements are not relevant to our principal topic they will not be described further.

4.3. *Comparisons with Previous Work*

4.3.1. *Parahydrogen*

The measurements listed above 10°K are all in good agreement; the present measurements fit smoothly into them but do not overlap. Thus direct comparisons are possible only with the work of Mendelssohn, Ruhemann and Simon, and that of Hill and Ricketson using essentially the present apparatus. At temperatures above 5°K there is good agreement with the latter data, but at lower temperatures the orthohydrogen impurity in the older specimen makes direct comparison impossible. When comparison is made with the values of Mendelssohn *et al.*, however, serious differences are found. The older results are always higher than the present ones, and it is believed that this discrepancy is due to the sample used by the older authors having contained appreciable orthohydrogen impurity. It is for this reason that their sample is described as doubtful in the table of § 2.

4.3.2. *Orthodeuterium*

At temperatures above 12°K, comparisons can be made with the data of Kerr, Rifkin, Johnston and Clarke and with those of Clusius and Bartholomé. No significant differences were found. Below this temperature, but above 6°K, comparison can be made with the data of Gonzales, White and Johnston, but at still lower temperatures comparison is again impossible because of the different paradeuterium concentrations. Within the 6 to 12°K range, however, appreciable discrepancies are found, as was shown in fig. 4, where the two relevant runs of this research are compared with the older values. As the present data are fuller and show considerably less scatter, it is felt that they are to be preferred.

§ 5. THE C_p–C_v CORRECTION

When the expansion coefficient α and the isothermal compressibility κ are known at all relevant temperatures, the C_p–C_v correction can be calculated from the thermodynamic relation $C_p - C_v = VT\alpha^2/\kappa$. In the present case these data do not exist; all that is known is the compressibility and molar volume at 4·2°K (Megaw 1939, Stewart 1955) and the molar volume at the triple point (Bartholomé 1936). However, if Grüneisen's law is assumed to hold, and the variation of compressibility with temperature neglected, $C_p - C_v = ATC_v^2$ where A is a constant, the value of which can be determined from the Bartholomé and Eucken values for C_v. In the range where both C_p and C_v measurements exist, it is found that $C_p - C_v = 1{\cdot}60 \times 10^{-3} TC_v^2$ for hydrogen and $2{\cdot}25 \times 10^{-3} TC_v^2$ for deuterium. These equations were solved to find C_v at all other temperatures; the correction proves to be negligible at temperatures below 5°K.

This calculation is admittedly approximate, and has the particular defect that the C_v values are made to agree with those of Bartholomé and

Eucken, so that these latter are in no sense confirmed. It is, however, the best that can be done until measurements of the expansion coefficient are made. Smoothed values of C_p, C_v and the Debye temperature θ are given in table 4.

Table 4

The thermal unit is millijoules deg^{-1} mole^{-1}. The deuterium values in brackets are taken directly from Bartholomé and Eucken (1936)

T°K	Parahydrogen			Orthodeuterium		
	C_p	C_v	θ	C_p	C_v	θ
2	9·95	9·95	116·0	13·1	13·1	106·0
3	34·8	34·7	114·8	45·2	45·2	105·1
4	86·1	85·6	113·2	111	111	103·9
5	178	176	111·3	226	225	102·6
6	327	317	109·8	410	408	100·9
7	558	527	108·1	688	681	99·2
8	899	813	106·9	1091	1070	97·4
9	1380	1170	106·0	1630	1580	95·9
10	2060	1570	104·5	2260	2160	95·4
12				3730	3410	96·4
14				5620	(4870)	(97·0)
16				8040	(6490)	(97·0)

§ 6. DISCUSSION

Specific heat data are conveniently displayed by plotting θ/θ_0, the ratio of the effective Debye temperature to its value at absolute zero, as a function of T/θ_0. This has been done in fig. 5, and typical curves computed for the f.c.c. lattice by Leighton (1948) have been added. The points of interest which emerge are that the curves for hydrogen and deuterium are very similar, both being rather similar to Leighton's curves.

The fact that the hydrogen and deuterium curves are so similar may not seem surprising, but the similarity could not have been predicted with any certainty because the effects of zero point energy are different in the two cases. Apart from such effects, the ratio of the values of θ_0 for hydrogen and deuterium should be $\sqrt{2}$; in fact it is much closer to unity. It appears, then, that the effects of zero point energy on the variation of θ/θ_0 is rather small compared with that on θ_0.

The similarity of the hydrogen curves and those for the f.c.c. lattice is also unpredictable but not too surprising. Here the problem is that the hydrogen solids have a h.c.p. structure, not a f.c.c. one. Since these structures are identical so far as nearest neighbours are concerned, the similarity might have been anticipated. However, the h.c.p. lattice has two particles in unit cell, while the f.c.c. lattice has only one. Thus the formulation of the dynamical problem of the lattice vibration spectrum is rather different in the two cases. No calculations comparable with those of Leighton have been made for the h.c.p. lattice, but from a study of the moments of the frequency spectra Barron and Domb (1955) have shown that differences in behaviour between the specific heats for the two structures are likely to be small. Their analysis, however, is restricted to the case where the effects of zero point energy are negligible, so that its applicability to the hydrogen istopes is doubtful.

Fig. 5

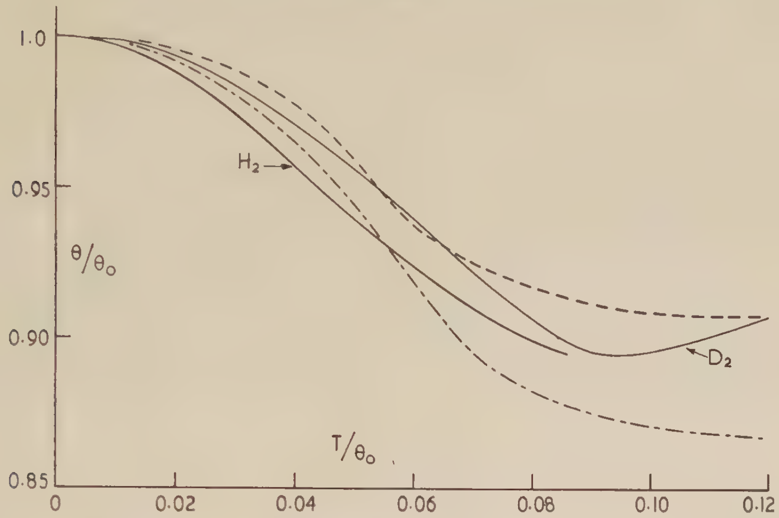

The reduced Debye temperatures as a function of reduced temperature. Dashed curves from Leighton (1948). ——— $\gamma/\alpha=0$. - - - $\gamma/\alpha=-0{\cdot}1$.

Acknowledgments

The authors wish to acknowledge the assistance of Mr. A. Anderson in these experiments. One of us (O.V.L.) is indebted to the Suomen Kultuurirahasto and the British Council for scholarships.

References

Barron, T. H. K., and Domb, C., 1955, *Proc. roy. Soc.* A, **227,** 447.
Bartholomé, E., 1936, *Z. phys. Chem.*, B, **33,** 387.
Bartholomé, E., and Eucken, A., 1936, *Z. Elektroch.*, **42,** 547.
Clusius, K., and Bartholomé, E., 1935, *Z. phys. Chem.* B, **30,** 237.
Clusius, K., and Hiller, K., 1929, *Z. phys. Chem.* B, **4,** 158.
Gonzales, O. D., White, D., and Johnston, H. L., 1957, *J. phys. Chem.*, **61,** 773.
Hill, R. W., 1954, *J. sci. Instrum.*, **30,** 331.
Hill, R. W., and Ricketson, B. W. A., 1954, *Phil. Mag.*, **45,** 277.
Johnston, H. L., Clarke, J. W., Rifkin, E. B., and Kerr, E. C., 1950, *J. Amer. chem. Soc.*, **72,** 3933.
Kerr, E. C., Rifkin, E. B., Johnston, H. L., and Clarke, J. W., 1951, *J. Amer. chem. Soc.*, **73,** 282.
Leighton, R. B., 1948, *Rev. mod. Phys.*, **20,** 165.
Megaw, H. D., 1939, *Phil. Mag.*, **28,** 129.
Mendelssohn, K., Ruhemann, M., and Simon, F. E., 1931, *Z. phys. Chem.* B, **15,** 121.
Stewart, J. W., 1955, *Phys. Rev.*, **97,** 578.

The Reaction $^{7}Li(\alpha\gamma)^{11}B$ †

By G. A. Jones‡, C. M. P. Johnson and D. H. Wilkinson§
Cavendish Laboratory, Cambridge

[Received January 28, 1959]

Abstract

The gamma rays following excitation by the $^{7}Li(\alpha\gamma)^{11}B$ reaction of levels in ^{11}B at 9·28 Mev, 9·19 Mev and 8·93 Mev have been studied with sodium iodide scintillation counters and a scintillation pair spectrometer. The decay schemes of these levels have been elucidated and angular distributions of some of the gamma rays have been measured. From these data, and a consideration of the reaction widths of the levels in ^{11}B, assignments of spins and parities have been made for some of these levels. In particular it has been established that the characteristics of the 4·46 Mev and 9·28 Mev levels in ^{11}B are 5/2− and 5/2+ respectively, and that the M1 radiation from the 4·46 Mev level is mixed with a small proportion of E2 radiation.

§ 1. Introduction

The properties of the excited states of ^{11}B are of considerable interest, along with other nuclei of the p shell, since a considerable amount of theoretical work has been done in this region by Inglis (1953) and more rigorously by Kurath (1956 and 1957). The positions of some eleven levels up to 9·28 Mev excitation had been determined by Van Patter *et al.* (1951), who measured the energies of proton groups in the $^{10}B(dp)^{11}B$ reaction. The $^{7}Li(\alpha\gamma)^{11}B$ reaction was discovered by Bennett *et al.* (1951), using a conversion electron spectrometer. They found resonances at 401 kev, 819 kev and 958 kev, corresponding to levels in ^{11}B at 8·93 Mev, 9·19 Mev and 9.28 Mev. This paper describes experiments in which the radiations from each of these three levels have been measured and correlated with transitions between known levels in ^{11}B. In an early series of experiments, scintillation counters consisting of one inch cube crystals of NaI(Tl) and E.M.I. photomultipliers type 6262 were used to study gamma ray spectra (and α–γ and angular correlations) at the three resonances. A brief report on these measurements has already appeared (Jones and Wilkinson 1952), but since then the stripping data of Evans and Parkinson (1954) on the reactions $^{10}B(d, p)^{11}B$ have become available, and further work has been done here on the $^{7}Li(\alpha\gamma)^{11}B$ reaction using a scintillation pair spectrometer and larger NaI crystals.

---

† Communicated by the Authors.
‡ Now at the Atomic Energy Research Establishment, Harwell.
§ Now at the Clarendon Laboratory, Oxford.

§ 2. The Decay Scheme

By using thin targets, the gamma rays following the decay of the three levels mentioned above were separately investigated. Scintillation spectra at the upper resonance contained a prominent peak just above 4 Mev, and two weaker lines of higher energy (fig. 1). Comparison of the peaks with calibration spectra of known energies showed that the main peaks contained two components at (4·806 ± 0·013) Mev and (4·464 ± 0·013) Mev and that the other gamma rays had energies (6·83 ± 0·03) Mev and (9·27 ± 0·03) Mev. These results were arrived at from several careful runs, using different calibration gamma rays and correcting for the effect of magnetic fields on the photomultiplier. Comparison with the level scheme established by Van Patter *et al.* suggested that these gamma rays correspond to a ground state transition, a cascade via the 4·46 Mev level (since the sum of the components of the double

Fig. 1

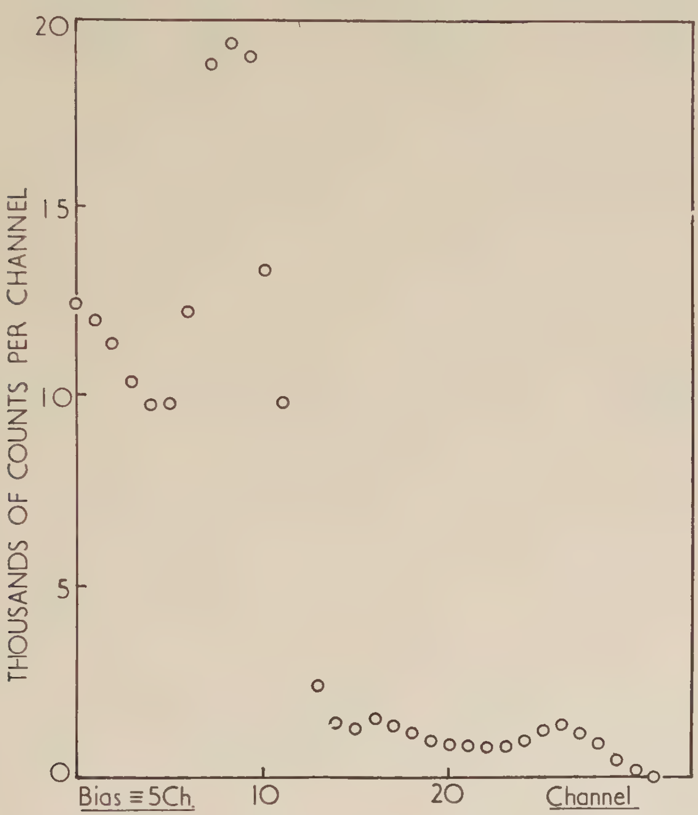

Scintillation pulse height spectrum of gamma rays from the 958 kev resonance in the ^{7}Li$(\alpha\gamma)^{11}$B reaction.

peak is 9·27 MeV), and a cascade via the doublet at 6·8 MeV. The other component of this latter cascade was measured by observing coincidences with the 6·8 MeV pulses in other counters; from the spectrum shown in fig. 2 its energy measured in this way was (2·53 ± 0·06) MeV.

Figure 3 shows typical pair spectrometer results in two regions, from 1 MeV to 5 MeV and from 4 MeV to 10 MeV. The presence of the main cascade peaks in each of these spectra enabled relative intensity measurements to be made. The mean of several runs gave (6·815 ± 0·030) MeV and (2·485 ± 0·020) MeV for the energies of the two components of the cascade, which agreed with the single crystal work in suggesting that the 6·81 MeV level is probably the one more concerned in the cascade. Relative intensities were obtained by adding the number of counts in each peak and subtracting pulses arising from 'tails' of other gamma rays. Since the total cross section of sodium iodide is nearly constant for the gamma rays of interest here, the numbers of counts were corrected simply by dividing each peak area by the relevant pair production cross section. Where necessary a correction for the angular distribution was applied. The results for two separate comparisons with the 4·82 MeV line are summarized in table 1, in which the relative intensities are subject to an error of about 20% arising mainly from uncertainty in background subtraction.

Fig. 2

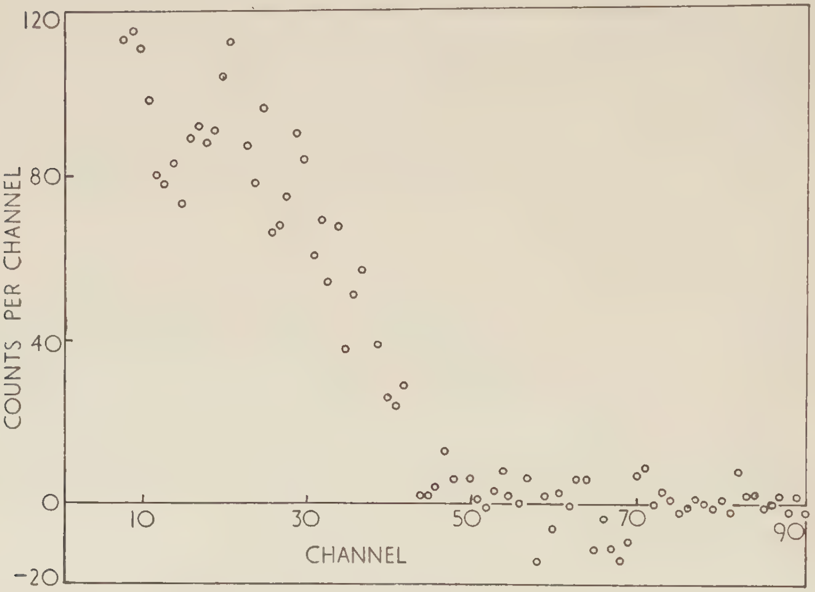

Spectrum in coincidence with 6·8 MeV radiation from the 958 kev resonance after subtraction of background.

Fig. 3

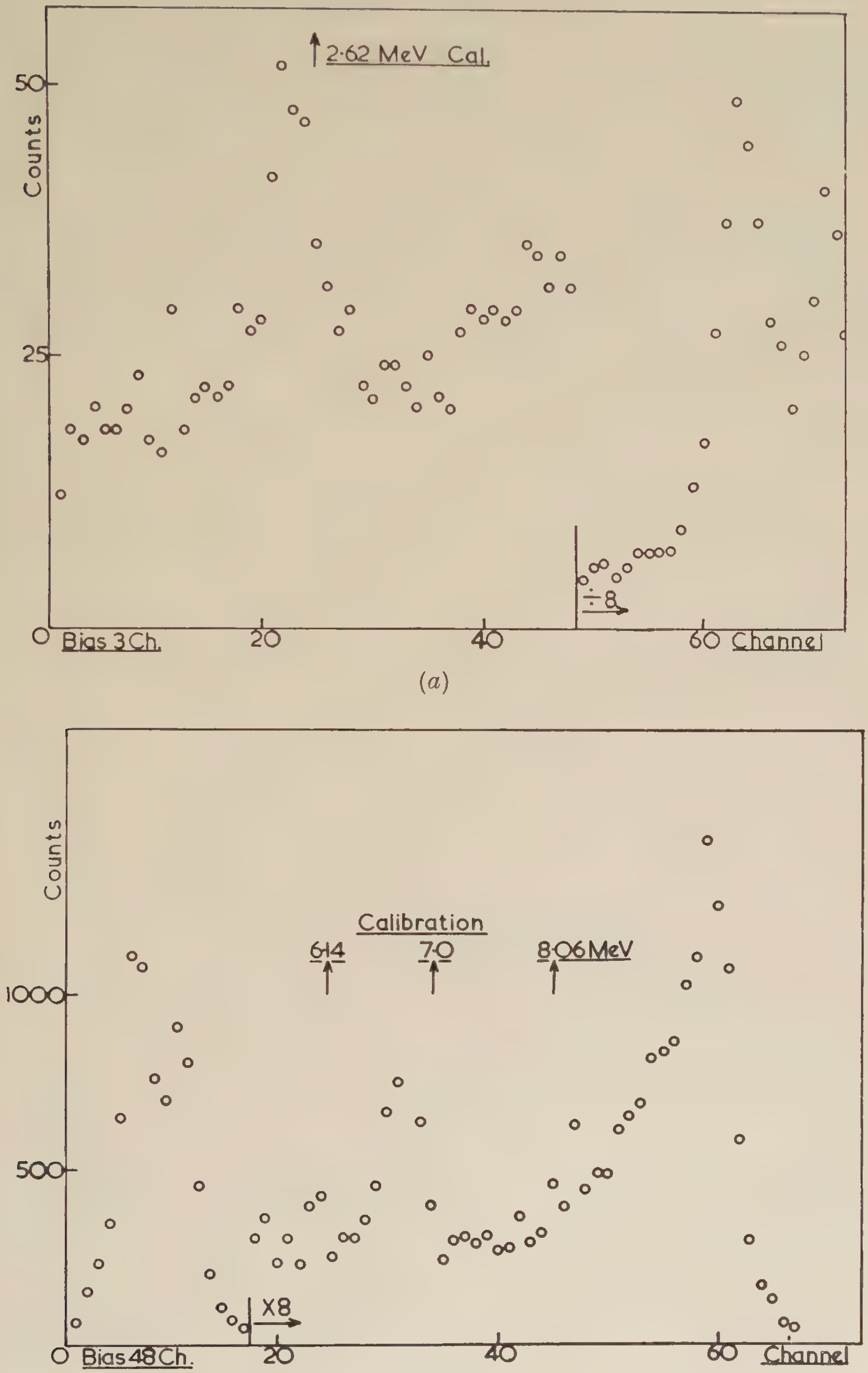

(*a*)

(*b*)

Pair spectrometer spectra of gamma rays from the 958 kev resonance. (*a*) 0–5 MEV region, (*b*) 4–10 MEV region.

Table 1

γ ray energies (MeV)	2·49	4·82	4·82	6·81	9·28
Number of counts	268	2570	3050	406	1707
Corrected	179	605	717	74	165
Relative intensity	0·29	1	1	0·10	0·23

It is evident from these figures that the decay of the 6·8 MeV level is not solely to the ground state: there must be a further cascade. This cannot be via the 5·03 MeV level since a 1·8 MeV gamma ray would be seen separated from the 2·5 MeV peak, and an upper limit of 5% relative to the main cascade was placed on the existence of this gamma ray. Furthermore a 5·03 MeV gamma ray would be expected also, since this level has been shown by Ferguson *et al.* (1958), using the ^{9}Be(^{3}He, pγ)^{11}B reaction, to decay 88% to the ground state and 12% to the 2·14 MeV state. A careful study of this region with the pair spectrometer (fig. 4) enabled an upper limit of 2% to be placed on the presence of the 5·03 MeV gamma ray. A cascade from the 6·8 MeV level(s) via the 4·46 MeV level is possible since the resulting 2·35 MeV gamma ray would just cause a widening of the 2·5 MeV peak, which is in fact observed. A study of the main cascade peaks, described

Fig. 4

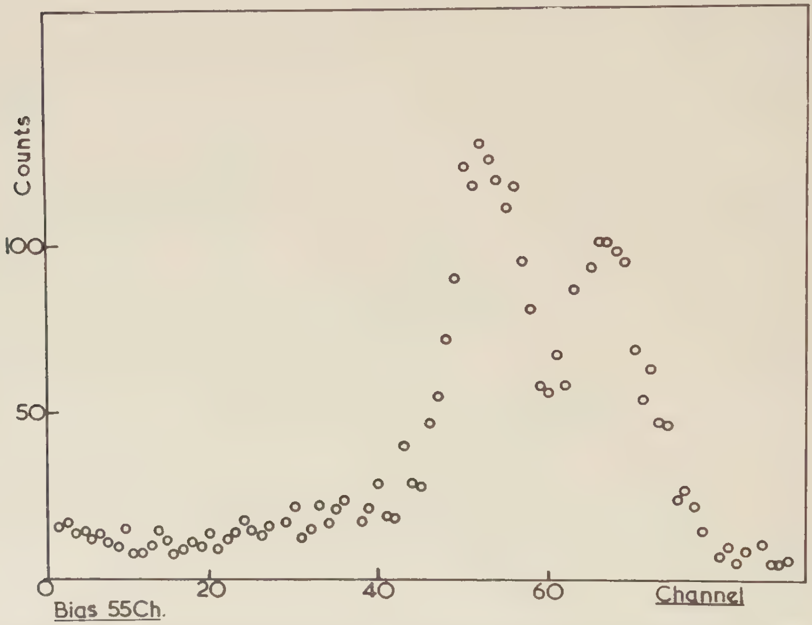

Pair spectrometer spectrum of the main cascade gamma rays from the 958 kev resonance.

later, showed that the 4·46 Mev gamma ray is about 16% more intense than the 4·82 gamma ray. The observed intensities could now be explained if a transition of about 20% of the main cascade strength took place to the 6·81 Mev level, which then decayed with comparable probability direct to the ground state and by cascade through the 4·46 Mev level.

Fig. 5

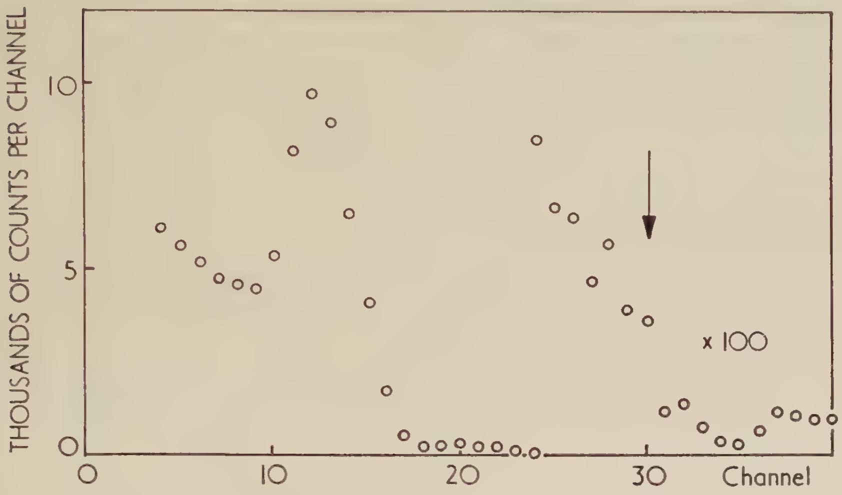

Gamma-ray scintillation spectrum from bombardment of a thin target at the 819 kev resonance. The arrow shows where the peak arising from a ground state transition would be.

The radiations following bombardment at the 819 kev resonance were studied in the same way. Figure 5 shows the single crystal spectrum obtained with a thin target at the resonance. The principal component was a double peak in the 4·5 Mev region, and careful comparison with the main cascade peaks at the upper resonance showed that the position of the lower peak was unchanged while that of the upper peak was lowered. This adds conviction to the previous interpretation of the cascade from the upper resonance. The adopted values of the energies of the two components were (4·470 ± 0·023) Mev and (4·728 ± 0·023) Mev, which add up to 9·198 ± 0·032 Mev, according very well with the available energy of 9·190 ± 0·012 Mev. There was also a weak component near 7 Mev, and a similar comparison showed that its position is unchanged in energy, confirming the previous interpretation that the gamma ray is the second in the cascade. The pair spectrometer spectra are shown in fig. 6, the energies of the weak gamma rays being (6·82 ± 0·04) Mev and (2·44 ± 0·05) Mev; the relative intensities were found as before and are shown in table 2.

Fig. 6

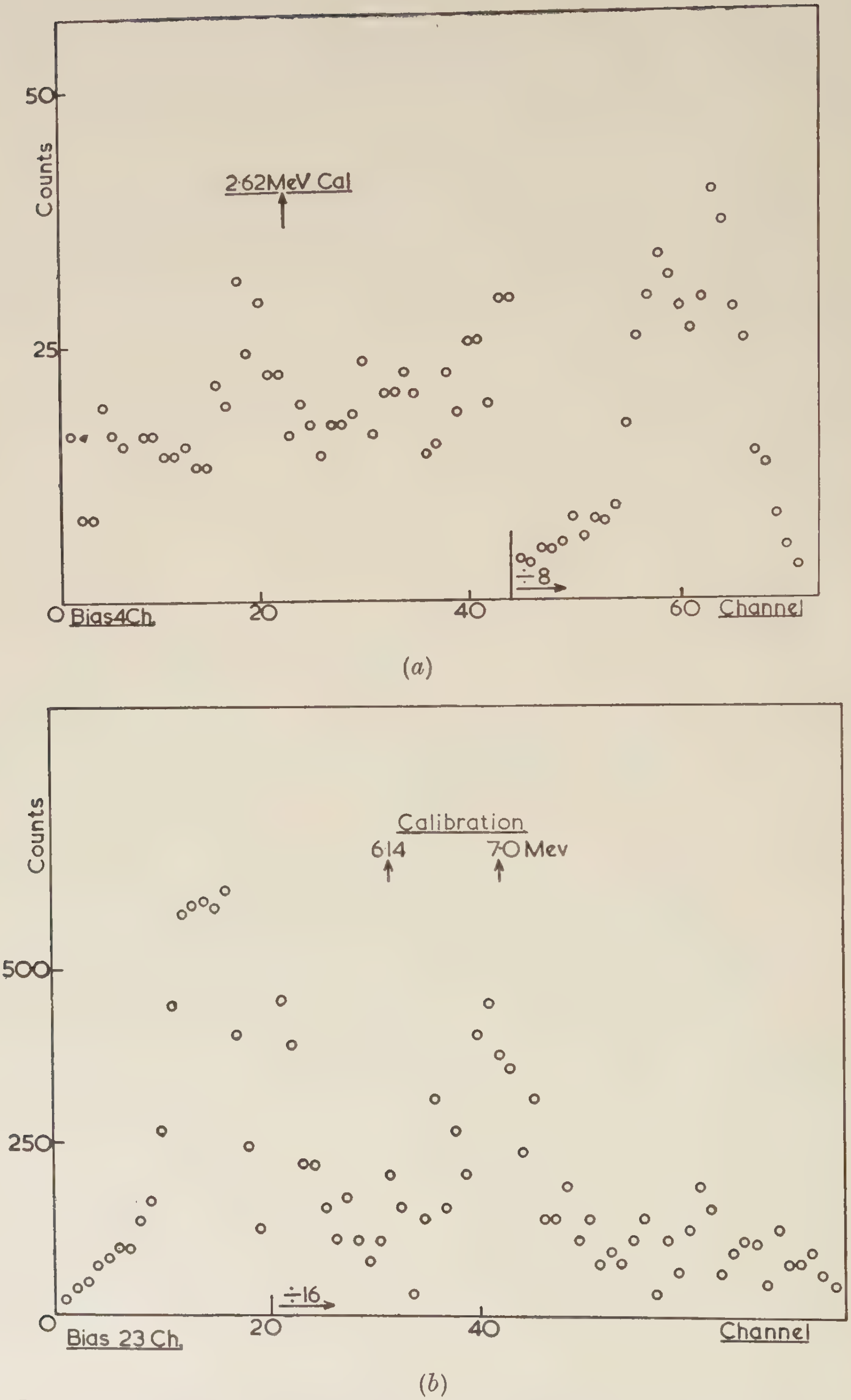

Pair spectrometer spectra of gamma rays from the 819 kev resonance. (*a*) 0–5 Mev region, (*b*) 4–10 Mev region.

Table 2

γ energies (MEV)	2·44	4·73	4·73	6·82
Number of counts	101	2200	2700	151
Corrected	67·5	525	645	27
Relative intensity	0·13	1	1	0·045

From the high energy spectrum there was slight evidence for a very weak ground state transition, about 2% of the main cascade. A careful study of the radiation with a large single crystal showed no evidence for a ground state transition and enabled an upper limit of 0·5% to be placed on its intensity relative to the main cascade radiation. Observation of the main cascade radiation at 0° and 90°, described later, showed that the 4·46 MEV gamma ray is about 3% stronger than

Fig. 7

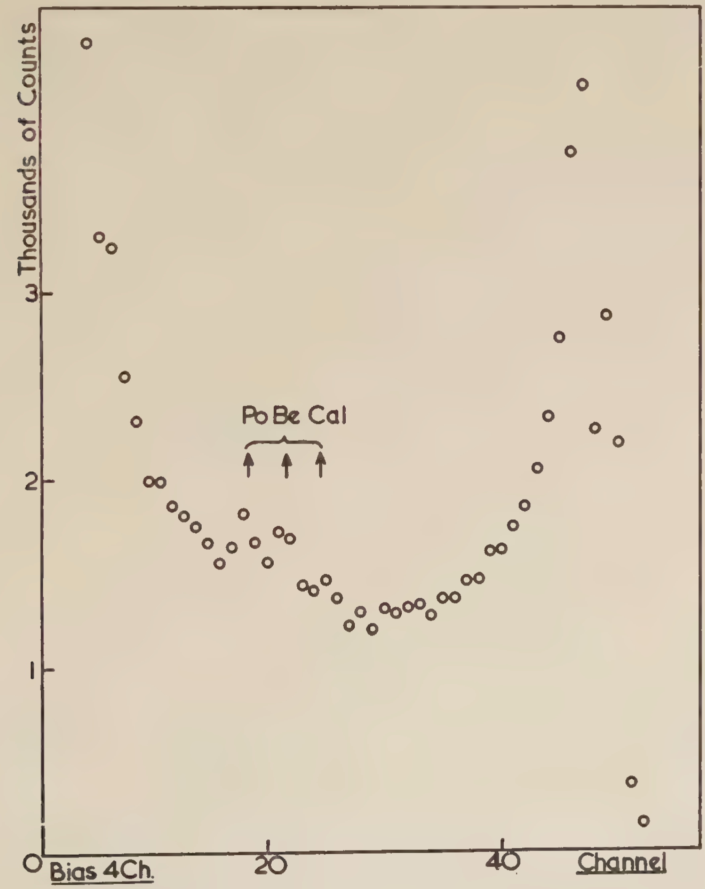

Gamma-ray scintillation spectrum at the 401 kev resonance. The arrows show the positions of the three peaks in the 4·43 MEV calibration spectrum.

the 4·73 MeV gamma ray. This fact, and the relative intensities in table 2, suggest that the decay scheme of the 6·8 MeV level is the same as observed following decay of the 9·28 MeV level, branching to the ground state and the 4·46 MeV level.

The yield at the 401 kev resonance is rather low, and it was not possible to carry out pair spectrometer observations. Figure 7 shows a typical spectrum, obtained with a $2\frac{1}{2}$ in. × $1\frac{1}{2}$ in. cylinder of NaI(Tl). In addition to a strong ground state gamma ray there were three well defined peaks, in almost the same position as the 4·43 MeV calibration gamma ray from the ^{9}Be(αn)^{12}C reaction. This suggested that the 8·93 MeV level decays

Fig. 8

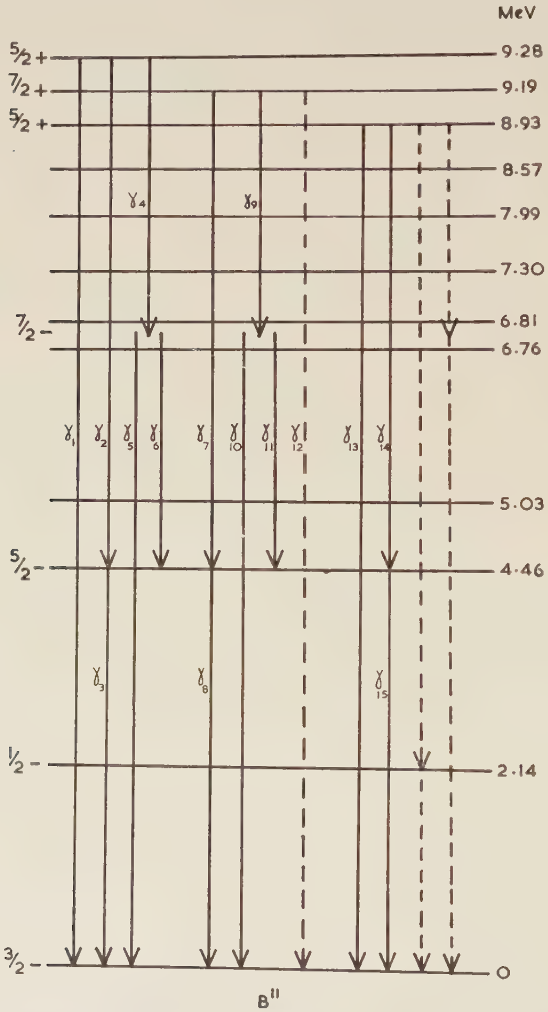

Decay scheme of the levels of ^{11}B following the ^{7}Li(αγ)^{11}B reaction, including the assignments resulting from this work and from the ^{10}B(dp)^{11}B stripping results.

also by cascade through the 4·46 MEV level, since the two members of the cascade would be 4·46 MEV and 4·47 MEV. To check that the three peaks are associated with two gamma rays very close together a run was carried out using a smaller (inch cube) crystal, when only the 'double escape' peak was seen. The intensity of the compound gamma ray was about 10% of the ground state transition, so the intensity of the cascade is 5%. An upper limit of 2% was placed on the presence of a cascade via the 5·03 MEV level. There were slight signs of the high energy component of a cascade via either the 2·14 MEV level or the doublet at 6·5 MEV, but the statistics did not permit a conclusion more definite than an upper limit of 5%. The decay scheme following the $^7\mathrm{Li}(\alpha\gamma)^{11}\mathrm{B}$ reaction at the three resonances is shown in fig. 8. Table 3 shows a comparison between the observed gamma ray energies (measured at 90° to the incident beam to avoid Doppler corrections) and the appropriate level differences. The relative probabilities of the modes of decay are indicated for each resonance.

Table 3

Gamma ray	Probability	Expected energy (MEV)	Measured energy (MEV)
γ_1	0·16	9·276 ± 0·012	9·27 ± 0·03
γ_2	0·70	4·817 ± 0·018	4·806 ± 0·013
γ_3	0·77	4·459 ± 0·014	4·464 ± 0·013
γ_4	0·14	2·468 ± 0·018	2·485 ± 0·020
γ_5	0·07	6·808 ± 0·013	6·815 ± 0·03
γ_6	(~0·07)	2·349 ± 0·018	
γ_7	0·91	4·731 ± 0·018	4·728 ± 0·023
γ_8	0·95	4·459 ± 0·014	4·470 ± 0·023
γ_9	0·09	2·382 ± 0·018	2·44 ± 0·05
γ_{10}	0·05	6·808 ± 0·013	6·82 ± 0·04
γ_{11}	(~0·05)	2·349 ± 0·018	
γ_{12}	⩽0·005	9·190 ± 0·012	
γ_{13}	0·95	8·926 ± 0·012	8·91 ± 0·03
γ_{14}	0·05	4·467 ± 0·018	4·43 ± 0·10
γ_{15}	0·05	4·459 ± 0·014	

§ 3. THE ANGULAR DISTRIBUTIONS

Because of the fairly complicated scheme of cascade gamma rays, two methods were used for the measurement of angular distributions. The more intense radiations were measured by the normal method using reasonably good geometry, and the feebler radiations were measured relative to these by noting the change in shape of the spectra with angle. In this way it was possible to make measurements in poor and uncertain geometry and to make long runs at each angle without fear of beam wander on the target, since this effect is eliminated on comparison of the feebler line with the stronger one of known angular distribution. In the 'good geometry' measurements, the detector was an inch cube NaI(Tl) crystal, and a similar detector in a fixed position was used as a monitor counter. Runs were performed at 10° intervals, over the range $-20°$ to $+110°$, and background runs were taken with the beam striking a shutter in front of the target. Corrections, amounting in each case to not more than 5%, were made for the effect of magnetic field on the gain of the photomultiplier, the change in distance from the target with angle, the Doppler shift in gamma ray energy, and for absorption in the target backing. The counters were about 7 cm from the target, and in better geometry accurate values of the 90° to 0° intensity ratio were measured and corrected for the effective location of the beam on the target.

To measure the feebler radiations, the shapes of the spectra were measured at the same angles using the same scintillation counter. For the main cascade radiations from the two higher levels, it was found convenient to measure the spectra at 0° and 90° with the scintillation pair spectrometer, since the two components of the cascade have nearly the same energy and are therefore very difficult to separate using single crystals. From the angular distribution of the combined radiation the distributions of the separate components were then obtained. The results are described below for each resonance in turn, together with the conclusions drawn from the measurements.

3.1. *The* 958 *keV Resonance* (9·28 *MeV Level*)

Figure 9 shows the angular distribution of the ground state transition, obtained by biasing the detector at 7·3 MeV; the value of the 90° to 0° ratio was $I_{90°}/I_{0°} = 1{\cdot}76 \pm 0{\cdot}04$. It is evident from the figure that any $\cos^4 \theta$ contribution is small, and the distribution can quite well be represented by $1{\cdot}75 - 0{\cdot}75 \cos^2 \theta$. Theoretical angular distributions were calculated for all possible combinations of ingoing alpha-particle orbital angular momenta, compound nucleus spins and radiation mixtures that may occur in the reaction. For the 9·28 MeV level spin 1/2 may be ruled out since the distribution is anisotropic, spin 7/2 may be ruled out since the intensity variation is in the wrong sense. 3/2+ gives a good fit and 5/2 ± give fair fits for appropriate values of the mixing ratios.

The angular distribution of the combined components of the main cascade is shown in fig. 10; the 90° to 0° intensity ratio was measured to be $0{\cdot}895 \pm 0{\cdot}015$. Single crystal spectra were taken at 10° intervals, enabling the distributions of the components to be separated. This was difficult to do with any accuracy, but was sufficient to show that any $\cos^4 \theta$ term in the distribution is small. The pair spectrometer was able to resolve the two gamma rays as shown in fig. 11 and was used to measure the 90° to 0° ratio for each; the values of the intensity ratios used were weighted averages of the singles and pair spectrometer values. After correction for change in pair cross section, and for finite solid angle, the distribution functions were

$$\gamma_2 = (0{\cdot}70 \pm 0{\cdot}07) + (0{\cdot}37 \pm 0{\cdot}10) \cos^2 \theta, \quad \gamma_3 = 1 - (0{\cdot}17 \pm 0{\cdot}08) \cos^2 \theta,$$

indicating that γ_3 is perhaps about 12% more intense than γ_2.

The stripping work of Evans and Parkinson showed unambiguously that the parity of the 4·46 MeV level must be odd; the following characteristics

Fig. 9

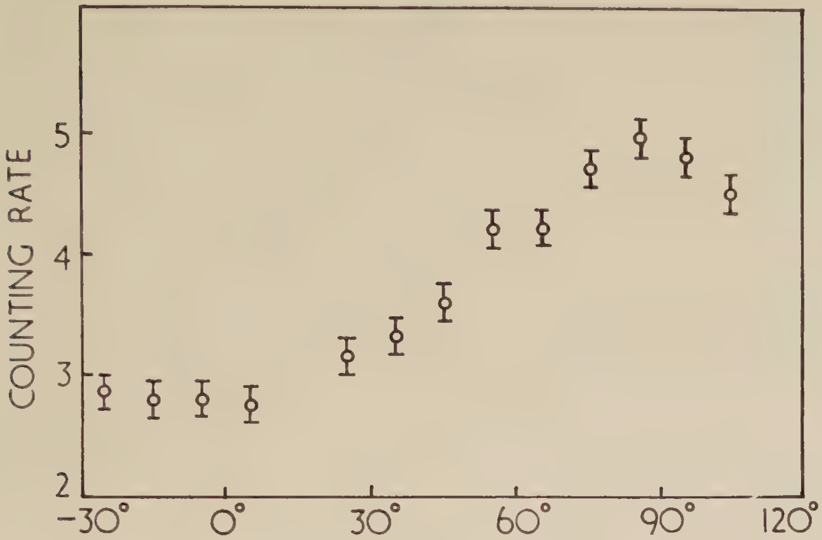

Angular distribution of the ground state transition from the 9·28 MeV level.

Fig. 10

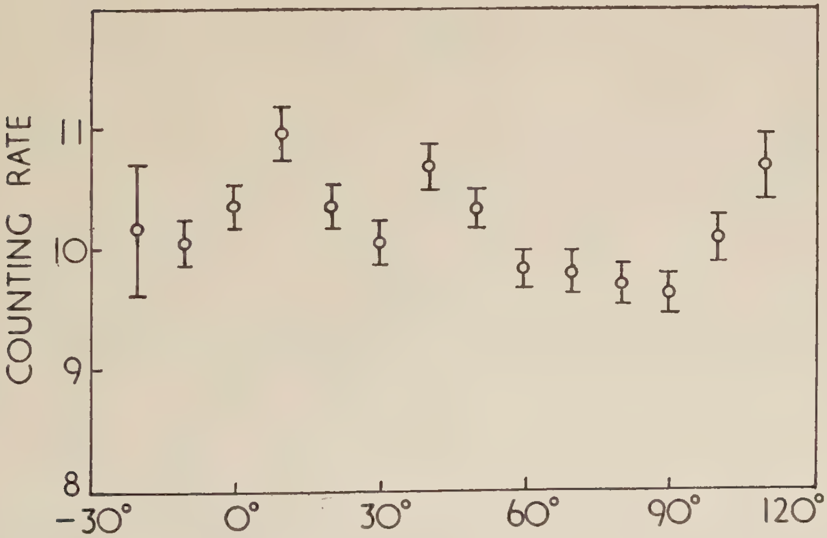

Angular distribution of the combined components of the main cascade from the 9·28 MeV level.

will fit in with this observation and with the observed decay schemes. Some of the possibilities are ruled out by comparison of experimental with theoretical distribution functions for the components of the main cascade.

Fig. 11

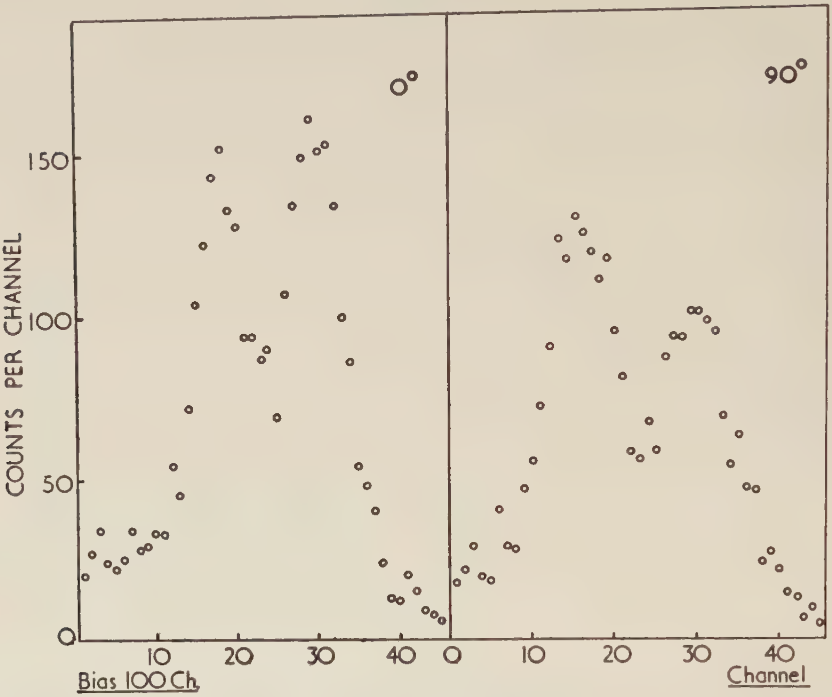

Pair spectrometer spectra at 0° and at 90° of the main cascade gamma rays from the 9·28 Mev level.

9·28 Mev	4·46 Mev	Remarks
5/2 ±, 3/2 +	3/2 −	γ_2 distribution varies in the wrong sense.
5/2 ±	5/2 −	Both components can be fitted.
3/2 +	5/2 −	γ_2 (experimental) has too extreme a pattern.
5/2 +	7/2 −	γ_2 distribution varies in the wrong sense.
5/2 −	7/2 −	γ_2 can only be fitted with too large an E2 mixing in the M1 transition.

Recently the lifetime of this level has been measured to be $1{\cdot}2 \times 10^{-15}$ sec (Rasmussen *et al.* 1958) which is consistent with magnetic dipole decay to the ground state, not pure electric quadrupole. Kurath (1957) has calculated the lifetime: his value agrees with experiment. We therefore conclude that the 9·28 Mev level is 5/2 ± and that the 4·46 Mev level is 5/2 −.

The angular distribution of 6·8 MeV radiation is shown in fig. 12, derived from the measurements of spectra as a function of angle. For the possible characteristics of the 9·28 MeV level, the assignments 3/2 ± or 7/2 ± for the 6·8 MeV level(s) could give the observed pattern; 7/2 + may be rejected because it makes the ground state transition magnetic quadrupole.

Fig. 12

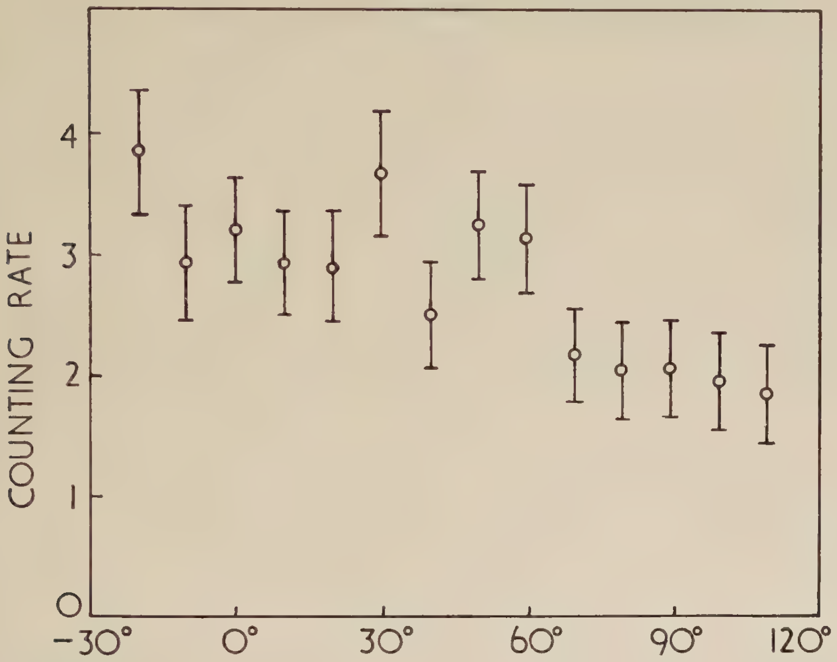

Angular distribution of the 6·8 MeV gamma ray from the 958 keV resonance.

3.2. *The* 819 *keV Resonance* (9·19 *MeV Level*)

It was impossible with single crystals to say more than that the departure from isotropy of the main cascade components was small, but using the pair spectrometer (fig 13), intensity ratios were found as follows :

$$\gamma_7(90°/0°) = 1{\cdot}27 \pm 0{\cdot}09; \quad \gamma_8(90°/0°) = 0{\cdot}95 \pm 0{\cdot}07$$

γ_8 is about 3% more intense than γ_1.

From the decay scheme of the 9·19 MeV level, the only assignments at all likely for it are 3/2 ±, 5/2 ±, 7/2 ± and 9/2 −, since it is very unlikely that γ_7 is not dipole or electric quadrupole in character. The theoretical ratios for each of these possibilities were compared with the measured ratios (using $J = 5/2-$ for the 4·46 MeV level):

3/2 + : Requires too large a proportion of the higher l wave in the alpha-particles.

3/2 − : Possible anisotropy too small, also cannot give a fit for the 6·8 MeV distribution.

5/2 + : Intensity of γ_7 varies in the wrong sense.

5/2 – : Intensity of γ_8 varies in the wrong sense, though cannot be ruled out in view of the experimental error.
7/2 + : Can be fitted assuming 0·1% intensity of M2 relative to E1 in γ_7 and a mixture of M1 and E2 radiation for γ_8.
7/2 – : Can be fitted for a mixture of M1 and E2 radiations.
9/2 – : Intensity of γ_7 varies in the wrong sense.

Fig. 13

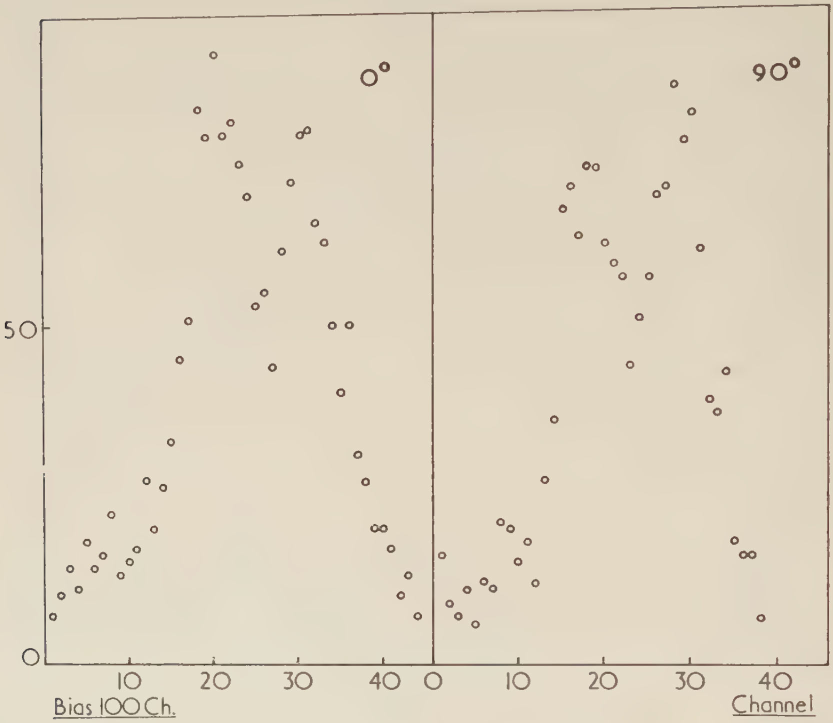

Pair spectrometer spectra at 0° and at 90° of the main cascade gamma rays from the 9·19 MeV level.

The most likely assignment for the 9·19 MeV level from our work alone is therefore 7/2 –, the very weak ground state transition being evidence against the 5/2 – possibility. We note that this conflicts with the recent stripping evidence (Bilaniuk and Hensel 1958) which suggests that this level is 5/2 + or 7/2 +. In view of this, the only alternative which fits both experiments is the 7/2 + assignment; this possibility will be discussed further in terms of the reaction widths.

The 90° to 0° intensity ratio of the 6·8 MeV line was measured, in poor geometry, by the method described above using a single crystal. This ratio was $I_{90°}/I_{0°} = 0{\cdot}71 \pm 0{\cdot}05$, and was compared with the theoretical values for the two possible assignments for the 9·19 MeV level, combined with the three assignments for the 6·8 MeV level which fit the data from the upper resonance.

9·19 MEV	6·8 MEV	Remarks
7/2 −	3/2 −	Theoretical value agrees with experiment.
7/2 −	3/2 +	Ruled out since γ_9 would be M2.
7/2 −	7/2 −	Large E2 component required in γ_9.
7/2 +	3/2 −	Ruled out since γ_9 would be M2.
7/2 +	3/2 + or 7/2 −	Theoretical value agrees with experiment.

3.3. *The* 401 *keV Resonance* (8·93 *MeV Level*)

The 90° to 0° ratio of the ground state transition was measured by comparison with the main cascade at the intermediate resonance by using a thick target. It was $I_{90°}/I_{0°} = 1{\cdot}26 \pm 0{\cdot}04$, which eliminated the possibility of spin 1/2 for the 8·92 MEV level. It would fit in well with 3/2 ± or 5/2 − assignments, but does not rule out the possibility of 5/2 +. It is worth noting in this connection that the branch to the 4·46 MEV level has about the correct intensity for the competition of two dipole transitions with a factor of two energy difference.

§ 4. REACTION WIDTHS OF LEVELS IN ^{11}B

The width of the 958 kev resonance, as measured by Bennett *et al.* (1951), is 6 kev (in E_α) while the yield of gamma-radiation indicates a controlling width $(2J+1)\Gamma \sim 14$ ev (an average of our present results and Bennett's). Comparison of these widths with Weisskopf's estimates for gamma-radiation makes it evident that $(2J+1)\Gamma_\gamma \sim 14$ ev and $\Gamma_\alpha \sim 4$ kev. The characteristics required for the resonance level are (5/2 +), formed by p-wave plus 10% (intensity) f-wave alpha-particles and decaying by E1 radiation; alternatively (5/2 −) formed by d-waves followed by emission of M1 (+ small amount of E2). Taking as large an effective radius as 5×10^{-13} cm to compute penetrabilities the former assignment leads to a p-wave reduced width of about 10% of the Wigner Limit and an f-wave reduced width of about 80%; the latter gives a d-wave width of 60%; the radiation widths to lower-lying levels are compared with Weisskopf units for the alternative schemes in table 4. It appears that, in either case, an uncomfortably large alpha-width is required, though it should be realized that for the collision of two light nuclei such as ^{4}He and ^{7}Li a simple description in terms of a conventional (if rather large) radius may be inadequate. The smoothing of the potential barrier because of diffuseness of the nuclear surface now commonly accepted for heavier nuclei might lead to greatly enhanced penetrabilities in the present instance—a similar state of affairs for light nuclei seems to occur in the reaction ^{9}Be(α, n)^{12}C (James *et al.* 1956). The radiation widths seem more appropriate to E1 radiation and this favours the characteristics 5/2 + for the 9·28 MEV level in ^{11}B. This accords with the recent stripping evidence of Bilaniuk and Hensel (1958).

Table 4

Transition	Energy (Mev)	Γ_γ(ev)	($J=5/2+$) Type	$\lvert M\rvert^2$	($J=5/2-$) Type	$\lvert M\rvert^2$
γ_1	9·28	0·34	E1	0·0011	M1 1%E2	0·017 0·034
γ_2	4·82	1·48	E1	0·037	M1 1%E2	0·74 5·0
γ_4	2·49	0·44	E1	0·09	M1 (1%E2	1·47 40)

At $E_\alpha = 819$ kev, the controlling width is probably again a measure of $(2J+1)\Gamma_\gamma$ rather than of Γ_α for the formation of the 9·19 Mev level with characteristics $7/2-$ or $7/2+$; from the gamma ray yield $(2J+1)\Gamma_\gamma = 2{\cdot}5$ ev. In table 5 the radiation widths of the gamma rays following decay of the 9·19 Mev level are compared with Weisskopf units for the level assignments which fit the angular distribution data.

Table 5

Transition	Energy (Mev)	Γ_γ(ev)	($J_{9\cdot 19}=7/2-$) Type	$\lvert M\rvert^2$	($J_{9\cdot 19}=7/2+$) Type	$\lvert M\rvert^2$
γ_{12}	9·19	$\leqslant 0{\cdot}006$	E2	$\leqslant 0{\cdot}06$	M2	$\leqslant 2$
γ_7	4·73	0·27	M1 +1%E2	0·13 1	E1 +0·1%M2	0·007 2
γ_9	2·39	0·037	E2	370 ($J_{6\cdot 8}=3/2-$)	E2	370 ($J_{6\cdot 8}=3/2+$)
			50%M1 +50%E2	0·053 185 ($J_{6\cdot 8}=7/2-$)	E1	0·007 ($J_{6\cdot 8}=7/2-$)

It is clear from the table and from the stripping data that much the most likely assignments are $J=7/2+$ for the 9·19 Mev level and $J=7/2-$ for the 6·8 Mev level, since the resulting widths follow the systematic trends so far as they are known. There are at the moment insufficient data available for us to compare our limit for the radiative width of the ground state transition with the resonant absorption measurement of Meyer-Schützmeister and Hanna (1958).

For the 400 kev resonance the controlling width from the measured yield is $(2J+1)\Gamma \sim 0{\cdot}10$ ev but it is no longer obvious whether this refers to Γ_α or Γ_γ. Ferguson *et al.* (1958) show that Γ_α is roughly the same as Γ_γ, so $(2J+1)\Gamma_\gamma \sim (2J+1)\Gamma_\alpha \sim 0{\cdot}2$ ev. For assignments $3/2+$ or $5/2+$ for the 8·92 Mev level in ^{11}B, Γ_α is about 0·4% of the Wigner limit for p-wave alpha-particles, and $\Gamma_\gamma \sim 5 \times 10^{-4}$ Weisskopf units for the ground state E1 radiation. For the 3/2 − assignment $\Gamma_\alpha \sim 0{\cdot}1\%$ or the Wigner limit for s-wave alpha particles and $\Gamma_\gamma \sim 0{\cdot}01$ Weisskopf units for M1 radiation. For 5/2 −, $\Gamma_\alpha \sim 0{\cdot}03$ of the Wigner limit for d-wave alpha-particles and $\Gamma_\gamma \sim 0{\cdot}01$ Weisskopf units for M1 radiation. All these are quite reasonable; with the stripping data the choice of 5/2 + is indicated.

§ 5. DISCUSSION

The weakness of transitions to the 2·14 MeV level from the three levels excited suggests that the spin of this latter level is 1/2, in conflict with the stripping data of Evans and Parkinson which give $l_n = 1$. The conclusion of spin 1/2 has however been supported by the measured isotropy of gamma ray distributions from this level following the ^{10}B(dp)^{11}B reaction (Thirion 1953), and the ^{11}B(pp′)^{11}B reaction (Bair *et al.* 1955). Metzger *et al.* (1958) have shown that the lifetime of this level is $(4{\cdot}7 \pm 0{\cdot}6) \times 10^{-15}$ sec and therefore that the transition is dipole in character, confirming the assignment of spin 1/2 for this level—see Wilkinson (1957) for a general discussion. It has been suggested by Evans and French (1958) that the stripping curve may be explained by a reversal of intrinsic spin between the incoming and the departing protons, and polarization measurements on the proton groups by Hensel and Parkinson (1958) demonstrated anomalous polarization of the first excited state, which is further evidence for some type of exchange process. The assignments made possible by this work, together with the stripping data, are shown on fig. 8.

Kurath (1956) has calculated the position of odd parity levels in ^{11}B belonging to p^7 as a function of the intermediate coupling parameter a/K. For a value of a/K in the region of 6 the first five levels agree fairly well with our present proposals if one assumes that the $J = 5/2$ and $J = 7/2$ levels have changed order. It is rather disturbing, however, that this assignment suggests that the spin of the 5·03 MeV level is 7/2. This does not accord well with the observation of Ferguson *et al.* that this level decays in 8% of cases by cascade via the 1/2 − first excited state, whose assignment is now a reasonably firm one.

Kurath (1957) has also calculated radiative transition probabilities in the 1p shell. He found that reasonable agreement with experiment was achieved only when the radiation was pure M1 while in the case of E2 transitions the predicted values were too low. This appears to be an indication that collective motions take place even in the 1p shell, giving rise to enhanced E2 transitions. Wilkinson (1958), in a survey of the meagre data on well established E2 transitions in light nuclei, has concluded that they are often enhanced, with values of $|M|^2$ distributed about 2 with a spread of a factor 5 in either direction. The calculated widths only seem to agree well when they concern the lower excited states, such as the 4·46 MeV transition to the ground state. To fit the theoretical angular distribution for the main cascade from the 9·28 MeV and 9·19 MeV levels the same proportion ($\sim 5\%$) of E2 radiation relative to M1 radiation is required for the 4·46 MeV gamma ray. This agrees with the measurement of Rasmussen *et al.* (1958) who found an E2 : M1 intensity ratio of $\leqslant 0{\cdot}2$; Kurath's prediction is here 5%–10%, in excellent agreement with our conclusions. The prediction of branching ratios from the upper states would be affected by the fact that the calculation neglects contributions from possible double excitation.

ACKNOWLEDGMENTS

We are indebted to Mr. D. D. Stewart for operating the H.T. set. One of us (C.M.P.J.) wishes to thank D.S.I.R. for a maintenance grant during the course of the work.

REFERENCES

BAIR, J. K., KINGTON, J. D., and WILLARD, H. B., 1955, *Phys. Rev.*, **100,** 21.
BENNETT, W. E., ROYS, P. A., and TOPPEL, B. J., 1951, *Phys. Rev.*, **82,** 20.
BILANIUK, O. M., and HENSEL, J. C., 1958, *Amer. phys. Soc.*, **3,** 188.
EVANS, N. T. S., and FRENCH, A. P., 1958, *Phys. Rev.*, **109,** 1272.
EVANS, N. T. S., and PARKINSON, W. C., 1954, *Proc. phys. Soc. Lond.* A, **67,** 684.
FERGUSON, A. J., GOVE, H. E., KUEHNER, J. A., LITHERLAND, A. E., ALMQVIST, E., and BROMLEY, D. A., 1958, *Phys. Rev. Letters*, **1,** 414.
HENSEL, J. C., and PARKINSON, W. C., 1958, *Phys. Rev.*, **110,** 128.
INGLIS, D. R., 1953, *Rev. mod. Phys.*, **25,** 390.
JAMES, D. B., JONES, G. A., and WILKINSON, D. H., 1956, *Phil. Mag.*, **1,** 949.
JONES, G. A., and WILKINSON, D. H., 1952, *Phys. Rev.*, **88,** 423.
KURATH, D., 1956, *Phys. Rev.*, **101,** 216 ; 1957, *Phys. Rev.*, **106,** 975.
METZGER, F. R., SWANN, C. P., and RASMUSSEN, W. K., 1958, *Phys. Rev.*, **110,** 906.
MEYER-SCHÜTZMEISTER, L., and HANNA, S. S., 1958, *Bull. Amer. phys. Soc.*, **3,** 188.
RASMUSSEN, W. K., METZGER, F. R., and SWANN, C. P., 1958, *Phys. Rev.*, **110,** 154.
THIRION, J., 1953, *Ann. Phys.*, **8,** 489.
VAN PATTER, D. M., BUECHNER, W. W., and SPERDUTO, A., 1951, *Phys. Rev.*, **82,** 248.
WILKINSON, D. H., 1956, *Phil. Mag.*, **1,** 127 ; 1957, *Phys. Rev.*, **105,** 666 ; 1958, *Proceedings of the Rehovoth Conference on Nuclear Structure* (North-Holland Publishing Company).

Lattice Spacing Relationships in Magnesium Solid Solutions†

By D. HARDIE and R. N. PARKINS
Department of Metallurgy, University of Durham, King's College,
Newcastle upon Tyne, 1

[Received January 31, 1959]

ABSTRACT

Accurate measurements have been made of the lattice spacings in binary magnesium solid solutions containing aluminium, bismuth, cadmium, indium, lead, lithium, silver, tin and zinc. The results show that the lattice distortion accompanying the introduction of a solute depends on the difference in size of the solute and solvent atoms, their relative electronegativity and, where the valency of the solute differs from that of magnesium, the electron : atom ratio in the solution. Where the solute is not divalent, variation of the number of electrons in the conduction band seems to be entirely associated with the c dimension of the lattice, in such a way that a regular increase in axial ratio takes place as the electron concentration increases. The manner in which this affects the accepted picture of the distribution of electrons in the Brillouin Zones of magnesium is discussed.

§ 1. INTRODUCTION

DURING an investigation into the correlation between solid solution hardening and lattice distortion (Hardie and Parkins 1957) it was necessary to determine the actual variations in lattice spacing which occurred in various magnesium alloys. Several interesting relationships were demonstrated by the subsequent results.

Previous examinations of lattice spacing variations produced in magnesium solid solutions by the addition of various solutes have been carried out by Hume-Rothery and Raynor (1938), Raynor (1940, 1942), Busk (1950), and Von Batchelder and Raeuchle (1957). In curves representing the relationship between lattice spacing and composition in solutions of metals having a higher valency than magnesium Raynor observed certain inflections which he attributed to the occurrence of Brillouin Zone overlap brought about by increasing electron concentration. Considerable doubt as to the validity of this assumption was aroused by Von Batchelder and Raeuchle who, despite their examination of a large number of alloys in the composition range concerned, observed no such inflection in the case of aluminium and only a slight one in the case of indium and therefore concluded that electron zone overlap does not necessarily lead to axial ratio anomalies. They also found that two distinct lines were obtained (each passing through the value for the pure solvent) when the unit cell volume was plotted against the concentration of magnesium solid solutions containing indium. Extrapolation of these lines to 100% solute gave two distinct apparent atomic sizes for indium when dissolved in magnesium. It was suggested that this, and the anomalies observed by Raynor, was due to short-range ordering in the alloys concerned.

---

† Communicated by the Authors.

By a statistical examination of his own and earlier lattice spacing measurements Busk reached the conclusion that there was a distinct relationship between electron concentration and axial ratio in the alloys, although the specific nature of this depended on whether the electron concentration, calculated from the 'relative effective valence' of the solute, was below, within or above the range 1·994 to 2·005. On this basis less than half the solutes he examined were ascribed their normal group valency.

The present paper presents results which disagree with those obtained by Raynor mainly with respect to the lack of evidence for inflections in the *c* parameter curves for tri, quadri, and pentavalent solutes and the distinct evidence to the contrary in the case of indium. The results for solution of aluminium and indium are in very close agreement with those of Von Batchelder and Raeuchle. Similar, but rather less complex, relationships between axial ratio and electron concentration, and change in *a* parameter and radius of the solute atom, were observed to those reported by Busk.

§ 2. EXPERIMENTAL PROCEDURE

The alloys used in the present investigation were those previously employed in the examination of solid solution hardening in magnesium. The solutes were Al (99·99%), Bi (99·9%), Cd (99·9%), In (99·96%), Pb (99·98%), Li (99·9%), Ag (99·99%), Sn (99·96%), and Zn (99·99%). The magnesium itself was 99·95% pure.

Lattice constants were determined from Debye–Scherrer photographs of −200 mesh filings removed from the alloys after homogenization in the lump form. The filings were annealed to remove strains introduced by filing and to achieve complete solid solution, and then subsequently quenched in a blast of cold nitrogen to retain solid solutions.

Elaborate precautions during the preparation of filings were found unnecessary but contamination of the filings during heat treatment was avoided by enclosing in small steel tubes and then sealing these in pyrex tubes containing argon. Except in the case of alloys containing lithium, no change in composition was found to occur as a result of this treatment†.

The x-ray specimens were prepared by rolling the sieved filings with gum tragacanth. Powder photographs were taken using Cr $K\alpha$ radiation

---

† The filings used by Raynor, on the other hand, were prepared, annealed and sieved in argon or *in vacuo* to ensure elimination of contamination, and were rapidly air-cooled after solution treatment.

Table 1. Lattice Parameters of Binary Magnesium Solid Solutions (all Values in Angstrom Units Corrected to 25°c)

Solute	Atomic %	*c*	*a*	*c/a*
Magnesium	—	5·2108	3·2099	1·6234
Aluminium	0·96	5·2061	3·2052	1·6243
	2·78	5·1958	3·1979	1·6247
	4·67	5·1851	3·1908	1·6250
	6·89	5·1739	3·1817	1·6262
Bismuth	0·13	5·2119	3·2097	1·6238
	0·34	5·2130	3·2105	1·6237
	0·54	5·2146	3·2106	1·6242
Cadmium	0·90	5·2082	3·2071	1·6239
	6·40	5·1883	3·1939	1·6244
	14·40	5·1617	3·1763	1·6250
	18·26	5·1405	3·1661	1·6236
Indium	0·92	5·2109	3·2088	1·6240
	3·01	5·2116	3·2064	1·6254
	5·56	5·2110	3·2040	1·6264
	7·23	5·2128	3·2003	1·6289
Lead	0·76	5·2145	3·2108	1·6241
	2·11	5·2200	3·2115	1·6254
	4·11	5·2297	3·2129	1·6277
	5·99	5·2409	3·2132	1·6311
Lithium	1·03	5·2073	3·2089	1·6228
	4·66	5·2011	3·2071	1·6218
	9·93	5·1759	3·2008	1·6171
	14·03	5·1702	3·1994	1·6160
Silver	0·78	5·2021	3·2048	1·6232
	1·62	5·1928	3·2008	1·6223
	2·55	5·1806	3·1945	1·6217
Tin	0·89	5·2121	3·2092	1·6241
	1·89	5·2135	3·2075	1·6255
	2·58	5·2149	3·2068	1·6262
Zinc	1·03	5·2029	3·2049	1·6234
	2·00	5·1947	3·2006	1·6231
	2·81	5·1882	3·1957	1·6235

($\alpha_1 = 2{\cdot}28962$ Å; $\alpha_2 = 2{\cdot}29351$ Å) and a 9 cm Unicam camera. With exposure times of the order of 15 min this gave films of a higher quality than those obtained with Cu $K\alpha$ radiation. The temperature during exposure was measured by a thermometer placed beneath the camera and all calculated spacings were corrected to a standard temperature of 25°C on the assumption that the effect of difference in coefficients of expansion between the alloys and pure magnesium would be negligible for the temperature ranges involved.

Fig. 1

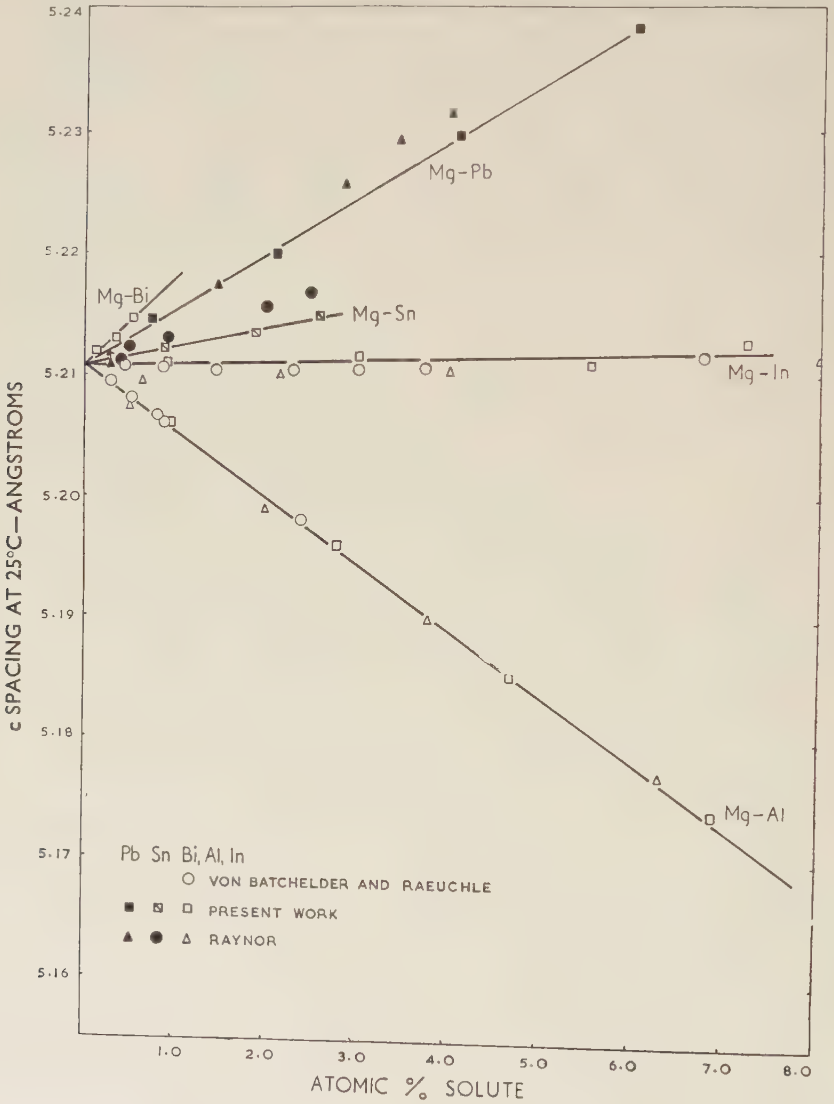

c spacings in magnesium solid solutions containing metals with higher valency than magnesium.

Chromium radiation produced a combination of lines in the diffraction pattern which was eminently suitable for the extrapolation technique involved. The five high angle lines, (10·4), (20·2), (00·4), (20·1) and (11·2), were measured on an accurate travelling microscope reading to 0·01 mm and lattice parameters calculated after correction for film shrinkage. The calculation was based upon the high sensitivity of the (10·4) reflection to variation in the c parameter and the invariance of the (00·4) reflection due to the fact that $h=k=0$. A graphical method of successive approximations using the extrapolation function of Nelson and Riley (1945) to correct for systematic errors was used. The value of a/c for a particular film could thus be established to ± 0·00005 Å, the values of c to ± 0·0002 Å, and the value of a therefore to ± 0·0003 Å.

§ 3. Results

The lattice parameters obtained for pure magnesium at 25°C were 3·2099 Å, $c=5{\cdot}2108$ Å and $c/a=1{\cdot}6234$, which are in good agreement with the values reported by Von Batchelder and Raeuchle for magnesium ($a=3{\cdot}2095_6$ Å, $c=5{\cdot}2107_1$ Å, $c/a=1{\cdot}6235_0$ Å).

When the values for the a and c spacings observed in the present work are plotted against the alloy composition a series of straight lines is obtained from which no point deviates by more than 0·0005 Å, although the majority of results are well within this limit. In general the slope of the lines obtained also shows negligible deviation from those observed by Raynor (1940, 1942). The lattice parameters are given in table 1.

In fig. 1 the spacings in alloys containing solutes of higher valency than magnesium are compared with similar results obtained by Raynor, and Von Batchelder and Raeuchle.

§ 4. Discussion

The lattice spacing-composition curves for magnesium containing tri, quadri, and pentavalent solutes show a notable lack of evidence for the inflections observed by Raynor and attributed to the occurrence of electron overlap at the faces of the first Brillouin Zone in a direction perpendicular to the c axis. In the case of solutions containing indium the difference between the present results and Raynor's is particularly marked. Whereas Raynor observed a contraction along the c direction with small additions followed by an expansion with larger additions, the present results agree very closely with those of Von Batchelder and Raeuchle, which indicate that a continuous slight increase in c spacing occurs with all indium additions. Similar close agreement with the latter workers, and absence of inflections is also observed for solutions containing Al, Bi, Pb and Sn. The anticipated Brillouin Zone overlap does not therefore seem to give rise to the anomalies in the lattice spacings of the solid solutions observed by Raynor, whose results could possibly be attributed to changes in short-range order.

The occurrence of inflections in the c spacing curves is also responsible for the discontinuous relationship between axial ratio and electron concentration suggested by Busk. On such a relationship also was based the theoretical treatment of the subject by Jones (1950). However, the results of the present work reveal a continuous linear relationship between the axial ratios and the electron : atom ratios in the solutions (fig. 2). With a few minor exceptions the relationship can be represented by

$$c/a = 1{\cdot}50319 + 0{\cdot}060085E$$

where E is the electron concentration based on the normal group valencies associated with the solutes concerned. Almost all the axial ratios are within ± 0·0017 of this line. Improved agreement is however obtained for alloys containing aluminium if a valency of 2·7 electrons per atom is assumed for the solute. In contrast Busk had to assume unusual valencies for Ag (0·66), Al (2·49), Bi (3·50), Li (0·84), Pb (3·55) and Sn (3·50).

Fig. 2

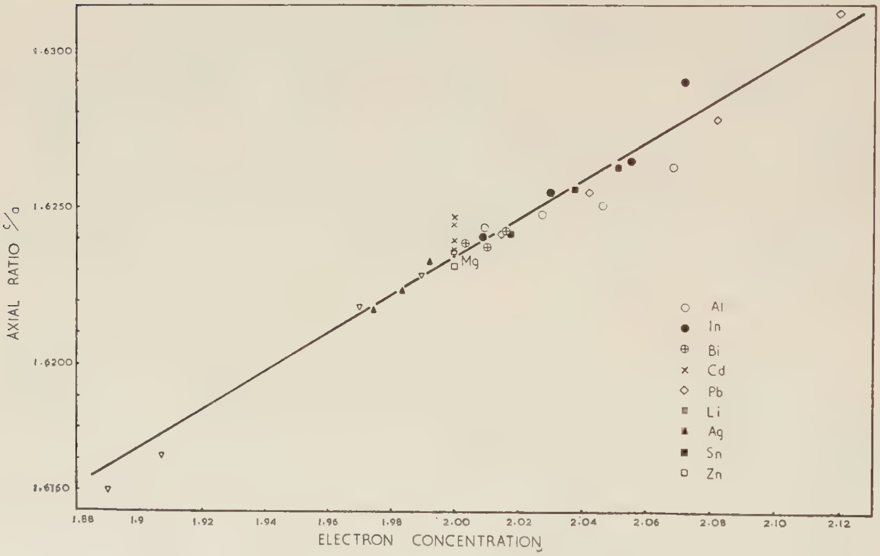

Variation of axial ratio with electron concentration in magnesium solid solutions.

On the assumption that any shearing strain resulting from the introduction of solute elements into the magnesium lattice is due to the effect of the Brillouin Zone structure on the valence electrons of the metal, and is therefore largely dependent on the electron–atom ratio, Jones used his earlier Brillouin Zone theory (1934) to derive a simple model to fit Raynor's experimental results and obtained a theoretical relationship between axial ratio and electron concentration. However, the occurrence of electron overlap at about 2·005 electrons per atom necessitated a discontinuous relationship such that the shearing strain at constant volume $(S-S_0/S_0)_v$ is given by

$$\begin{aligned}(S-S_0/S_0)_v &= -0{\cdot}213n^2+0{\cdot}150(n-0{\cdot}005)^{3/2} && \text{for} \quad n>0{\cdot}005\\ &= -0{\cdot}213n^2 && \text{for} \quad n<0{\cdot}005\end{aligned}$$

where $n=E-2$.

When he compared this calculated curve with the experimental results he found reasonable agreement in the region where $n>0{\cdot}005$, where the relation is substantially linear. However, in the region where n is negative and the relation is parabolic the experimental points indicated some deviation. In actual fact they showed the tendency, so clearly demonstrated in the present work where the variation of axial ratio may be taken as a measurement of shearing strain (fig. 2), to follow a linear relationship for all values of n. An alternative theoretical treatment of the effect of 'electron stress' on the axial ratio in a hexagonal lattice by McClure (1955) provides the same qualitative interpretation of the effects of alloying as the Jones model.

Fig. 3

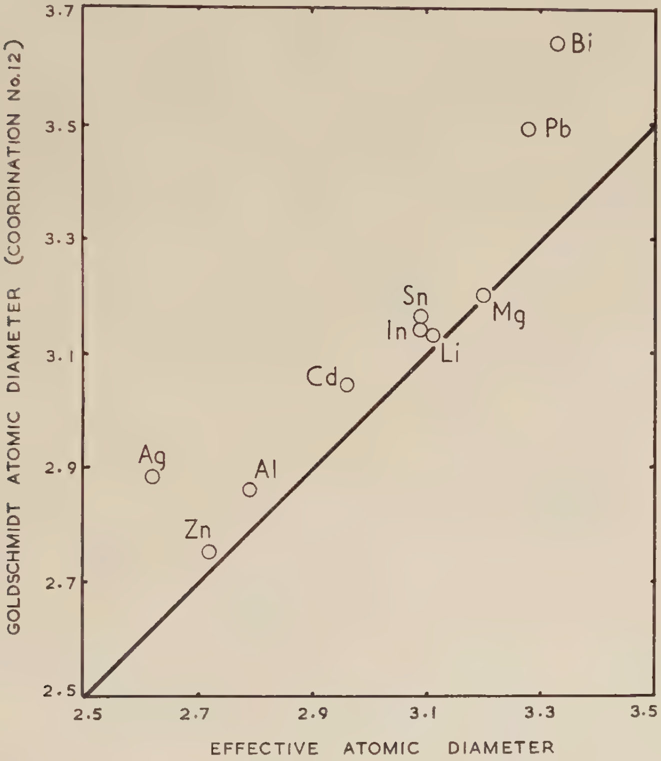

Graph showing deviation from Vegard's law.

Quite apart from electron concentration effects the lattice of magnesium is distorted by solute elements as a result of a 'size effect' and a 'shrinking effect'. The spacing of atoms in the basal plane is dependent on these effects alone whilst the electron concentration affects the axial ratio. As shown in fig. 3 the 'effective atomic diameter' of any solute element in magnesium approximates within 10% to the Goldschmidt Atomic Diameter (Coordination Number 12) representing the size of the atom in the elemental crystal. The deviations which do in fact occur are all such that the solute atom occupies a smaller volume in the magnesium lattice than it does in its own lattice. In other words there is a greater attraction between a solvent and a solute atom than between two like atoms, and the mean interatomic distance is thus decreased. Such a tendency is also revealed in the contraction which occurs with ordering in alloys of magnesium with cadmium, silver, etc. The contraction appears to be closely related to the relative electronegativities of the solute and solvent (except in the case of Sn), see fig. 4 (the electronegativity values used are those quoted by Laves (1956)). The scatter of the points in this figure is no doubt due in part to the lack of precise values for electronegativities. The a spacing of an alloy is nevertheless given fairly precisely by

Fig. 4

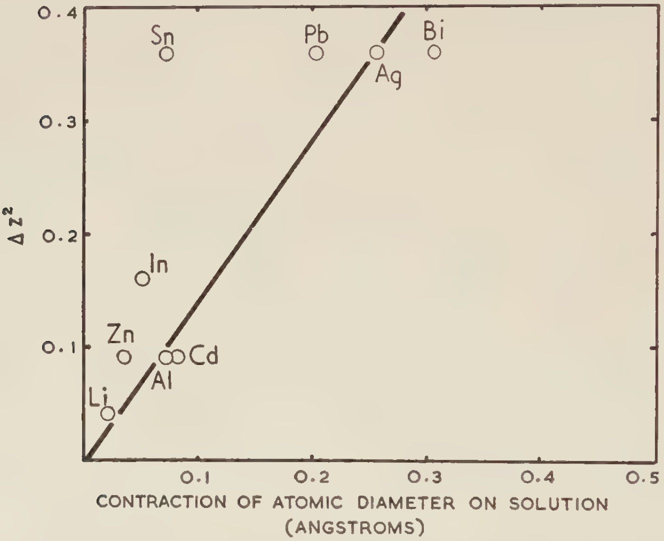

Relationship between the contraction of an atom on solution and its difference in electronegativity from the solvent.

$$a_x = a_{\mathrm{Mg}} + x(D_x - D_{\mathrm{Mg}} - 0{\cdot}693\Delta Z^2)$$

where x is the atomic concentration of the solute, D_x and D_{Mg} are the Goldschmidt Atomic diameters of the solute and solvent respectively, and ΔZ is the difference in electronegativity between solute and solvent.

The fact that the a spacing of the solid solution lattice depends solely on size effects, completely independent of the solute valency, whereas the

Fig. 5

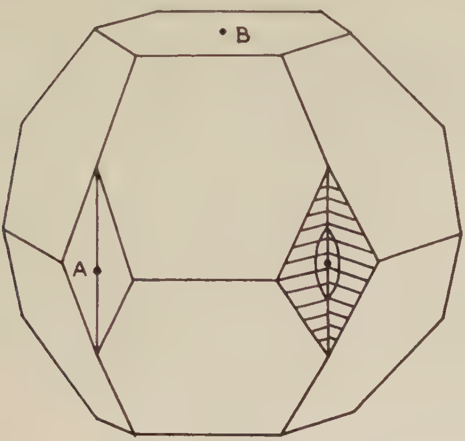

Brillouin Zone for magnesium (after Jones).

Table 2. Rates of Change of Lattice Parameters with Composition, and Effective Atomic Diameters of Solutes Derived Therefrom

Solute	Rate of change of lattice parameter. Angstroms × 10^{-4} per at. %		Effective atomic diameter	Goldschmidt atomic diameter (C.N. = 12)
	a	c		
Magnesium	—	—	3·20	3·20
Aluminium	−41·1	−54·0	2·79	2·86
Bismuth	+13·0	+69·1	3·33	3·64
Cadmium	−23·8	−34·9	2·96	3·042
Indium	−10·9	+1·9	3·09	3·14
Lead	+8·3	+47·6	3·28	3·49
Lithium	−9·2	−35·7	3·11	3·13
Silver	−57·5	−116·4	2·62	2·883
Tin	−10·9	+15·2	3·09	3·164
Zinc	−48·1	−80·6	2·72	2·748

axial ratio is decided by the electron concentration, indicates that electrons added or subtracted from the lattice are associated with the interplanar bonds rather than those in the basal planes. The application of Brillouin Zone theory to alloy structures inevitably involves certain simplifying assumptions and, since it neglects local disturbance of the lattice around solutes, electron–electron interaction, and also the bond electrons, must always be rather tentative. Knowledge of the exact form of the Fermi surface at increasing values of energy within zones of different structures is lacking. The quantitative prediction of electron : atom ratios at which overlap in different directions of a Brillouin Zone occurs is therefore impossible unless the Fermi surface is assumed to retain its spherical shape as the electron concentration increases. The dependence of axial ratio on electron concentration in the range 1·9 to 2·1 for magnesium solid solutions shown in fig. 2 could be an indication of zone overlap across the B faces of the zone structure proposed by Jones (1934) just as the decrease in c/a ratio with increasing electron concentration in close-packed hexagonal Cu–Ga–Ge alloys, and close-packed hexagonal ζ phases in binary alloys based on Cu and Ag, is interpreted by Raynor and Massalski (1955) as evidence of overlap of electrons from the appropriate Brillouin Zone in directions at right angles to the hexagonal axis. In a similar way the increase of axial ratio c/a with increasing electron concentration in face-centred tetragonal indium-rich solid solutions is attributed by Tyzack and Raynor (1954) to overlap of electrons across the {002} faces of the first Brillouin Zone. According to the Jones hypothesis overlapping of electrons across the face of a Brillouin Zone results in its displacement towards the origin of k space, which corresponds with an expansion of the lattice in the corresponding direction (the c axis) in real space.

Extensive studies of the electronic properties of magnesium alloys (Salkovitz *et al.* 1957 a, b) have however provided alternative evidence for the occurrence of Brillouin Zone overlap in dilute alloys containing In and Al which do not occur in pure magnesium. The curves representing variation of Hall constant, the thermal coefficient of resistivity and the thermoelectric power with concentration all exhibit discontinuities at electron concentrations between 2·010 and 2·013. Interaction between the Fermi surface and the Brillouin Zone faces on close approach has been proposed by Goodenough (1953) and Schubert (1952) to give distortion of the Brillouin Zone in k space similar to that produced by overlap. If, however, the axial ratio variations at electron concentrations below 2·010 were attributed to these effects a discontinuity in the relationship would still be expected when overlap occurred since its effects are of much greater magnitude (Massalski 1958). On the other hand, a linear relationship still can be consistent with Jones' theory if the shearing strain is considered as resulting from alteration in the balance between the oppositely directed stresses which arise from the 'holes' in the first zone and the electrons overlapping into the second zone (Jones 1959, private communication).

ACKNOWLEDGMENTS

The authors wish to express their thanks to Magnesium Elektron Limited for the supply of high-purity magnesium and assistance with the chemical analysis of the alloys, to the Department of Scientific and Industrial Research for financial aid, to their colleagues for helpful discussion, and to the late Professor A. Preece for facilities provided for the research.

REFERENCES

BUSK, R. S., 1950, *Trans. Amer. Inst. min. (metall.) Engrs.*, **188,** 1460.
GOODENOUGH, J. B., 1953, *Phys. Rev.*, **89,** 282.
HARDIE, D., and PARKINS, R. N., 1957, *J. Inst. Met.*, **85,** 449.
HUME-ROTHERY, W., and RAYNOR, G. V., 1938, *J. Inst. Met.*, **63,** 227.
JONES, H., 1934, *Proc. roy. Soc.* A, **147,** 396 ; 1950, *Phil. Mag.*, **41,** 663.
LAVES, F., 1956, *Theory of Alloy Phases* (Cleveland, Ohio : American Society for Metals), p. 124.
MASSALSKI, T. B., 1958, *Met. Rev.*, **3,** 45.
MCCLURE, J. W., 1955, *Phys. Rev.*, **98,** 449.
NELSON, J. B., and RILEY, D. P., 1945, *Proc. phys. Soc. Lond.*, **48,** 297.
RAYNOR, G. V., 1940, *Proc. roy. Soc.* A, **174,** 457 ; 1942, *Ibid.*, **180,** 107.
RAYNOR, G. V., and MASSALSKI, T. B., 1955, *Acta Met.*, **3,** 480.
SALKOVITZ, E. I., SCHINDLER, A. I., and KAMMER, E. W., 1957 a, *Phys. Rev.*, **105,** 887 ; 1957 b, *Ibid.*, **107,** 1549.
SCHUBERT, K., 1952, *Z. Metallk.*, **43,** 1.
TYZACK, C., and RAYNOR, G. V., 1954, *Trans. Faraday Soc.*, **50,** 675.
VON BATCHELDER, F. W., and RAEUCHLE, R. F., 1957, *Phys. Rev.*, **105,** 59.

Brillouin Zones and Crystal Structure Factors†

By T. H. K. Barron
Department of Physical and Inorganic Chemistry, University of Bristol
and Gaston Fischer
Division of Pure Physics, National Research Council of Canada, Ottawa

[Received April 10, 1959]

Abstract

Brillouin zones in reciprocal space are most logically defined by Brillouin's original method, solely in terms of the Full Bravais Lattice giving the full translational symmetry of the crystal. Another method, which rejects zone boundaries of vanishing structure-factor, is illogical, both because it is possible to have an energy discontinuity of electron states across a plane of zero structure-factor, and because it ignores the energy continuity within Brillouin's original zones. The energy is always continuous within the true Brillouin zones, which must contain two electron states for each unit cell of the Full Bravais Lattice.

During an enquiry carried out at the National Research Laboratories on the properties of compounds crystallizing in the nickel–arsenide structure (Pearson 1957, Fischer and Pearson 1958), it was brought to our attention that there are two different methods of determining the Brillouin zone-structure in reciprocal space (Kittel 1956, Reitz 1955), and that these do not always lead to the same zone-structure.

The original definition of Brillouin (1930, 1931, 1953) depends only upon the basic Bravais lattice of the crystal structure. Care must be taken to ensure that we have the Bravais lattice describing the full translational symmetry of the crystal, and not some lattice of larger unit cell: we shall call this lattice the ' Full Bravais Lattice ' of the crystal. Once the Full Bravais Lattice has been identified, the reciprocal lattice and Brillouin zone-structure are determined uniquely, and are independent of the detailed configuration of atoms within the unit cell and of all considerations of structure-factor. Zones thus obtained have the following properties:

(i) they contain two electron states for each unit Full Bravais cell in the crystal;

(ii) the energy is continuous throughout each zone (the continuity between different regions comes about because the energy is equal along boundaries of the same zone separated by a reciprocal lattice vector);

---

† Communicated by the Authors.

(iii) the pieces of each higher zone can be reduced into the first zone by shifting the separate regions by appropriate reciprocal lattice vectors, and the states of each zone then form a continuous energy band over the first zone;

(iv) cells of the shape of the first Brillouin zone can be fitted together to fill completely reciprocal space, leaving no gaps between neighbouring cells (the first zone is thus a 'repeating unit' of the reciprocal lattice).

This original method has been consistently followed in papers by Hund (1936), Bouckaert *et al.* (1936), Herring (1937, 1942), Herring and Hill (1940), Herman (1955, 1958) and others.

The other method of obtaining Brillouin zones accepts as true zone boundaries only those planes which have a non-vanishing structure-factor associated with the corresponding Bragg reflection. This has the advantage that we do not then have to identify the Full Bravais Lattice, since if we choose a Bravais lattice of coarser mesh the structure-factor vanishes for all the false zone boundaries thus introduced; for example, the method as used in Wilson (1953) for the face-centred and body-centred cubic lattices gives zones identical to Brillouin's. But while such false zone boundaries have zero structure-factors because of the translational symmetry of the crystal, other planes may have zero structure-factors because of screw axes, glide planes and other special atomic arrangements; if this is so we are then led to discard planes which are true Brillouin zone boundaries.

The idea of demanding that a zone boundary should have a non-vanishing structure-factor is suggested by the simple correspondence between x-ray reflections from a crystal and Brillouin zone boundaries in the reciprocal lattice. It has at times been implied that there is an exact equivalence between the strength of an x-ray reflection and the energy discontinuity between electron states on either side of the corresponding zone boundary; in particular, a vanishing structure-factor for the reflection has been taken to indicate that there is no discontinuity across the boundary. This in turn led to the rejection of such boundaries as true zone boundaries, and hence to a definition of zones different from Brillouin's (Jones 1934 b). This definition (which may give zones which do not possess the properties we have just outlined for Brillouin's zones) has appeared regularly in well-known treatises and textbooks for many years (e.g. Mott and Jones 1936, Wilson 1953†, Hume-Rothery and Raynor 1954, Kittel 1956), and has been used in attempts to interpret experimental results (e.g. Jones 1934 b, Makarov 1943). It is our purpose here to point out: (*a*) that a vanishing structure-factor does not necessarily indicate that there is no energy discontinuity, and (*b*) that even where there is no discontinuity of energy across a zone boundary, modification of Brillouin's definition is not justified.

(*a*) The structure-factor can be only a rough guide to the energy discontinuity, since the structure-factor is a single constant while the energy discontinuity varies over the zone boundary (see, for example, the detailed calculations of Herman and others (Herman 1955, 1958) on the electronic structure of germanium and silicon). In fact the structure-factor is a measure of only the first-order term obtained when the crystal field is treated as a perturbation on the free electron wave functions (Jones 1934 a); and while first-order perturbation theory is adequate for x-rays with their relatively high energy, it is totally inadequate and qualitatively misleading for valence or conduction electrons in a solid. In particular, the energy discontinuity across a plane of zero structure-factor will not vanish unless all the higher order terms are zero; this will not happen if one can express the reciprocal lattice vector bisected perpendicularly by the plane as the sum of other reciprocal lattice vectors with non-vanishing structure-factors. This point is clearly stated by Chambers (1956) in a discussion of the energy discontinuities in tin.

---

† Wilson's treatment is criticized in a review in the *Philosophical Magazine* (1954, **45**, 108), but not in detail.

A particular example which has been the source of much confusion in the past is that of the hexagonal close-packed structure, whose first Brillouin zone is a hexagonal ' pill-box ' (shown for example in Kittel 1956, p. 316). The hexagonal top and bottom faces have zero structure-factor; but Dr. Heine has informed us that from space group considerations (Herring 1942, Koster 1957) one can deduce that the energy gap need be zero *only* along the edges and along lines joining opposite corners, and *not* necessarily over the rest of these faces.

(*b*) Whether or not there is discontinuity of energy across all zone boundaries there is certainly continuity of energy within each of Brillouin's zones. This can be seen particularly clearly from the reduced zone scheme, in which the states of each zone in the extended scheme now form a continuous band within the first zone. If the discontinuity vanishes across certain zone boundaries in the extended scheme, then corresponding energy bands in the reduced scheme will indeed meet each other; but this does not destroy the continuity within each band. It therefore seems quite illogical to ascribe parts of the same band to different zones.

Let us suppose, for example, that the structure-factor criterion rejects some of the zone boundaries between the first and second of Brillouin's zones, but none of those between the second and third. Adoption of the criterion results in a new zone-structure in which the new first zone contains part of Brillouin's second zone. This has at least two serious disadvantages:

(i) different parts of Brillouin's second zone are assigned in the new scheme to different zones, although the electron-states form a continuous band throughout the original zone; and

(ii) the new first zone is not a repeating unit of the reciprocal lattice, and is therefore not suitable as a basis for a reduced zone scheme.

By retaining Brillouin's definition we ensure that we have consistent reduced and extended zone schemes, with energy continuity throughout each zone. We have merely to remember that if the structure-factor corresponding to a zone boundary vanishes, the energy discontinuity across that boundary will probably be small and may even vanish; 'Umklapp' processes associated with this boundary will therefore be correspondingly unlikely and may not occur at all.

ACKNOWLEDGMENTS

We should like to thank Drs. R. G. Chambers, M. Bailyn, J. S. Dugdale and A. V. Gold for helpful discussions, and Dr. V. Heine for his many valuable comments.

REFERENCES

BOUCKAERT, L. P., SMOLUCHOWSKI, R., and WIGNER, E., 1936, *Phys. Rev.*, **50,** 58.
BRILLOUIN, L., 1930, *J. Phys. Radium*, **1,** 377; 1931, *Quantenstatistik* (Berlin: Springer); 1953, *Wave propagation in periodic structures*, 2nd Edition (New York: Dover).
CHAMBERS, R. G., 1956, *Canad. J. Phys.*, **34,** 1405.
FISCHER, G., and PEARSON, W. B., 1958, *Canad. J. Phys.*, **36,** 1010.
HERMAN, F., 1955, *Proc. Inst. Radio Engrs*, **43,** 1703; 1958, *Rev. mod. Phys.*, **30,** 102.
HERRING, C., 1937, *Phys. Rev.*, **52,** 361; 1942, *J. Franklin Inst.*, **233,** 525.
HERRING, C., and HILL, A. G., 1940, *Phys. Rev.*, **58,** 132.
HUME-ROTHERY, W., and RAYNOR, G. V., 1954, *The structures of metals and alloys* (London: Institute of Metals).
HUND, F., 1936, *Z. Phys.*, **99,** 119.
JONES, H., 1934 a, *Proc. roy. Soc.* A, **144,** 225; 1934 b, *Ibid.*, **147,** 396.
KITTEL, C., 1956, *Introduction to solid state physics*, 2nd Edition (New York: Wiley).
KOSTER, G. F., 1957, *Solid State Physics*, **5,** 235 (New York: Academic Press).
MAKAROV, E. S., 1943, *Akad. Nauk. Dokl.*, **40,** 191.
MOTT, N. F., and JONES, H., 1936, *The theory of the properties of metals and alloys* (Oxford: University Press).
PEARSON, W. B., 1957, *Canad. J. Phys.*, **35,** 886.
REITZ, J. R., 1955, *Solid State Physics*, **1,** 1 (New York: Academic Press).
WILSON, A. H., 1953, *The theory of metals*, 2nd Edition (Cambridge: University Press).

Time-dependent Spectra of Electroluminescent ZnS:Cu, Pb†

By J. Weiszburg, J. Schanda and Z. Bodó
Industrial Research Institute for Telecommunication Technique and
Institute for Technical Physics of the Hungarian Academy of Sciences, Budapest

[Received February 3, 1959]

The electroluminescent emission spectrum of the green ZnS:Cu, Pb phosphors prepared by the well-known method (Homer *et al.* 1953) consists, as is already known, of two bands with peaks at 5200 and 4700 Å (Destriau 1947, Waymouth 1953). Though the spectra published up to now, with one exception (Loebner 1953) give the results without time resolution, it has become a generally accepted assumption, based on investigations of different types (Burns 1953, Destriau 1953, Destriau and Ivey 1955, Henderson 1958, Jerome and Gungle 1953, Matossi 1957, Waymouth and Bitter 1953), that the single bands, which can be identified with the photoluminescent bands (Bowers and Melamed 1955) are not emitted simultaneously. Loebner measured the time–brightness wavelength correlation of the emission directly with an AO scanning spectrograph. Plotting the data on a three-dimensional surface the 'brightness time' cuts showed sharp asymmetrical peaks and shallow minima, like the well-known brightness waves of the total light.

A relative phase shift with the wavelength became apparent. The cuts parallel with the 'brightness wavelength' plane give the time spectrum in question. This spectrum can be separated into a 'constant' and time-dependent component. Loebner thought that the fine structure consisting of ten bands in the spectrum range of 4000–5800 Å must have been caused by the Stark effect of the strong electric field. Zalm *et al.* (1954) mention that according to Loebner the radiation of the secondary maximum of the brightness wave as compared with the primary maximum is shifted towards the longer wavelength.

For a more detailed knowledge of the mechanism it seems to be essential to understand also the field-dependence of this phenomenon. The investigation of the frequency and field dependence of the electroluminescent brightness wavelength versus time relations with the methods generally adopted seems to be rather difficult, especially at small frequencies and field strengths, because of the small brightness. This made it necessary to work out a new measuring method. The method makes use of the stroboscopic effect already described by Destriau (1947) and later used by Zalm *et al.* (1954). The stroboscopic picture was projected on the entrance slit of a spectrograph in such a way, that the light emitted

---

† Communicated by the Authors.

Fig. 1

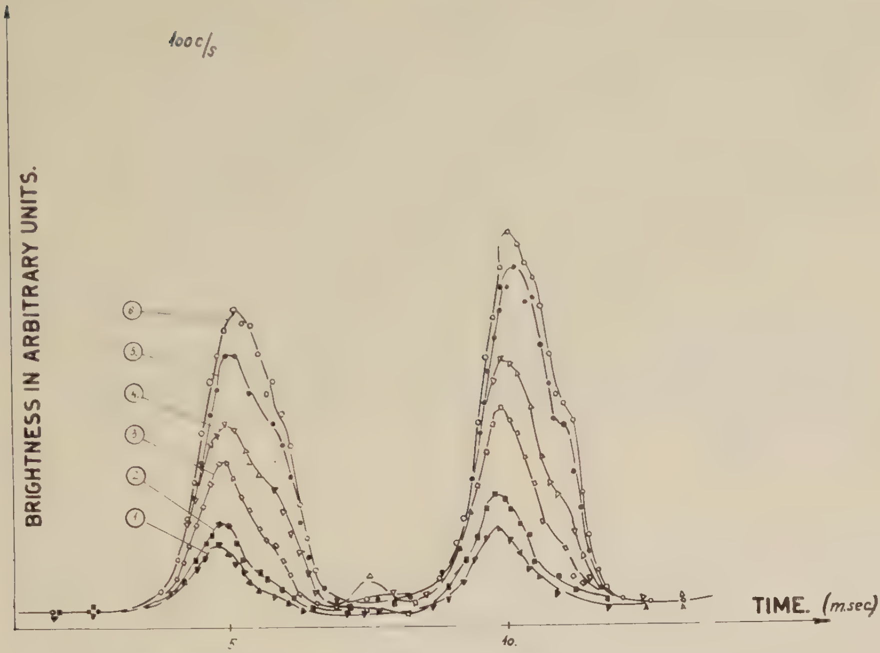

Time-dependence of an electroluminescent spectrum at 100 c/s. The wavelengths of the ' brightness-time ' sections visible above are as follows:

1 = 4450 A.U., 2 = 4550 A.U., 3 = 4740 A.U.,
4 = 4920 A.U., 5 = 5250 A.U., 6 = 5330 A.U.

Fig. 2

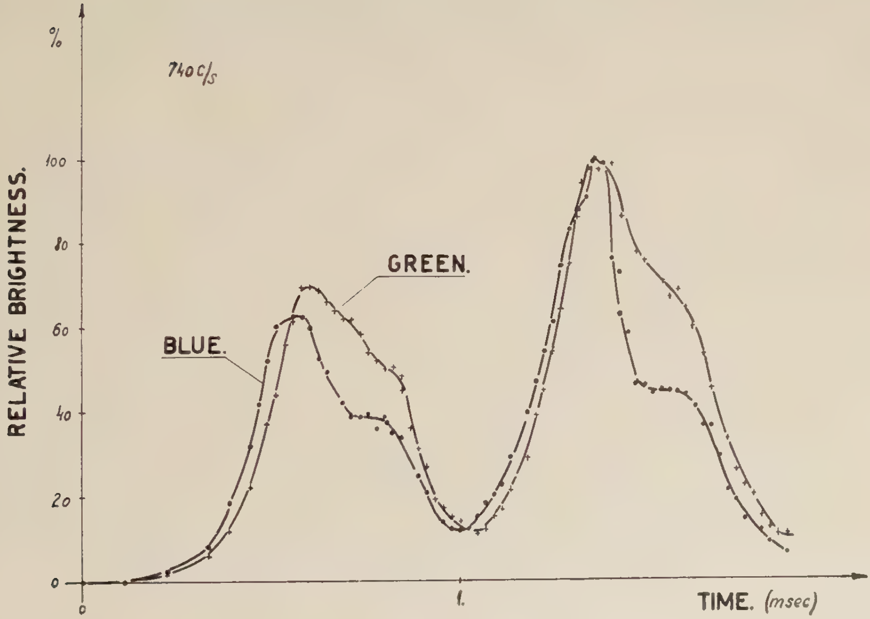

Time-dependence of spectra of the respective bands at 740 c/s.

at different instants from various picture elements, should be projected to different heights of the entrance slit. Evaluating the densities obtained on the photographic plate we obtain the proper time–brightness wavelength relations.

A graph taken with this method is presented in fig. 1. The curves of the phosphor emitting green light taken at 100 c/s show good agreement with Loebner's results. Only a slight phase shift between the bands is apparent, hardly to be observed at 100 c/s and at 740 c/s it does not exceed 3% of the period-time measured at the brightness peaks (fig. 2). At 740 c/s the light of the cell apparently becomes bluish. We could not observe the fine-structure in the spectrum formerly found by Loebner. The cause of this was probably the relatively small field strength used in our measurements. The difference between the decay time of the blue and green band is evident from fig. 2. Similar measurements are at present in progress, so a detailed discussion will be given when abundant data are available.

REFERENCES

BOWERS, R., and MELAMED, N. T., 1955, *Phys. Rev.*, **99,** 1781.

BURNS, L., 1953, *J. electrochem. Soc.*, **100,** 572.

DESTRIAU, G., 1947, *Phil. Mag.*, **38,** 700; 1953, *J. Phys. Radium*, **15,** 13.

DESTRIAU, G., and IVEY, H. F., 1955, *Proc. Inst. Radio Engrs, N.Y.*, **43,** 1911.

HENDERSON, S. T., 1958, *Brit. J. appl. Phys.*, **9,** 45.

HOMER, H. H., RULON, R. M., and BUTLER, K. H., 1953, *J. electrochem. Soc.*, **100,** 566.

JEROME, C. W., and GUNGLE, W. C., 1953, *J. electrochem. Soc.*, **100,** 34.

LOEBNER, E. E., 1953, *Phys. Rev.*, **92,** 846.

MATOSSI, F., 1957, *Elektrolumineszenz und Elektrophotolumineszenz* (Braunschweig: Verlag Friedrich Vieweg & Sohn), p. 42.

WAYMOUTH, J. F., 1953, *J. electrochem. Soc.*, **100,** 81.

WAYMOUTH, J. F., and BITTER, F., 1953, Paper presented at the Spring Meeting of the Electrochemical Society, *Enlarged Abstracts*, p. 50.

ZALM, P., DIEMER, G., and KLASENS, H. A., 1954, *Philips res. Rep.*, **9,** 81.

The Specific Heat of Cerium Magnesium Nitrate below 10°K†

By C. A. Bailey
The Clarendon Laboratory, Oxford

[Received March 24, 1959]

Abstract

The specific heat of cerium magnesium nitrate has been measured in the range 1·5°K to 10°K where the magnetic specific heat is negligible compared with the lattice specific heat. It was found that above 3°K the lattice specific heat cannot be represented by a single Debye term but below this temperature it is given by

$$C_L = 1{\cdot}13 \times 10^{-3}\, RT^3.$$

Cerium magnesium nitrate is widely used in obtaining temperatures below 1°K by the method of adiabatic demagnetization and in measuring these temperatures. The magnetic specific heat, which is extremely small, has been measured by Cooke *et al.* (1953) in the helium range and is given by $C_I = 7{\cdot}5 \times 10^{-6} R/T^2$. Daniels and Robinson (1953) showed that the susceptibility obeys Curie's law to within an accuracy of 2% down to a temperature of six millidegrees. This combination of properties makes it an ideal substance for a magnetic thermometer. The smallness of the magnetic specific heat also implies that the salt can readily be cooled to very low temperatures using only moderate fields. The maximum in the magnetic specific heat occurs at a temperature of about three millidegrees and is extremely pronounced. Thus most of the anomalous entropy is contained in a small temperature interval and if sufficiently large demagnetization fields have been applied a nearly constant temperature of three millidegrees can be maintained for some time. Therefore it is also a very good coolant.

The majority of salts used for demagnetization experiments have a lattice specific heat which is negligible compared with the magnetic specific heat at 1°K. In the case of cerium magnesium nitrate with its extremely small magnetic specific heat this is not so. Observations by Cooke *et al.* (1953) on the rate of warming up of specimens cooled below 1°K indicated that the magnetic specific heat only becomes comparable with the lattice specific heat at about 0·5°K. For a complete understanding of the properties of the salt around 1°K a knowledge of the lattice specific heat is therefore required. This can best be obtained by extrapolation from measurements made in the liquid helium range where the magnetic specific heat is negligible compared with the lattice specific heat.

---

† Communicated by the Author.

Cerium magnesium nitrate is one of the isomorphous series of rare earth double nitrates which have the formula $A_2B_3(NO_3)_{12} . 24 H_2O$ where A is the trivalent rare earth ion and B is a divalent metal. The salt is very soluble in water from which it crystallizes readily in thick plates of trigonal symmetry. The crystals were prepared by mixing solutions of cerium nitrate and magnesium nitrate in the correct proportions and then seeding the resultant saturated solution and allowing the crystals to grow slowly at a constant temperature. It is extremely difficult to prevent the inclusion of water in the crystals and therefore density measurements were carried out to select the best crystals. The density was measured by weighing the crystals in air, benzene and carbon tetrachloride and crystals with the maximum density of 2·02 g per cm^3 were selected from those available. The only density measurement available is that due to Jantzsch (1912) who gives a value of 2·002 g per cm^3.

Measurements of the specific heat of these cerium magnesium nitrate crystals were carried out in the temperature range 1·5°K to 10°K. The apparatus used and the experimental procedure have been described by Smith and Wolcott (1956). A small amount of helium gas was introduced into the calorimeter to ensure good thermal contact between the crystals and the calorimeter. In the liquid helium range the phosphor-bronze wire was replaced by a 47 ohm L.A.B. radio resistor as resistance thermometer but constantan wire was used above these temperatures.

The experimental specific heat values are given in table 1 and smoothed specific heat values in half degree intervals up to 4°K then in one degree intervals up to 10°K are given in table 2. Above 3°K the lattice specific heat cannot be represented by a single Debye term but below this temperature it was found to be given by

$$C_L = 1{\cdot}13 \times 10^{-3} RT^3.$$

The figure shows both the lattice specific heat and the magnetic specific heat below 1°K. It will be seen that the two are of equal magnitude at a

Table 1

°K	C_p/R	°K	C_p/R	°K	C_p/R
1·640	0·00503	3·452	0·0502	7·12	0·722
1·884	0·00773	3·680	0·0646	7·52	0·873
2·042	0·00968	3·893	0·0800	7·92	1·025
2·194	0·0118	4·16	0·112	8·30	1·17
2·333	0·0143	4·68	0·171	8·68	1·31
2·465	0·0172	5·10	0·233	9·04	1·45
2·602	0·0196	5·46	0·295	9·45	1·67
2·773	0·0240	5·78	0·371	9·92	1·89
3·002	0·0307	6·20	0·469	10·42	2·15
3·237	0·0397	6·70	0·590		

Table 2

°K	C/R	°K	C/R
0·5	0·000141	4·0	0·124
1·0	0·00113	5·0	0·216
1·5	0·00380	6·0	0·416
2·0	0·00901	7·0	0·694
2·5	0·0176	8·0	1·05
3·0	0·0304	9·0	1·47
3·5	0·0533	10·0	1·93

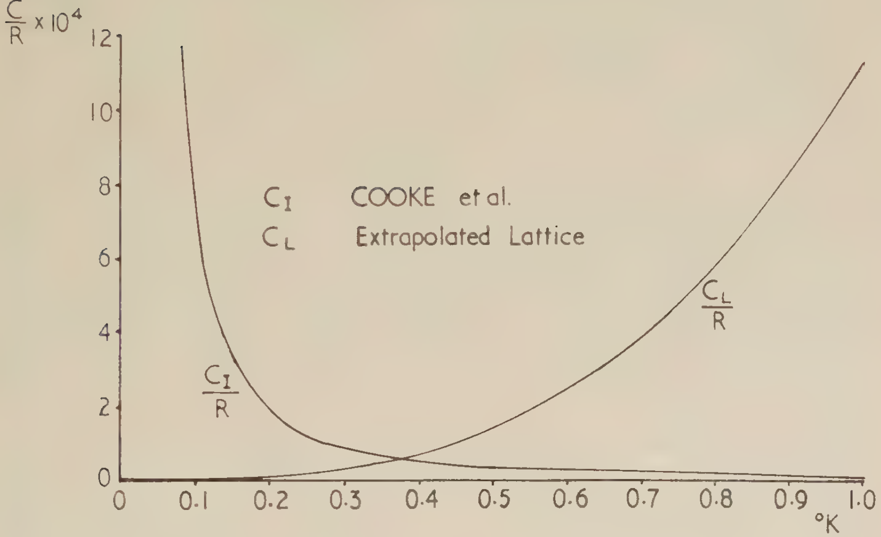

The lattice and magnetic specific heats of cerium magnesium nitrate below 1°K.

temperature of 0·37°K. Although the lattice specific heat at 1°K is 150 times the magnetic specific heat the lattice entropy is only 1/2000 of the magnetic entropy of $R \log_e 2$.

The main errors in calculating the heat capacities from the experimental data arise from an inaccurate knowledge of the temperature heating interval and the change of thermometer resistance with temperature. Taking account of all the various sources of error the total error in the range 10°K to 4°K should be ±2% increasing to ±3% at 2°K.

References

Cooke, A. H., Duffus, H. J., and Wolf, W. P., 1953, *Phil. Mag.*, **44,** 623.
Daniels, J. M., and Robinson, F. N. H., 1953, *Phil. Mag.*, **44,** 630.
Jantzsch, H., 1912, *Z. anorg. Chem.*, **76,** 303.
Smith, P. L., and Wolcott, N. M., 1956, *Phil. Mag.*, **1,** 854.

Optical Transition Radiation from Protons Entering Metal Surfaces†

By P. Goldsmith and J. V. Jelley
Atomic Energy Research Establishment, Harwell

[Received February 9, 1959]

Abstract

Transition Radiation is the term adopted to describe a feeble radiation emitted when a charged particle crosses the boundary between two media having different optical properties. The paper describes experiments to establish the existence of this effect, which has previously only been studied theoretically. The results, obtained from studies of the polarization of the radiation, its excitation function and its absolute yield, confirm the predictions of theory.

§ 1. Introduction

When a charged particle enters a metal surface, the annihilation of the dipole formed by the charge and its image, causes the emission of an exceedingly weak pulse of electromagnetic radiation. This effect, which is known as Transition Radiation, has not previously been studied experimentally though it has been discussed theoretically by a number of authors, namely Frank and Ginsburg (1945 a, b), Beck (1948), Klepikov (1951) and Garibian (1957).

Although transition radiation is expected to occur when a charged particle traverses a sharply defined boundary between *any* two media having different optical properties, we here restrict ourselves to the specific case of a vacuum-metal boundary, to minimize fluorescence and to avoid Čerenkov radiation which might be present if dielectrics were used. Further, protons rather than electrons were used in these experiments, to avoid background effects from scattered particles and Bremsstrahlung.

Frank and Ginsburg show that in the case of non-relativistic particles of charge e moving with a constant velocity v normal to the surface, the energy radiated by a single particle into solid angle $d\Omega$ at an angle θ to the trajectory of the particle is given by:

$$dW = \frac{e^2 v^2 \sin^2 \theta}{\pi^2 c^3} \, d\omega \, d\Omega \quad . \; . \; . \; . \; . \; . \; . \quad (1)$$

for the transition from a vacuum to a perfect conductor, in a bandwidth of circular frequency $d\omega$. The total radiation within the hemisphere in front of the surface is thus

$$W_T = \frac{4e^2 v^2 \, d\omega}{3\pi c^3} .$$

---

† Communicated by the Authors.

Rewriting (1), the yield of the number of photons N_p within a wavelength interval $d\lambda$ at a wavelength λ in the direction $\theta = \pi/2$ is:

$$N_p = \frac{2e^2v^2}{\pi hc^3\lambda} d\Omega d\lambda. \qquad (2)$$

To indicate the magnitude of the effect, we find for 1 MeV protons ($v = 1{\cdot}39 \times 10^9$ cm sec^{-1}), $N_p = 3{\cdot}6 \times 10^{-10}$ photons proton^{-1} Å^{-1} sterad^{-1} at $\theta = \pi/2$ and $\lambda = 4400$ Å, the wavelength of the maximum response for a Cs–Sb photocathode. For a beam of protons this amounts to $2{\cdot}24 \times 10^6$ photons $(\mu c)^{-1}$ sterad^{-1} at $\theta = \pi/2$, between wavelength limits 3900–4900 Å.

At non-relativistic energies, transition radiation is polarized in a similar manner to dipole radiation, that is with the electric vector parallel to the dipole, or in this case, the proton beam, when $\theta = \pi/2$. It is this property which enabled the transition light to be distinguished from the various background sources.

§ 2. EXPERIMENTAL ARRANGEMENTS

The proton beam B from the 5 MeV Van de Graaff generator was collimated at D to impinge on a selected target T, mounted within a cylindrical shielding mask M and connected to a current integrator. The target, inclined at an angle of 4° to the plane normal to the beam axis, was set up so that the area struck by the proton beam could be viewed by the photomultiplier PM through the slit S_1 (cut in M, see inset in fig. 1) via a $\frac{1}{4}$ in. thick plate glass vacuum window W. The mask M served both as a Faraday cage to retain secondary electrons, and as a mask, to exclude as much as possible of the ionization glow from the residual gas (pressure about 10^{-5} mm of Hg) from reaching the phototube. In control runs, T and M could be rotated and withdrawn together, so that a second slit S_2 was brought opposite W, whereby light from the gas could be separately studied. When M was turned through 180°, all light other than that arising in W was excluded, and so the background light, due to neutrons and γ-rays, was obtained.

The polarization of the light was investigated by rotating a disc of polaroid P_1 (type KN36). The phototube was followed by conventional electronic units consisting of an amplifier (time constants 0·08 μsec), a fast discriminator and cascaded scalers. The CO_2 cooling depressed the dark current rate of the phototube to about 50 pulses per second at the standard bias (see below).

§ 3. TARGETS

Three metals were selected for study, aluminium, silver and gold; these were chosen in anticipation of good optical properties whilst having markedly different atomic numbers. In the preparation of the targets, the best results were obtained by first grinding them reasonably flat, hand polishing to remove all scratches, cleaning in solvents, and finishing by evaporating a layer of the metal onto this surface. It was found, however, that the yield of polarized light from the surface when subjected to the proton beam often varied considerably between targets of the same material prepared in identical ways. This is apparent from the table where, for example, in the case of aluminium targets, the maximum yield observed was three times the average. Various modifications in the preparation technique were tried, including that of grinding the surface optically flat; these targets, however, showed no improvement on those produced by the above standard method and, in fact, were usually inferior.

Good polarization curves were often obtained with targets prepared in the standard manner but *without* the final evaporation. On investigating the excitation function of these targets, however, it was often found that the yield decreased with increasing proton energy. No explanation of this phenomenon is offered.

Fig. 1

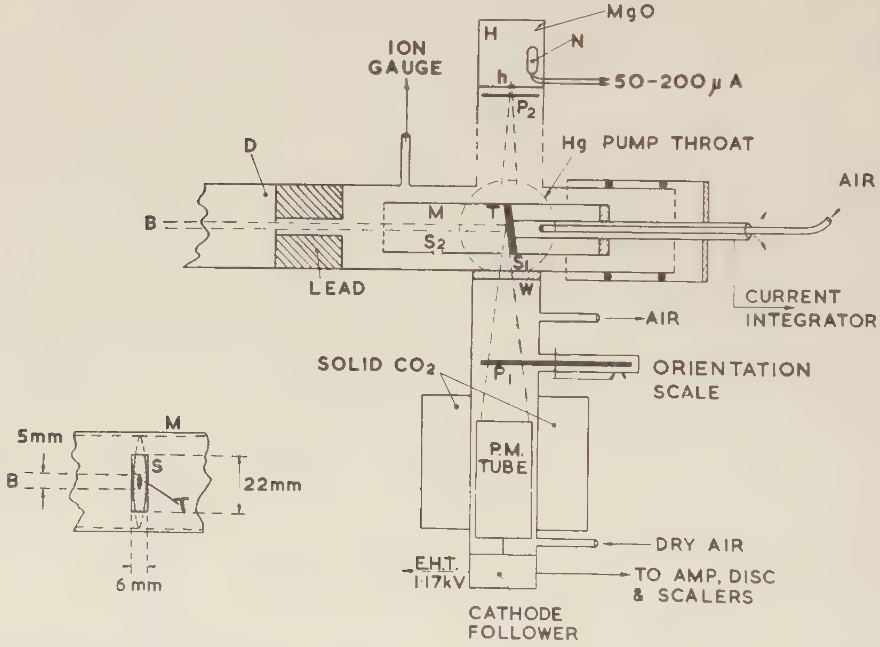

Experimental arrangement. The proton beam B is collimated at D and impinges on the target T. The photomultiplier PM receives that resultant light emitted from the target at 90° to the proton beam via the vacuum window W and the polaroid P_1.

§ 4. Tests and Calibrations

Throughout the experiments the discriminator was set at a bias corresponding to the average pulse height for single photoelectrons. This was carried out by a development of the method described by Morton (1949), from a photoelectron pulse-height distribution using a weak light source. For this, a small lamp N, located in the housing H coated with MgO on the inside, gave ample light from the small pin-hole *h* (see fig. 1).

With unpolarized light emerging from *h*, the transmission of the polaroid P_1 was measured as a function of its orientation and it was checked that the variation of transmission was independent of the colour of the light. All the results shown have been corrected for this transmission factor.

Finally, the efficiency of the polaroid P_1 to plane polarized light was tested, by inserting a second polaroid P_2 in the light path, from which the polarization curve in fig. 2 (*d*) was obtained. The efficiency of cut-off for crossed polaroids was found to be 99%, so that the efficiency of P_1 alone, to obtain a cut-off for a truly plane polarized source, was nearly 100%.

Fig. 2

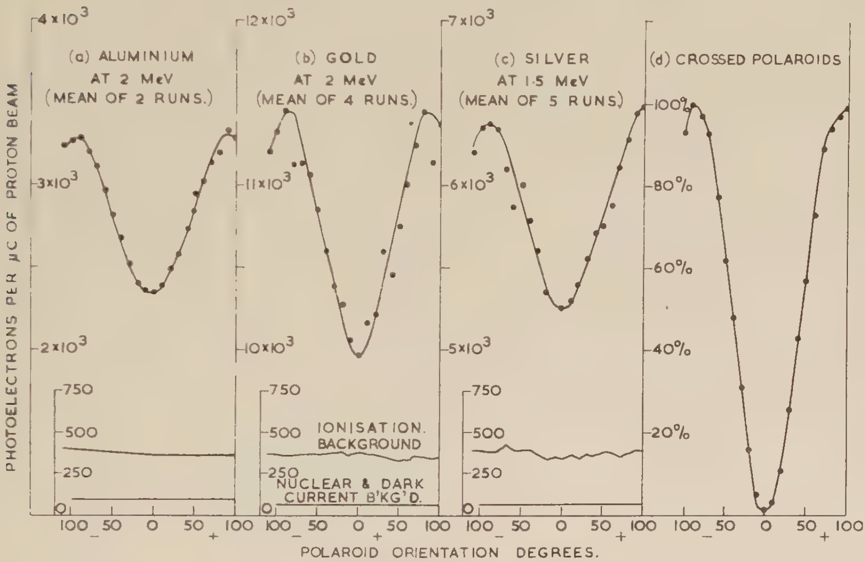

Polarization curves. The output of the photomultiplier in photoelectrons per μc of proton beam is plotted against the polaroid orientation for three metals (*a*) aluminium, (*b*) gold and (*c*) silver. The efficiency of the polaroid is demonstrated in (*d*), where the relative yield is plotted against polaroid orientation for the case of crossed polaroids.

§ 5. Results

5.1. *Polarization*

As already mentioned, transition radiation may be identified by its polarization. Figure 2 (*a*), (*b*) and (*c*) shows the results of typical polarization runs for aluminium, gold and silver targets. The number of photoelectron counts per micro-coulomb of proton beam is plotted against the polaroid orientation; it is seen that the polarized light is superimposed on a background of non-polarized light. The level of this background was found to vary with the mode of taget preparation and type of target. Also shown are the backgrounds due to ionized residual gas, the phototube dark current and nuclear radiations, these effects being isolated as described earlier in § 2. The orientation of the plane of polarization was consistent with the assumption that the polarized light was transition radiation.

5.2. *Excitation Function*

From eqn. (1), it is seen that the yield of transition radiation varies as the square of the proton velocity, that is linearly with proton energy.

Fig. 3

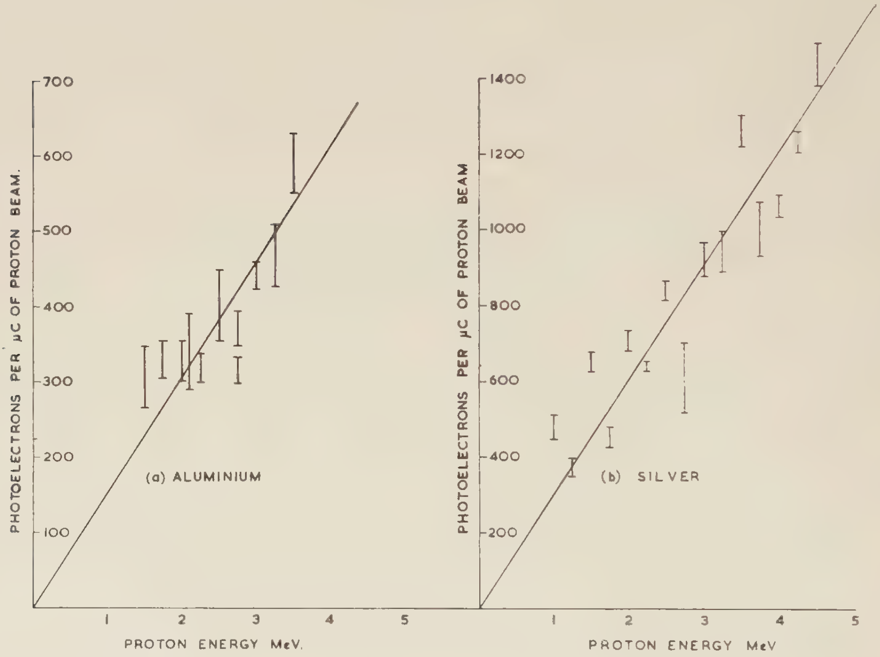

Excitation function. The photomultiplier output, for polarized light only, plotted as a function of the energy of protons incident on targets of aluminium and silver.

Runs were therefore made over a range of proton energies. The yields for the polarized component of the light from aluminium and silver targets are shown in fig. 3. It is seen that although there is considerable scatter in the points, the general trend is consistent with a linear excitation function.

The scatter is not unexpected since targets tended to deteriorate under prolonged proton bombardment; also, changes of proton energy necessitated slight refocusing which caused the beam to fall on different parts of the target. It should be mentioned that other runs with a silver target were again consistent with the linear excitation function, but gave markedly different slopes.

5.3. *Absolute Intensities*

The observed photoelectron counting rates were used to obtain figures for absolute light yields, for comparison with the theory. We may rewrite eqn. (2) in the form:

$$N_e = \frac{2e^2v^2}{h\pi c^3}\, d\Omega \eta_0 \int (1/\lambda) P(\lambda) S(\lambda)\, d\lambda \quad . \quad . \quad . \quad . \quad . \quad (3)$$

where N_e is the number of photoelectrons emitted from the photocathode for each proton striking the target, η_0 is the absolute quantum efficiency of the photocathode (at the wavelength corresponding to maximum response), $S(\lambda)$ is the spectral distribution of the sensitivity of the photocathode (normalized to unity at the peak of the curve) and $P(\lambda)$ is the spectral transmission curve of the polaroid and glass window for

Fig. 4

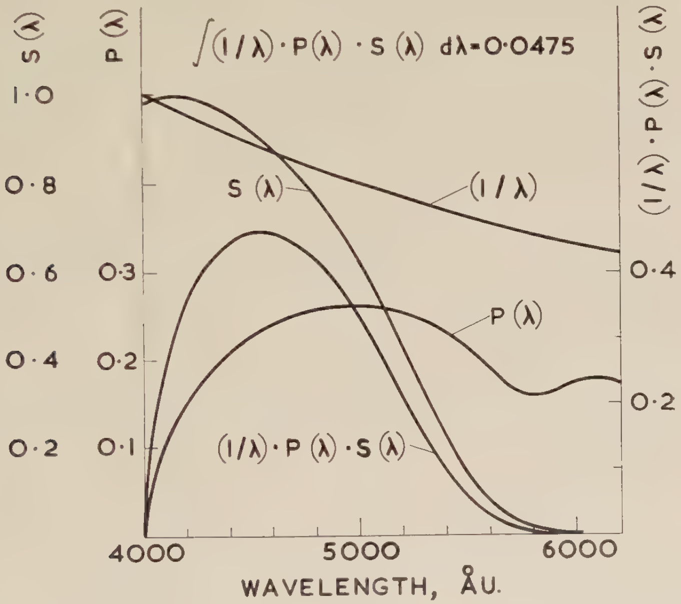

The variations of the photomultiplier sensitivity $S(\lambda)$, the polaroid and window transmission $P(\lambda)$, the reciprocal of the wavelength $(1/\lambda)$ and their product $(1/\lambda)P(\lambda)S(\lambda)$ with wavelength are shown. The area of the latter curve gives $\int (1/\lambda)P(\lambda)S(\lambda)\, d\lambda$, which is used in the comparison between the theoretical and experimental yield of polarized light.

unpolarized light. The various factors in the integral of (3), and their product, are shown in fig. 4, $S(\lambda)$ has been redrawn from curves published by the E.M.I. for a typical Cs–Sb surface, and $P(\lambda)$ was measured on a spectrophotometer. From a measured figure of 56 μA per lumen for the absolute sensitivity of the phototube, η_0 was calculated to be 13% at λ max = 4200 Å (see for example, Jelley 1958).

In our particular case a numerical evaluation of the integral gives 0·0475, while $\eta_0 = 0{\cdot}13$, $v^2 = 1{\cdot}92 \times 10^{18}$ cm^2 sec^{-2} (at 1 Mev), $d\Omega$ (measured) = 0·0117 steradians, from which $N_e = 710$ photoelectrons emitted per microcoulomb of 1 Mev protons. This figure is now compared (see table) with the observed counting rates of the *polarized* component, reduced to 1 Mev.

Target	Number of runs	Average number of photoelectrons per μc of protons at 1 Mev	The highest yield of photoelectrons/μc at 1 Mev observed
Aluminium	24	370 ± 60	1180
Silver	33	530 ± 40	1050
Gold	6	830 ± 60	1110
Theoretical yield :		710	

It may be that the theoretical value should be compared with the highest yield observed rather than the average yield, the results for which are given in the last column of the table. The satisfactory similarity of this yield for all three metals is pointed out.

In view of the many uncertainties in comparisons of this nature, in particular, lack of information on the optical properties of the target surfaces, the theoretical and observed intensities are in satisfactory agreement with each other.

§ 6. DISCUSSION AND CONCLUSIONS

From the results of the experiments described above, it is concluded that the polarized component of the light observed from aluminium, silver and gold targets is transition radiation. The evidence for this stems mainly from the polarization experiment and the estimates of the absolute intensity, while the excitation functions of this polarized light are also consistent with this conclusion.

We now discuss five other effects which may also be present in these experiments, the first two of which are closely associated with transition radiation. As the proton approaches the metal surface, the attraction between it and its image charge will give rise to acceleration radiation. This effect, which Klepikov has termed 'Approach Radiation', is however several orders of magnitude weaker than the transition radiation for a

1 MeV proton. Similarly, there is an acceleration when the proton finds itself in the lower potential environment inside the metal. This effect, which arises from the work function of the surface, is also quite negligible, being of the same order as that for the 'approach radiation'.

The possibility of Bremsstrahlung in the optical band is now considered. Assuming that the spectral distribution given by Heitler (1953) for screened nuclei is valid down to optical frequencies, it is deduced that for silver ($Z=47$) the radiation yield for fast electrons is $\sim 6\times 10^{-13}$ ergs cm^{-1} per electron in the band 3900–4900 Å. Assuming a skin-depth in silver of $\sim\lambda/10$, the depth from which radiation can escape, and assuming the Bremsstrahlung from protons to be weaker than that for electrons by the factor $(M/m)^2$, the light yield will amount to $\sim 10^{-4}$ photons $(\mu\mathrm{C})^{-1}$ Å^{-1} sterad^{-1}, which again is negligible.

We have also to imagine that a fraction of the unpolarized light from the column of ionized residual gas just in front of the target will reach the phototube by specular reflection from the target, and hence will be polarized to a degree depending upon the optical properties of the metal surface. This contribution to the polarized light is however negligible, because, although the total amount of light from ionization is comparable to the polarized light from the target (see fig. 2) only a small proportion of this light can reach the phototube through specular reflection at the target's surface; and moreover this reflected light would be only partially polarized. Furthermore, such reflected light would in any case be polarized in a plane orthogonal to that for transition radiation.

Finally we must consider the contribution to the transition light made by secondary electrons leaving the target surface. A single electron is required to have an energy of ~ 500 ev for the same velocity as a 1 MeV proton. It is suggested by Sternglass (1957) that secondary electrons will seldom have energies greater than about 20 ev and that for protons within the Van de Graaff energy range, a multiplication factor of not greater than one may be expected. Thus the upper limit for the contribution from these secondary electrons will be weaker by a factor of about 25 relative to the proton contribution.

We believe that the main sources of the *unpolarized* background light arise from fluorescence from impurities and oxide layers on the target surface, and scattered protons and γ-rays producing fluorescence and Čerenkov radiation in the glass window.

Owing to the very low light yield from transition radiation, it is clear that the effect cannot be used as the basis of a detector of single particles of unit charge; it might however serve as a flux monitor for beams of particles of high current, using a very thin foil. Such a monitor would present a minimum of disturbance to the beam through energy loss and scattering.

It is quite possible that the residual light sometimes found in experiments on Čerenkov radiation, below the normal threshold, may arise from the transition effect, e.g. in the experiments of Richards (1956), in which electrons enter water after emerging from a metal foil. In conclusion, it may be mentioned that Askarian (1956 a, b) has proposed a millimetre-wave generator based on this effect.

ACKNOWLEDGMENTS

The authors would first like to thank Dr. E. B. Paul and his team for their assistance on the Van de Graaff generator. Thanks are also due to Mr. J. C. Robins, and Miss J. R. Murray of the Metallurgy Division, for preparation of the targets, and to Mr. M. W. J. Elliott who took part in some of the initial experiments. In conclusion we wish to express our gratitude to Dr. E. Bretscher for his interest in the work.

REFERENCES

ASKARIAN, G. A., 1956 a, *Zh. Eksper. Teor. Fiz.*, **30,** 584 ; 1956 b, *Soviet Phys.* (*J.E.T.P.*), **3,** 613.
BECK, G., 1948, *Phys. Rev.*, **74,** 795.
FRANK, I. M., and GINSBURG, V. L., 1945 a, *Zh. Eksper. Teor. Fiz.*, **16,** 15 ; 1945, *J. Phys.* (*U.S.S.R.*), **5,** 353.
GARIBIAN, G. M., 1957, *Zh. Eksper. Teor. Fiz.*, **33,** 1403 ; 1958, *Soviet Phys.* (*J.E.T.P.*), **6,** 1079.
HEITLER, W., 1953, *Quantum Theory of Radiation* (Oxford), 3rd edn., p. 250.
JELLEY, J. V., 1958, *Čerenkov Radiation and its Applications* (London : Pergamon Press), p. 111.
KLEPIKOV, N. P., 1951, *Bulletin Moscow State University*, **8,** 61.
MORTON, G. A., 1949, *RCA Rev.*, **10,** 525.
RICHARDS, E. W. T., 1956, *A.E.R.E. Report* No. C/R 1901, Harwell.
STERNGLASS, E. J., 1957, *Phys. Rev.*, **108,** 1.

The Lattice Thermal Conductivity of Copper Alloys: Effect of Plastic Deformation and Annealing†

By W. R. G. Kemp, P. G. Klemens, and R. J. Tainsh
Division of Physics, Commonwealth Scientific and Industrial Research Organization, Sydney, Australia

[Received February 9, 1959; and in revised form April 6, 1959]

Abstract

The thermal and electrical conductivities were measured and the lattice thermal conductivities were deduced of two copper alloys (Cu–0·4% As and Cu–32% Zn) after severe torsional deformation and after subsequent annealing. Deformation and annealing conditions were selected to allow comparison of these measurements with studies of the release of stored energy made by Clarebrough, Hargreaves, Loretto, and West. In the case of arsenical copper the only observable change in lattice thermal conductivity is due to a removal of dislocations during the recrystallization stage. In the case of alpha–brass, the recovery phenomena are complex and not fully understood; annealing seems to remove dislocations, point defects, and probably also stacking faults. Dislocation densities deduced from the lattice thermal conductivity appear to be somewhat higher than those deduced from stored energy release and from changes in the density.

§ 1. Introduction

The lattice component of the thermal conductivity of metals and alloys is sensitive to physical imperfections (see, for example, Klemens 1956 a, 1958). The temperature dependence of the conductivity provides some information about the nature of the principal imperfections. Whereas it is usually not possible to measure the lattice thermal conductivity of pure metals, this may be done in the case of alloys, for their electronic thermal conductivity is small and can be calculated from the measured electrical resistivity.

A number of alloy systems have been investigated (e.g. Kemp *et al.* 1956, Kemp, Klemens, Tainsh, and White 1957; Birch *et al.* 1958). Most measurements were made on well annealed specimens, but some were also measured prior to annealing. The lattice thermal conductivity indicated the presence of dislocations and, in some cases, other imperfections, but no quantitative conclusions could be drawn, since the nature of the previous deformation was not known. This would require controlled deformations and parallel measurements of changes in other physical properties.

Clarebrough *et al.* (1955, 1956, 1957) have studied the release of stored energy of deformed metal specimens during isochronal annealing as

---

† Communicated by the Authors.

function of annealing temperature, and have made supplementary measurements of hardness, electrical resistivity, and density. Two of the materials studied are suitable for lattice thermal conductivity measurements: a dilute alloy of arsenic in copper (Clarebrough *et al.* 1955) and an alloy of copper with 32% zinc (Clarebrough *et al.* 1959, to be published). We have now measured the lattice thermal conductivity of these alloys under comparable conditions of deformation and annealing.

§ 2. Arsenical Copper: Measurements

Two rods of copper-arsenic (Cu 99·55%, As 0·35%, P 0·05%) taken from the same material as that used for the study of stored energy release by Clarebrough *et al.* (1955) were supplied by Dr. Clarebrough. Both rods had been drawn to 3·25 mm diameter and given a prolonged anneal at 450°c. One rod, about 8 cm long, served as control specimen (No. 0). The other rod was torsionally deformed to a value of $nd/l = 1{\cdot}29$, where n is the number of turns, d the diameter, and l the length. A similar specimen (No. 1) was cut from it.

The thermal and electrical conductivities of these two specimens were measured from 2° to 90°K in the manner previously described (Kemp *et al.* 1956).

After measurement, specimen No. 1 was annealed in an atmosphere of helium. To be comparable with the studies of Clarebrough *et al.* (1955) the annealing temperature was increased continuously at a rate of 6°/min. Annealing was interrupted at 175°c and 275°c to allow measurements to be made (specimens Nos. 2 and 3) and concluded at 450°c (specimen No. 4).

The thermal conductivities of specimens 0, 1, and 4 are shown in fig. 1 as functions of temperature; the conductivities of specimens 2 and 3 are practically indistinguishable from that of No. 1. The electrical resistivities at helium temperatures (ρ_0), at 90·2°K, and at 293°K are shown in table 1.

Table 1. Electrical Resistivities (in $\mu\Omega$-cm) of the Specimens at Helium, Oxygen, and Room Temperatures (suffices denote temperature in °K)

Specimen	Annealed to	ρ_{293}	ρ_{90}	ρ_0	$\rho_{293}-\rho_0$	$\rho_{90}-\rho_0$
Cu–0·35% As	°c					
No. 0	450 (prolonged)	4·51	3·04	2·71	1·80	0·33
1	Deformed	4·60	3·11	2·79	1·81	0·32
2	175	4·58	3·13	2·83	1·75	0·30
3	275	4·56	3·15	2·80	1·76	0·35
4	450	4·53	3·11	2·77	1·76	0·34
Cu–32% Zn						
No. 1	Deformed	7·27	5·11	4·59	2·68	0·52
2	250	6·88	4·84	4·20	2·68	0·64
3	290	6·58	4·49	3·90	2·68	0·59
4	400	6·31	4·27	3·66	2·65	0·61
Copper	—	—	—	—	1·68	0·28

Fig. 1

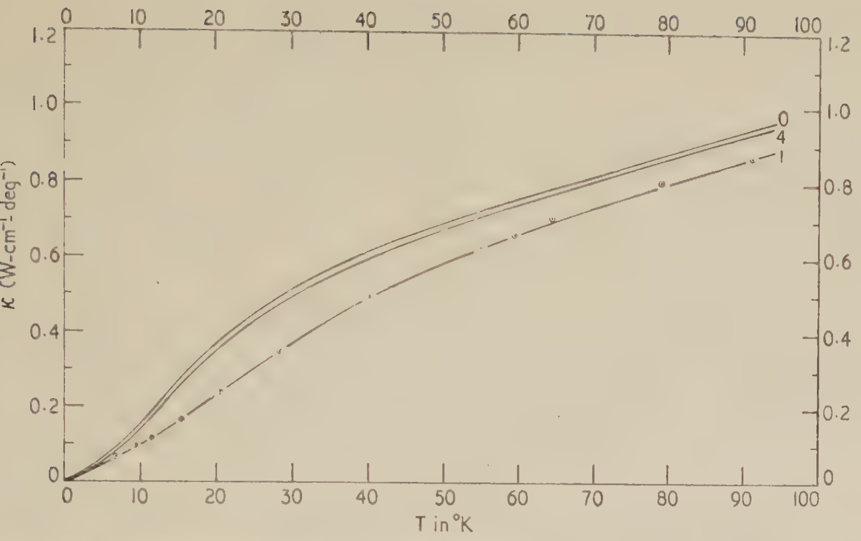

The total thermal conductivity of the arsenical copper specimens Nos. 0, 1, and 4. Experimental points for 0 and 4 are omitted for the sake of clarity.

Fig. 2

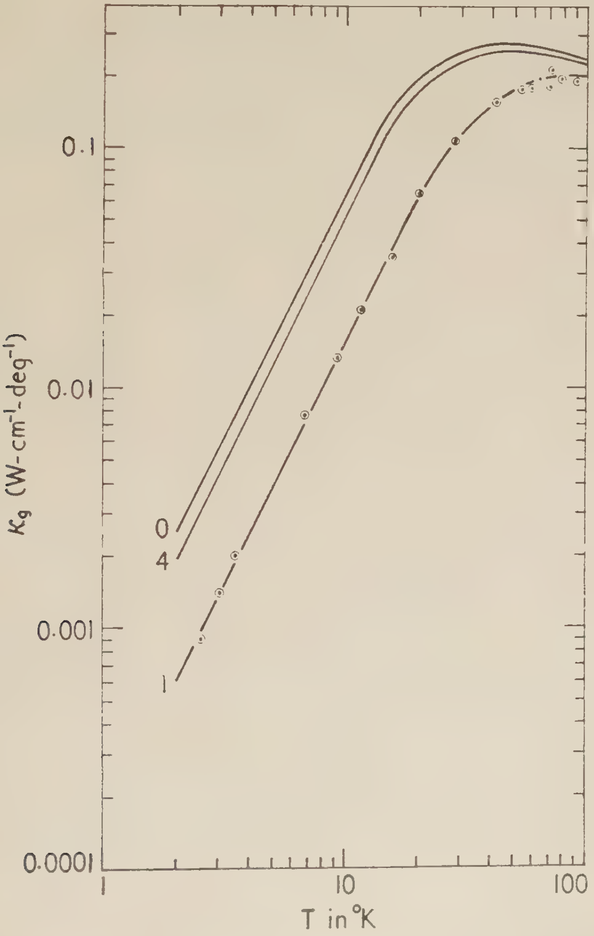

The lattice component of the thermal conductivity of the arsenical copper specimens Nos. 0, 1, and 4. Experimental points for 0 and 4 are omitted for the sake of clarity.

The measured thermal conductivity is composed of the electronic component κ_e and the lattice component κ_g, so that

$$\kappa = \kappa_e + \kappa_g \qquad (1)$$

and κ_e may be calculated from

$$\frac{1}{\kappa_e} = W_i + \frac{\rho_0}{LT} \qquad (2)$$

where ρ_0 is the residual electrical resistivity, which has been measured, L is the Lorenz number ($2{\cdot}45 \times 10^{-8}$ watt-ohm-deg^{-2}), T the absolute temperature, and W_i is the ideal thermal resistivity, and may be taken as that of pure copper, measured, for example, by White (1953).

The lattice conductivity κ_g, which has been calculated by means of (1) and (2) from the measured values of κ and ρ_0, is plotted as function of T in fig. 2 for the specimens Nos. 0, 1, and 4; the curves for Nos. 2 and 3 again coincide with that of No. 1.

§ 3. Arsenical Copper: Discussion

Clarebrough *et al.* (1955) had observed two stages of energy release. During stage I (from 80° to 300°c), energy was released slowly. During stage II (from 300° to 400°c) an approximately equal quantity of energy was released, but at a much higher rate, with a sharp peak at about 350°c.

No appreciable change in the lattice thermal conductivity was produced by annealing up to 275°c (stage I); on the other hand a substantial increase in κ_g resulted on annealing from 275° to 450°c, that is, through stage II. However, as curve 4 in fig. 2 is still below curve 0, annealing to 450°c did not produce complete recovery, in spite of the fact that no appreciable energy release had been observed above 400°c.

The variation of κ_g with temperature is governed by the scattering of phonons by electrons (producing a resistivity W_E), by dislocations (W_D), by point defects (W_P), and by the mutual interaction of the phonons (W_U). To a sufficient degree of approximation these resistivities contribute in an additive manner to the total resistivity, i.e.

$$\frac{1}{\kappa_g} = W_g = W_E + W_U + W_D + W_P + W_I \qquad (3)$$

where W_I is the resisitivity due to any imperfections not included in the above. Now $W_E \propto T^{-2}$, $W_D \propto T^{-2}$, $W_P \propto T$, and $W_U \propto T$ except at very low temperatures, where W_U decreases more rapidly than T.

Below about 15°K it has been found that $\kappa_g \propto T^2$, so that at these low temperatures the resistivity is due to dislocation and electron scattering. Since W_E cannot be altered by deformation or annealing, the differences in κ_g in the T^2 region between specimens 0, 1, and 4 must be due to differences in W_D.

Above about 50°K, κ_g decreases with increasing temperature. Here most of the resistivity arises from the mutual interaction of the phonons and possibly also from point defects. The principal point defects are the solute atoms; arsenic and phosphorus. From measurements of dilute copper alloys (White and Woods 1955) it appears that $W_U/T \simeq 0{\cdot}03$ watt^{-1}-cm. The curves 0 and 4 in fig. 2 approach a similar limit at high temperatures. It thus appears, at least in the annealed specimens, that W_P is not an important component of the resistivity. This seems reasonable, for the scattering due to the mass difference (Klemens 1955) of the arsenic atom is far too small to account for the observed resistance, and the phosphorus atoms are present in too small a concentration.

The difference in κ_g between Nos. 1 and 4 at liquid helium temperatures is clearly due to the removal of dislocations by annealing from 275° to 450°c during stage II. The number of dislocations thus removed have been estimated as 1×10^{11} cm^{-2} by Clarebrough *et al.* (1955) from the energy released during stage II, assuming an energy of 5×10^{-4} erg-cm^{-1} for a dislocation in copper according to Cottrell (1953).

An estimate of the dislocation density can also be made from the change in the lattice thermal conductivity. The scattering of lattice waves by dislocations and the consequent thermal resistivity have been calculated by Klemens (1955), who found that

$$W_D T^2 \simeq 1{\cdot}1 \times 10^{-2} \frac{vh^2}{K^3} b^2 N \quad . \quad . \quad . \quad . \quad . \quad . \quad . \quad (4)$$

where h and K are the Planck and Boltzmann constants respectively, v is the sound velocity, b the magnitude of the Burgers vector, and N the dislocation density. However, a revised treatment (Klemens 1958) leads to a scattering cross section increased by a factor 16. For copper, $v = 2{\cdot}4 \times 10^5$ cm sec, $b^2 = 6{\cdot}6 \times 10^{-16}$ cm^2, and including the above factor of 16, (4) becomes

$$W_D T^2 = 5 \times 10^{-9} N \quad . \quad . \quad . \quad . \quad . \quad . \quad . \quad . \quad (5)$$

where W_D is expressed in cm-deg-watt^{-1} and N in lines/cm^2.

The change in κ_g at low temperatures during stage II corresponds to a dislocation resistance $W_D T^2 \simeq 4{\cdot}5 \times 10^3$ watt^{-1}-cm-deg^3, so that the density of dislocations removed is $N = 9 \times 10^{11}$ cm^{-2}. This estimate exceeds the estimate from the stored energy release by a factor of 9.

On the scale of eqn. (5), the difference between Nos. 4 and 0 corresponds to a dislocation density of 7×10^{10} cm^{-2}. It should be noted that specimen No. 0 is probably not free of dislocations, since at helium temperatures $W_g T^2 \simeq 1{\cdot}5 \times 10^3$, while from theory and experiments $W_E T^2 \simeq 0{\cdot}5 - 0{\cdot}7 \times 10^3$ (Klemens 1958), so that there is a residual dislocation density, according to (4), of about 2×10^{11}. Similar residual dislocation densities have been found in other copper alloys (Kemp, Klemens, and Tainsh 1957).

Although the energy released during stage I was comparable to the energy released during stage II, there was no appreciable change in lattice thermal conductivity. Clarebrough, Hargreaves, and West have suggested that some rearrangement of dislocations occurred during stage I, but our results indicate that any such rearrangement did not appreciably alter the total number of dislocations.

A large part of the energy of a dislocation arises from the distant regions of its strain field; thus for a single dislocation in a large crystal, as in Cottrell's (1953) estimate of the stored energy, about two-thirds of the energy comes from the region more than 100 lattice spacings from the dislocation core. On the other hand, the major contribution to the phonon scattering comes from a cylindrical region of less than 100 lattice spacings radius (Klemens 1955). The average distance between dislocations is also of the order of 100 lattice spacings. Thus the dislocations may act as single dislocations when scattering phonons, while the total energy of the dislocation array may be sensitive to their arrangement. In particular the long-range strain energy (beyond 100 lattice spacings) may be considerably smaller than for a single dislocation, as dislocations would have a tendency to arrange themselves so as to minimize this part of the strain energy. Apparently such a rearrangement and long-range energy release occurred during stage I without appreciable reduction in their concentration. Thus during stage II the energy released pertains mainly to the short range strain field (within 100 lattice spacings) and the estimate of the density of dislocations removed must be increased, perhaps by a factor 3, since the fraction of energy in Cottrell's model pertaining to the short range field is 1/3, but at least by a factor 2, since the total energy released during stage I and II, rather than the energy of stage II only, is dislocation energy. This decreases the discrepancy between estimates of dislocation densities from stored energy and lattice thermal conductivity to a factor of from 3 to 4·5.

§ 4. ALPHA–BRASS: MEASUREMENTS

Measurements have also been made on a copper-zinc alloy (approx. 32% Zn) taken from the same material as was used by Clarebrough, Hargreaves, and Loretto to study stored energy release and changes in density.

In order to achieve a greater torsional deformation than could be obtained with a thin rod, a thick rod, which had originally been annealed at 700°C, was deformed torsionally ($nd/l = 1{\cdot}88$) and four thin specimens were afterwards cut from that rod, taken from regions of the rod symmetrically placed about the original axis. Since the machining was done after deformation, further deformation was confined to the specimen surface and was relatively unimportant.

These four equivalent specimens were used in order to avoid a series of measurements in an annealing range where no change in lattice conductivity occurred, as had been inevitable when all measurements and annealing were done on one specimen. Thus specimen No. 1 was measured as deformed, No. 4 was measured after an anneal at a temperature increasing at 6°/min up to 400°C, No. 2 after an anneal up to 250°C†, and since the major change in lattice thermal conductivity occurred between 250°C

---

† This temperature was suggested from data on the release of energy.

Fig. 3

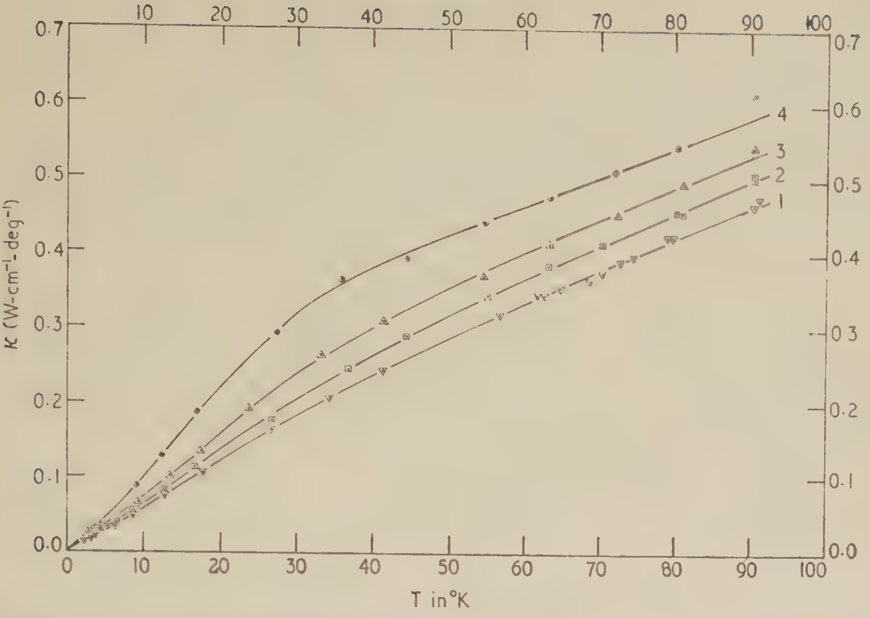

The total thermal conductivity of the alpha-brass specimens Nos. 1, 2, 3 and 4.

Fig. 4

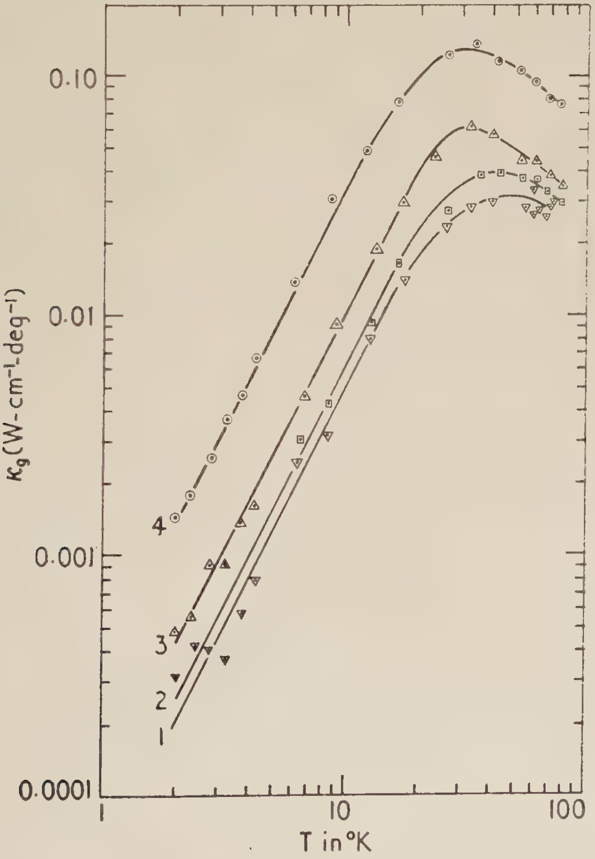

The lattice component of the thermal conductivity of the alpha-brass specimens Nos. 1, 2, 3 and 4.

and 400°C, the last specimen (No. 3) was annealed up to 290°C. These specimens were prepared and annealed by Dr. Clarebrough.

From measurements of the electrical and thermal conductivities the lattice thermal conductivities were deduced as before. Electrical resistance data are presented in table 1, the total thermal conductivities are shown in fig. 3, and the lattice thermal conductivities in fig. 4.

§ 5. ALPHA–BRASS: DISCUSSION

The lattice thermal conductivities of the deformed specimen (No. 1) and the annealed specimen (No. 4) generally confirm the results of earlier measurements made on deformed and fully annealed brass (Kemp, Klemens, Tainsh and White 1957), and indicate that both dislocations and point defects were removed during annealing.

Clarebrough, Hargreaves and Loretto noted two peaks in the energy release as a function of annealing temperature: the first (stage I) extends over a wide temperature interval (80° to 250°C); the second (stage II), from 270° to 340°C, with a maximum at 290°C, is rather sharper. The energy released during stage I (1·19 cal/g) is unusually high; the energy release during stage II (0·46 cal/g) is comparable to, but roughly twice, the energy released during the recrystallization stage in similarly deformed copper and nickel (Clarebrough *et al.* 1955). The electrical resistivity changes found by them are in essential agreement with our data of table 1. They also found a fractional increase in density of $7{\cdot}5 \times 10^{-4}$ during stage I and $2{\cdot}5 \times 10^{-4}$ during stage II.

The changes in lattice thermal conductivity during stage I are small (see fig. 4): there is a suggestion of a small change at high temperatures, indicating a change in point defect concentration, and there is a definite effect at low temperatures, indicating some change in dislocation density.

Stage II has been arbitrarily divided into two parts: II (*a*) from No. 2 to No. 3 and II (*b*) from No. 3 to No. 4. There is a substantial change in lattice conductivity during this stage, comprising a major change in dislocation density (change of κ_g at low temperatures), about evenly divided between II (*a*) and II (*b*), and a change in point defect concentration (change of κ_g at high temperatures), particularly during II (*b*).

The energy release during stage II has been interpreted by Clarebrough, Hargreaves, and Loretto as due to the removal of dislocations, analogously to the similar recrystallization stage in copper and nickel (Clarebrough *et al.* 1955). The density change during stage II is considered to be associated with the removal of these dislocations, as in nickel (Clarebrough *et al.* 1956) and copper (Clarebrough *et al.* 1957), and explained theoretically by Stehle and Seeger (1956) and by Lomer (1957). This is confirmed by the present lattice thermal conductivity results.

Changes in $W_D T^2$, and corresponding changes in dislocation densities estimated from (5), are given in table 2. It is seen that almost one-quarter of the dislocations are removed already during stage I. If we ascribe all the energy release of stage II to dislocations, then the energy release

Table 2. Changes in Conduction Properties of Brass†

Specimen No.	1		2		3		4	
Differences		2–1		3–2		4–3		4–2
Stage		I		II(a)		II(b)		II
$\rho_0(\mu\,\Omega\text{-cm})$	4·59		4·20		3·90		3·66	
$\Delta\rho_0(\mu\,\Omega\text{-cm})$		0·39		0·30		0·24		0·54
$(W_g T^2)_{\text{helium}}$	20×10^3		16×10^3		10×10^3		3×10^3	
$\Delta W_D T^2$		4×10^3		6×10^3		7×10^3		13×10^3
$\Delta N_{\text{disl.}}$ from (5)		8×10^{11}		12×10^{11}		14×10^{11}		26×10^{11}
ΔS (cal/g)		1·9		(0·23)		(0·23)		0·46
$\Delta N_{\text{disl,}}$ (stored energy)		—		(2×10^{11})		(2×10^{11})		4×10^{11}
$\Delta D/D$		$7{\cdot}5\times10^{-4}$		—		—		$2{\cdot}5\times10^{-4}$
$\Delta N_{\text{disl,}}$ (from density)		—		—		—		$2{\cdot}5\times10^{11}$
$(W_g/T)_{\text{oxygen}}$	0·48		0·42		0·33		0·16	
$\Delta W_P/T$		0·06		0·09		0·17		0·26
nS^2		$1{\cdot}5\times10^{-3}$		$2{\cdot}2\times10^{-3}$		$4{\cdot}2\times10^{-3}$		$6{\cdot}4\times10^{-3}$
$W_S T$	150		160		0		0	
$\Delta W_S T$		0		160		0		160
Δa from $\Delta W_S T$		0		$4{\cdot}5\times10^{-3}$		0		$4{\cdot}5\times10^{-3}$
Δa from $\Delta\rho_0$		—		$3{\cdot}5\times10^{-3}$		—		—

† Including stored energy and hydrostatic density changes investigated by Clarebrough, Hargreaves and Lorreto.

due to dislocations during stage I should be about 0·14 cal/g, perhaps more if there is also some rearrangement of dislocations as in arsenical copper. Thus, the major fraction of the energy release during stage I is due to some unknown process which does not seem to affect κ_g appreciably. No reliable interpretation of this release can be given at present.

There are also indications of the removal of a third type of imperfection during stage II (*a*), for curves 1 and 2 in fig. 4 are not of the same shape as curves 3 and 4, but appeared truncated beween 20°K and 50°K. By drawing curves in fig. 4 of the same shape as curves 3 and 4, but superimposed on the extremities of curves 1 and 2, it is possible to estimate this additional resistivity. Its temperature dependence is not inconsistent with the effect of stacking faults ($W_S \propto 1/T$, Klemens 1957). In the case of copper $W_S T$ would be expected to be $3{\cdot}5 \times 10^4\,\alpha$ where α is the stacking fault probability, i.e. the fraction of stacking faults per atomic plane. The value of $W_S T$ deduced from fig. 4 is about 160 w^{-1}–cm-deg^2: this corresponds to an α of $4{\cdot}5 \times 10^{-3}$, and this resistance was removed during stage II (*a*).

A second estimate of α can be obtained from the change in electrical resistivity. Since the electrical resistance due to the dislocations removed during stage IIa is probably relatively small, even when using Harrison's (1958) estimate rather than that of Hunter and Nabarro (1953). most of the change in ρ_0 of II (*a*) may be ascribed to the removal of stacking faults. The change in electrical resistivity due to the removal of stacking faults of probability α would be $2{\cdot}9 \times 10^{-4} p\alpha$ ohm-cm, where p is the average probability that an electron impinging on a stacking fault is specularly reflected. This probability may be taken as approximately 0·25 (Seeger 1956, Klemens 1956 b, 1957). Ascribing a change in resistivity of 0·25 $\mu\Omega$-cm to the removal of stacking faults, this gives α as $3{\cdot}5 \times 10^{-3}$, in reasonable agreement with the value derived from the lattice thermal conductivity.

The lattice thermal conductivity above 45°K clearly indicates a large change in point defect concentration during stage II, particularly during II (*b*). The additional resistivity due to point defects is given by

$$W_P/T = \frac{3(2\pi)^2}{0{\cdot}90}\frac{a^3}{hv^2}S^2 n \qquad . \quad . \quad . \quad . \quad . \quad . \quad . \quad (6)$$

where a^3 is the volume per atom, h and v are defined as in (4), n is the concentration of point defects per atom, and S^2 is a parameter, usually of order unity, describing the scattering cross section of the imperfection (Klemens 1955).

In the case of copper, (6) becomes (in watt^{-1} cm)

$$W_P/T = 40{\cdot}5 n S^2. \qquad . \quad . \quad . \quad . \quad . \quad . \quad . \quad (7)$$

Values of W_g/T at oxygen temperatures are given in table 2. The annealed specimen (No. 4) has a value of $W_g/T = 0{\cdot}16$; this exceeds substantially the resistance due to mutual interaction of the phonons, which in the arsenical copper was $W_p/T=0{\cdot}03$. The excess resistivity $W_p/T=0{\cdot}13$ must be due to the zinc atoms ($n=0{\cdot}3$), so that from (7), $S^2=0{\cdot}01$ for zinc in copper. However, as pointed out by Kemp, Klemens, Tainsh, and White (1957), even this relatively weak scattering parameter cannot arise from the small mass difference between zinc and copper for which S^2 should be 5×10^{-5}. Thus it arises most probably from a distortion of the lattice about the impurity atom.

The point defect resistivity of specimens 1, 2, and 3 is considerably higher, and the decrease in resistivity during stage II (*b*) corresponds to $nS^2=4{\cdot}2\times10^{-3}$. If the point defects were vacancies without lattice distortion, we would expect $S^2=0{\cdot}25$ (Klemens 1955). This would imply that during stage II (*b*) alone about 0·015 vacancies per atom were removed—an impossibly high concentration. The electrical resistivity change corresponding to that vacancy concentration, according to Jongenburger's (1953) estimate, would be about $2\,\mu\Omega$-cm, or about eight times the electrical resistivity change observed†. Furthermore, the change in density D observed by Clarebrough, Hargreaves, and Loretto during stage II (*b*) was far too small to be in accord with the removal of vacancies or, for that matter, any point defect in such large concentration. During all of stage II, $\Delta D/D=2{\cdot}5\times10^{-4}$, and this can be accounted for quite well in terms of the removal of dislocations.

The absence of any pronounced changes in the density may be explained by supposing that during stage II these point defects are not removed from the solid, but coagulate; thus if they are vacancies or small clusters of vacancies, they come together to form small but macroscopic voids, which do not scatter lattice waves as effectively. To account for the large value of W_p/T, one would have to suppose that the initial defect concentration is an order of magnitude smaller than estimated above, but that the defects form small groups already before annealing, leading to enhanced scattering of lattice waves by reinforcement. This would possibly imply a total vacancy concentration of say 2×10^{-3}, grouped in clusters of 8 to 10, and coagulating to form voids during annealing, particularly during stage II (*b*).

§ 6. CONCLUSION

It has been found possible to derive information about the removal of lattice imperfections during annealing of torsionally deformed copper alloys from the changes in their lattice thermal conductivity, thus supplementing the information derived from measurements of the release of stored energy and other properties. It has been verified that during recrystallization there is a large change in dislocation density. In the case of arsenical copper it has been shown that the early release of energy

---

† This difficulty had already been noted by Kemp, Klemens, Tainsh and White (1957), where the change in W_P/T was nearly three times too large compared with the change in ρ_0 if the point defects were vacancies.

(stage I) does not involve an appreciable change in the dislocation density. In the case of alpha–brass the early energy release (stage I) causes only a small change in lattice thermal conductivity, in spite of the large amount of energy released, and during recrystallization a large number of point defects disappeared: the nature of these defects is as yet unknown, and they did not show up unambiguously in any other physical property. There were also indications that stacking faults were removed by annealing during stage II (*a*), while part of the dislocations still remained.

The lattice thermal conductivity gives a good relative measure of dislocation densities, but, like other methods, gives absolute dislocation densities of considerable uncertainty, since the theory leading to (5) contains some unjustified approximations. By intercomparing the results of different methods, the limits of uncertainty may be decreased.

In the case of arsenical copper, the estimate of dislocation density from (5) exceeds that from the stored energy. However, the energy of a dislocation is uncertain because of the contribution from the long-range strain field; if this is allowed for, the discrepancy between estimates from (5) and from the stored energy is reduced to about 4·5 and possibly less, but not less than about 3. In the case of alpha–brass the discrepancy between (5) and the energy released during stage II is about 6·5 (see table 2), but this neglects any possible reduction of the long-range strain energy. The change in density indicates an even lower dislocation density, but since the ratio of $\Delta D/D$ to ΔS was lower in this case than in pure copper (Clarebrough *et al.* 1957), it is not clear what significance would be ascribed to this result.

Lomer and Rosenberg (1959) compared changes in lattice thermal conductivity of more dilute alpha–brass with dislocation counts from electron-micrographs obtained from sections polished down to a thickness of 1000 Å. They found a discrepancy by a factor of about 6, eqn. (5) again over-estimating the dislocation density. However, in polishing down to such thin sections, some dislocations which were originally pinned may have been released when the point of pinning was removed, so that the micrographs may have underestimated the dislocation density.

From the above it seems likely that (5) over-estimates the dislocation density in copper alloys by a factor of between 3 and 6. This is probably due to the inadequate treatment of the anharmonic component of the lattice forces in the theory of the scattering of lattice waves by strain fields, as discussed elsewhere (Klemens 1957). Consequently one cannot assume that the discrepancy from (5) will be the same in all classes of solids: however, the discrepancy deduced here should apply to all face-centred cubic metals and alloys.

ACKNOWLEDGMENT

We wish to thank Dr. L. M. Clarebrough who prepared the alloy specimens used in this work, made available to us the results of his investigations and gave us valuable advice at all stages of our work.

REFERENCES

BIRCH, J. A., KEMP, W. R. G., and KLEMENS, P. G., 1958, *Proc. phys. Soc., Lond.* A, **71,** 843.

CLAREBROUGH, L. M., HARGREAVES, M. E., and WEST, G. W., 1955, *Proc. roy. Soc.* A, **232,** 252; 1956, *Phil. Mag.*, **1,** 528; 1957, *Acta Met.*, **5,** 738.

COTTRELL, A. H., 1953, *Dislocations and Plastic Flow in Crystals* (Oxford: Clarendon Press).

HARRISON, W. A., 1958, *J. Phys. Chem. Solids*, **5,** 44.

HUNTER, S. C., and NABARRO, F. R. N., 1953, *Proc. roy. Soc.* A, **220,** 542.

JONGENBURGER, P., 1953, *Appl. Scientific Research*, B, **3,** 237.

KEMP, W. R. G., KLEMENS, P. G., SREEDHAR, A. K., and WHITE, G. K. 1956, *Proc. roy. Soc.* A, **233,** 480.

KEMP, W. R. G., KLEMENS, P. G., and TAINSH, R. J., 1957, *Aust. J. Phys.*, **10,** 454.

KEMP, W. R. G., KLEMENS, P. G., TAINSH, R J., and WHITE, G. K., 1957, *Acta Met.*, **5,** 303.

KLEMENS, P. G., 1951, *Proc. roy. Soc.* A, **208,** 108; 1955, *Proc. phys. Soc., Lond.* A, **68,** 1113; 1956 a, *Encyclopedia of Physics*, **14** (Berlin: Springer); 1956 b, *Canad. J. Phys.*, **34,** 1212; 1957, *Ibid.*, **35,** 441; 1958, *Solid State Physics*, **7** (New York: Academic Press).

LOMER, J. N., and ROSENBERG, H. M., 1959, *Phil. Mag.*, **4,** 467.

LOMER, W. M., 1957, *Phil. Mag.*, **2,** 1053.

SEEGER, A., 1956, *Canad. J. Phys.*, **34,** 1219.

STEHLE, H., and SEEGER, A., 1956, *Z. Phys.*, **146,** 217.

WHITE, G. K., 1953, *Aust. J. Phys.*, **6,** 397.

WHITE, G. K., and WOODS, S. B., 1955, *Canad. J. Phys.*, **33,** 58.

The Interactions of π^--mesons with Complex Nuclei in the Energy Range (100–800) MeV

I: The Interaction Lengths and Elastic Scattering of 88 MeV π^--mesons in G5 Emulsion†

By J. E. Allen, A. J. Apostolakis, Y. J. Lee‡,
J. V. Major and E. Perez Ferreira§
The Physics Department,
The Durham Colleges in the University of Durham, Durham,

[Received February 12, 1959]

Abstract

A block of emulsion has been exposed to the 96 MeV π^--meson beam of the Liverpool synchrotron and 92·5 m of track have been scanned in the region where the mean energy is 88 MeV. After correction for beam contamination, the interaction lengths for the production of inelastic events and for elastic scatters with projected angle of scatter $\geqslant 8°$ are $(20{\cdot}4 \pm 1{\cdot}1)$ cm and $(32{\cdot}3 \pm 2{\cdot}1)$ cm respectively. The geometrical interaction length is 29·3 cm. With the optical model of the nucleus, the absorption coefficient is found to be $K = (4{\cdot}0^{+2{\cdot}5}_{-0{\cdot}75})\,10^{12}\,\mathrm{cm}^{-1}$, and the change in wave number is given by $k_1 = -(1{\cdot}86 \pm 0{\cdot}20)\,10^{12}\,\mathrm{cm}^{-1}$. This absorption coefficient corresponds to a mean free path in nuclear matter $\lambda_\mathrm{n} = (2{\cdot}5^{+0{\cdot}6}_{-0{\cdot}7})\,10^{-13}$ cm, to an imaginary component of potential $V_i = -(32^{+20}_{-6})$ MeV, and with the value of the change in wave number to a real potential $V_r = -(28 \pm 3)$ MeV.

§ 1. Introduction

The first results are described of a systematic survey of the interaction characteristics of π^--mesons with G5 emulsion nuclei within the energy range (100–800) MeV. Within this range, the relative probabilities for absorption, charge exchange and inelastic scattering of the π^--meson vary greatly, and the analysis of the interactions is not complicated by excessive production of secondary π-mesons.

Emulsion blocks exposed to meson beams have been examined by scanning along meson tracks. Track scanning yields a considerable number of elastic scattering events, besides the inelastic interactions, and this allows an investigation of the energy variations of the optical model parameters. Some results on the elastic scattering only of π^--mesons at 88 MeV are presented in this paper.

---

† Communicated by Professor G. D. Rochester, F.R.S.
‡ On leave from the Atomic Energy Commission of the Republic of Korea.
§ On leave from the Comision Nacional de Energia Atomica, Argentina.

§ 2. THE OPTICAL MODEL

Throughout this work there will be constant reference to the optical model of the nucleus. Its essential features are summarized below.

2.1. *The Complex Potential*

The model describes the refraction, attenuation and diffraction of a matter wave by a complex nuclear potential which has real and imaginary components V_r and V_i. The reduced wave number, k, of the meson, is increased by the real component of potential to k'. For the non-relativistic case (Fernbach *et al.* (1949)) the complex potential is assumed constant within the nucleus and k' is given by

$$k' = k(1 + V_r/E)^{1/2}. \qquad \qquad (1)$$

For the relativistic case (Fowler and Perkins (1958, private communication))

$$k' = k[1 + 2V_r/p\beta c + (V_r/pc)^2]^{1/2} \qquad \qquad (2)$$

where E is the kinetic energy of the particle, p the momentum and βc the velocity. For small values of V_r relative to E and p, the change in wave number on entering the nucleus is

$$k_1 = kV_r/2E \quad \text{(from eqn. (1))} \qquad \qquad (3)$$

or

$$k_1 = kV_r/p\beta c \quad \text{(from eqn. (2)).} \qquad \qquad (4)$$

The attenuation length of the meson wave (or the mean free path for interaction of the meson within the nucleus), λ_n, is related to the imaginary component of potential by

$$\lambda_n = \hbar\beta c/2V_i. \qquad \qquad (5)$$

The absorption coefficient may be calculated assuming two models of the interaction between π-mesons and the nucleus.

In the first model the process of interaction is assumed to be due to the scattering of mesons by individual nucleons within the nucleus. From a knowledge of the $\pi^\pm$-meson cross sections on free nucleons the absorption coefficient is given by

$$K = (3A/4\pi R^3)[\{Z\sigma_{\pi\text{-p}} + (A-Z)\sigma_{\pi\text{-n}}\}/A] \qquad \qquad (6)$$

where A, Z and R are the atomic weight and number and the nuclear radius of the element, $\sigma_{\pi\text{-p}}$ and $\sigma_{\pi\text{-n}}$ are the cross sections for π^--meson interactions with the proton and the neutron. By charge independence $\sigma_{\pi\text{-n}}$ and $\sigma_{\pi^+\text{p}}$ are equal and K is determined by the ($\pi^\pm$-p) cross sections. Below 300 MeV the ratio of $\sigma_{\pi^+\text{p}}$ to $\sigma_{\pi\text{-p}}$ is 3 (see for example Bethe and Hoffmann (1956)), and

$$K = (3/4\pi r_0^3)\sigma_{\pi\text{-p}}(3 - 2Z/A) \qquad \qquad (7)$$

where the nuclear radius has been written as $r_0A^{1/3}$. The variations of Z/A with Z and A throughout the periodic table lead to corresponding changes in the value of K which for nuclear emulsion changes by about 10% from C to Ag.

The above estimates assume that the only process within the nucleus is the π-nucleon scattering and that all energy transfers are possible. The Pauli exclusion principle restricts the number of low energy transfers and leads to a reduction in K. However absorption of the meson by two or more nucleons will lead to an increase in K. The effects of the exclusion of low energy transfers and the absorption of the meson on the value of K have been estimated by Cronin *et al.* (1957) for 970 Mev π^--mesons for a variety of nuclei. It is found that the two corrections, being approximately equal in size, cancel, so that the value of K is given by eqn. (6).

The second model applies at energies ~ 100 Mev where the dominant process is absorption, not scattering, and K is largely determined by this process. The absorption coefficient is then given by

$$K=3N_D\sigma_D/4\pi R^3 \qquad \ldots\ldots\ldots \quad (8)$$

where N_D is the effective number of nucleon pairs in the nucleus and σ_D is the absorption cross section of deuterium at this energy. The analysis of Brueckner *et al.* (1951) suggests that N_D is equal to ΓZ and $\Gamma \sim 10$. Thus

$$K\approx 3\Gamma\sigma_D/8\pi r_0^{\,3}. \qquad \ldots\ldots\ldots \quad (9)$$

The absorption coefficient is then independent of the element to the extent that Γ is constant.

2.2. *Cross Sections*

The total cross sections for inelastic interaction σ_a, and elastic or diffraction scattering σ_d, are

$$\sigma_a=\pi R^2\{1-[1-(1+2KR)\exp(-2KR)]/2K^2R^2\}, \qquad \ldots \quad (10)$$

$$\begin{aligned}\sigma_d=\pi R^2\{&1+[1-(1+2KR)\exp(-2KR)]/2K^2R^2\\ &-(1/(K^2/4+k_1^{\,2})^2R^2)[(K^2/4-k_1^{\,2})+\exp(-KR)\\ &\times[2k_1R(K^2/4+k_1^{\,2})+k_1K]\sin 2k_1R-\exp(-KR)\\ &\times[(K^2/4-k_1^{\,2})+KR(K^2/4+k_1^{\,2})]\cos 2k_1R]\}. \qquad \ldots \quad (11)\end{aligned}$$

as given by Fernbach *et al.* (1949). The differential cross section for diffraction scattering is

$$d\sigma_d/d\Omega=(\sigma_d/\pi)[J_1(kR\sin\theta)/\sin\theta]^2[(1+\cos\theta)/2]^2 \qquad \ldots \quad (12)$$

where J_1 is the first order Bessel function and θ is the spatial angle of scatter. Equation (12) is an approximation to a more exact expression but for $KR=2$, the angular distributions calculated by both expressions agree to $\lesssim 10\%$.

It has been pointed out by Fowler and Perkins (1958, private communication) that the original optical model of Fernbach *et al.* (1949) does not take into account the effect of obliquity. The obliquity factor $[(1+\cos\theta)/2]^2$ (Brenner and Brown (1958, private communication)), is not important at high energies where the angular distribution is chiefly confined to small angles. When it is taken into consideration the value of σ_d in eqn. (12) is still computed by means of eqn. (11), but the cross section for diffraction scattering should be estimated by the integration of the differential cross section.

A further correction must be made at low energies when meson size becomes important. According to Feshbach and Weisskopf (1949) the maximum total cross section corresponding to a 'black' nucleus is given by $2\pi(R+\bar{\lambda})^2$ where $\bar{\lambda}$ is the reduced de Broglie wavelength of the meson. The cross sections given in eqns. (10) and (11) must then be modified to

$$\sigma_a{}' = (\sigma_a{}^{1/2} + \pi^{1/2}\bar{\lambda})^2 \quad \text{and} \quad \sigma_d{}' = (\sigma_d{}^{1/2} + \pi^{1/2}\bar{\lambda})^2. \qquad . \quad . \quad . \quad (13)$$

2.3. *Application of the Optical Model*

The comparison of the cross section for inelastic interactions with the predictions of the optical model leads to the determination of the absorption coefficient K. A similar comparison of either the cross section or the angular distribution for elastic scattering leads to the determination of k_1. The contamination from Rutherford scattering and the inefficiency of detection of small angles make the determination of the elastic interaction cross-section very difficult. Experimentally k_1 is obtained by fitting theoretical angular distributions to the experimental distribution at angles where these effects are unimportant.

If the angular distributions of $\pi^{\pm}$-mesons are compared in the region of Rutherford scattering contamination, the effects of the interference of the Coulomb and nuclear potentials can be observed (Williams *et al.* (1956 a, b) at 78 Mev). In one case the potentials have the same sign and the differential cross section is increased; in the other a decrease is observed. This leads to the determination of the sign of the nuclear potential which is normally not possible.

In the nuclear emulsion there are eight elements and the diffraction scattering at each type of nucleus has to be considered. It is assumed that the emulsion is composed of N_{i} nuclei/cm³ of the ith element each with an interaction cross section σ_{i} which is not necessarily the geometrical cross section. The mean cross-section in such a medium (e.g. $\bar{\sigma} = \bar{\sigma}_a$ or $\bar{\sigma}_d$) is obtained by adding together the various cross sections according to their frequency of occurrence. Thus

$$\bar{\sigma} = \sum(N_{\mathrm{i}}\sigma_{\mathrm{i}})/\sum N_{\mathrm{i}}. \qquad . \quad . \quad . \quad . \quad . \quad . \quad . \quad . \quad (14)$$

The quantity determined experimentally for emulsion is the interaction length λ which is given by

$$\lambda = 1/\sum(N_{\mathrm{i}}\sigma_{\mathrm{i}}). \qquad . \quad . \quad . \quad . \quad . \quad . \quad . \quad . \quad (15)$$

§ 3. Interaction Lengths and Elastic Scattering of 88 Mev π^--mesons in G5 Emulsion

3.1. *Experimental*

The emulsion block consisted of 20 strips each 20 cm × 10 cm × 0·04 cm and it was exposed to the 96 Mev π^--meson beam of the Liverpool synchrotron. The flux of particles was about 10^4 mesons/cm² on the end face of the block. During exposure the plates were kept at constant humidity which had a relative value of 55% at 19°c. The temperature cycle method of processing was used with a development temperature of 24°c. The curvature distortion vector is about 50 μ and there is negligible bubbling.

The plates were scanned by four observers by track scanning under a magnification of 45 × 15 × 1·5 on four Cooke 4000 microscopes. Tracks were selected at exactly 1 cm from the emulsion edge and followed either to an interaction, out of the plates, or for a maximum length of 1 cm. The 1 cm length was chosen to keep the energy loss small, while allowing relatively quick scanning. The beam energies at the beginning and end of the 1 cm strip were calculated to be 93 and 86 Mev, giving an average value of 88 Mev.

An eyepiece hairline was aligned on each track to be followed and the track compared to this direction every few fields of view. Because of the considerable multiple scattering, re-alignment was made at intervals. Only tracks lying within ± 6° of the general beam direction were followed.

Interactions of type ($n_h=0$, $n_s=1$) were classed as 'elastic scatters' and all other interactions as 'stars'. The latter group included 'disappearances' ($n_h=0$, $n_s=0$). The emulsion region up to 150 μ around each disappearance was scrutinized for a secondary track or continuing primary. Star-sizes were estimated visually. Those of type ($n_h=1$, $n_s=1$) were measured carefully and out of 22 events three were identified as elastic collisions with a visible recoiling nucleus. The three were identified on dynamical grounds as (π^--p) collisions and were classed as elastic scatters. It should be noted that with this classification, inelastic interactions of type ($n_h=0$, $n_s=1$) will be included as 'elastic scatters'. If the number of these events is comparable to the number of stars of type ($n_h=1$, $n_s=1$) the total number of stars will be underestimated by about 5%.

Elastic scatters were measured only if the projected angle was greater than 8° and estimated with an accuracy of 1°. The limit in this case was chosen to eliminate that part of the angular distribution which would be formed chiefly by the Rutherford Scattering and it corresponds to a scattering parameter just equal to the average nuclear radius for G5 emulsion.

3.2. *Beam Contamination*

At the time of exposure the beam consisted of 82% π^--mesons, 14% electrons and 4% μ-mesons (Cassels 1957, private communication). It is assumed that the track length followed is contaminated in these proportions. Spurious events which would simulate those produced by π-mesons are estimated to be small in number; the more important cases are given below.

The contribution of the elastic scattering of electrons to the spatial angular distribution at $\theta \geqslant 8°$ has been calculated from the Mott formula for a point nucleus for electrons of momentum equal to 180 MeV/c. Electrons are known to interact with nuclei with a cross section $\sim 10^{-29}\,\text{cm}^2$ and should thus lead to negligible contamination. However at the same momentum, Barkas *et al.* (1952) have observed the disappearance of two electron tracks in a track length of 103 cm. Such events simulate the π^--meson disappearances but, since the statistical weight is low, no correction has been made for this type of event. Instead it should be noted that this could lead to an overestimation of the inelastic cross section by about 5%.

3.3. *The Interaction Lengths*

In a total track length of 92·51 m, 235 elastic scatters with horizontally projected angles larger than or equal to 8° and 371 stars, which include 92 disappearances, have been found. Allowing for the beam contamination of 18%, the interaction length for the formation of inelastic events in G5 emulsion is $(20{\cdot}4 \pm 1{\cdot}1)$ cm and the interaction length for elastic scattering through a projected angle $\phi \geqslant 8°$ is $(32{\cdot}3 \pm 2{\cdot}1)$ cm.

3.4. *Comparison with the Optical Model*

The interaction length, λ_a, for inelastic events ('absorption' events) has been computed from eqns. (10), (13) and (15) as a function of the absorption coefficient K. The nuclear radius has been taken to be $r_0 A^{1/3}$ where r_0 is $1{\cdot}35 \times 10^{-13}$ cm. From eqns. (7) and (8) the value of K at a particular energy is expected to be approximately the same for all emulsion nuclei with the exception of hydrogen. Because of the small size of the hydrogen nuclei, their contribution to the interaction length is small and therefore K has been assumed constant. The variation of λ_a with K is shown in curve A of fig. 1. In curve C a similar relationship is shown where the finite size of the meson has been taken into account. The increase in cross section due to Coulomb attraction alone has been estimated and is shown in curve B for purposes of comparison. This correction, however, cannot be applied to curve C since it is valid only if the meson wavelength is small relative to nuclear size. Using curve C of fig. 1 the experimental value of the inelastic interaction length yields a mean value of the absorption coefficient $K = (4{\cdot}0^{+2\cdot5}_{-0\cdot75})\,10^{12}\,\text{cm}^{-1}$. With this value of the absorption coefficient, the horizontally projected angular distribution for scattering has been computed for assumed values of the change in wave number $k_1 = (0,\ \pm 1 \text{ and } \pm 2)\,10^{12}\,\text{cm}^{-1}$, which correspond to various values of the real nuclear potential.

It has been shown above that there will be Rutherford scattering at angles $\sim 8°$ and a preliminary comparison of the experimental angular distribution with the theoretical ones indicates that Rutherford scattering leads to an increase in the differential cross section. An approximate correction has therefore been made by adding the estimated angular distribution for Rutherford scattering for projected angles $\geqslant 8°$. This addition implies a nuclear potential of the same sign as the Coulomb potential.

The calculated distributions together with the experimental results are shown in fig. 2. A reasonable fit is obtained for $k_1 \sim (1-2)\, 10^{12}\,\mathrm{cm}^{-1}$. A more precise value of k_1 has been obtained by numerically integrating the functions in fig. 2 to determine the interaction length for elastic scattering through projected angles $\geqslant 8°$ as a function of k_1. The observed value of the mean free path corresponds to $k_1 = -(1{\cdot}86 \pm 0{\cdot}20)\, 10^{12}\,\mathrm{cm}^{-1}$.

Fig. 1

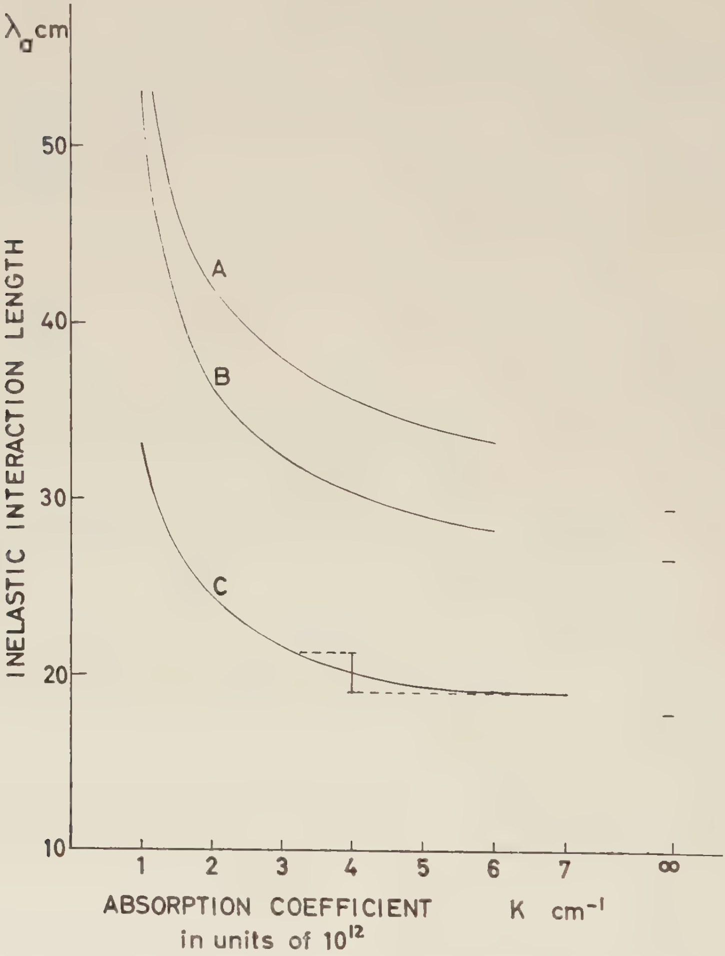

The variation of the inelastic interaction length with absorption coefficient. Curve A, computed from the optical model; curves B, C, computed from the optical model but with correction for Coulomb attraction and meson size respectively.

The error quoted on this value is due to the expected statistical uncertainty on the interaction length for scattering assuming the absorption coefficient is known exactly. The uncertainty in the determination of K leads to further error in the estimation of k_1. This value has been calculated approximately to be $\pm 0{\cdot}04\ 10^{12}\,\mathrm{cm}^{-1}$ and is negligible.

3.5. *Discussion and Conclusions*

The value of the absorption coefficient K can be compared with the predictions from eqns. (7) or (9). In the first case it is assumed that scattering of the meson is the process responsible for the inelastic interaction. Anderson *et al.* (1952) determined the cross section $\sigma_{\pi^- p}$ at 89 MeV to be (21 ± 8) mb. For $r_0 = 1{\cdot}35\ 10^{-13}$ cm, this leads to

$$K = (4{\cdot}3 \pm 1{\cdot}6)\ 10^{12}\ \mathrm{cm}^{-1}$$

for an average emulsion nucleus. In the second case the absorption of the meson by two or more nucleons is regarded as the only interaction process. Rogers and Lederman (1957) at 85 MeV observed a $\sigma_{\pi^+ D}$ cross section of $(7 \pm 1{\cdot}4)$ mb which with charge independence leads to

$$K \approx 3{\cdot}5 \times 10^{12}\ \mathrm{cm}^{-1}.$$

Fig. 2

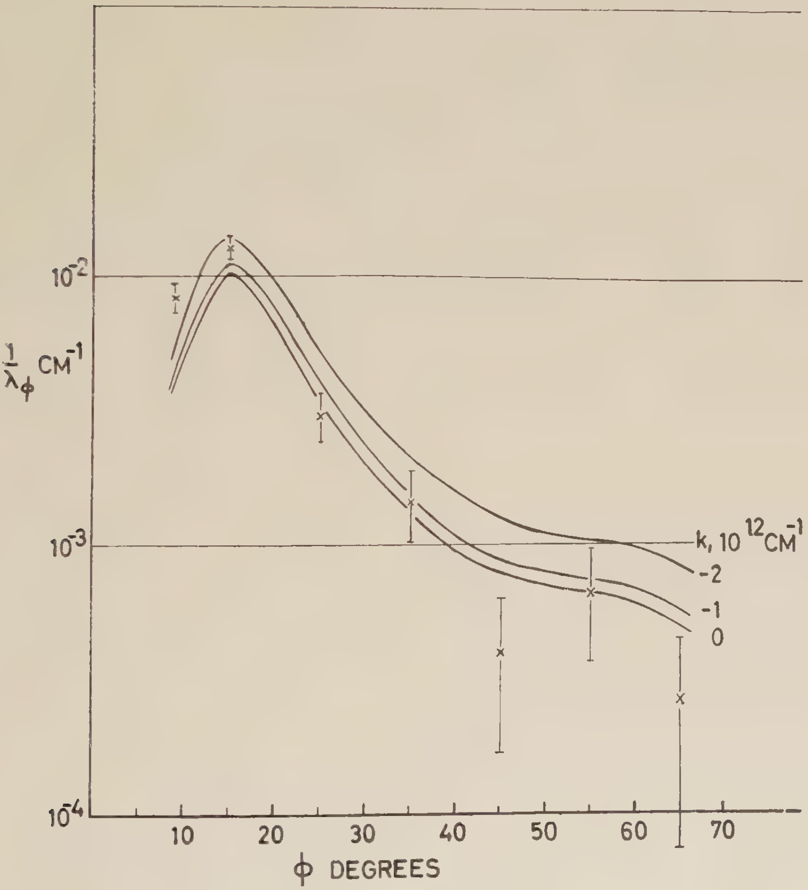

The observed distribution of horizontally projected angles of elastic scattering per 10° interval. The curves have been computed from the optical model for various assumed values of the real nuclear potential. The first experimental point is for the interval (8–10)° only.

Both estimates of K are consistent with the observed value. About 17% of the primary mesons emerged from the inelastic interactions. Thus it would appear that both mechanisms contribute to the process of inelastic interaction.

The attenuation mean free path of the meson wave in nuclear matter is $\lambda_n = 1/K$ and has been observed to be $(2{\cdot}5 \pm 0{\cdot}6)\ 10^{-13}$ cm; it corresponds to an imaginary component of nuclear potential $V_i = -(32^{+20}_{-6})$ Mev.

The observed value of k_1 may be compared with the values computed by Sternheimer (1956) over a range of meson energies. At 88 Mev the computed value of k_1 is $2{\cdot}4\ 10^{12}\ \mathrm{cm}^{-1}$ which is in reasonable agreement. The corresponding value of the real potential V_r is $-(28 \pm 3)$ Mev. The values of potential observed in other experiments near 88 Mev are shown in the table.

Meson energy (Mev)	Particle	Target element	V_r (Mev)	V_i (Mev)	Reference
48	$\pi^\pm$	C	$-(15 \pm 15)$	$-(22 \pm 7)$†	Shapiro (1951)
62	π^-	G5	—	~ -19	Ferretti *et al.* (1956)
80	π^+		—	~ -24	
120	$\pi^\pm$		—	~ -24	
70	$\pi^\pm$	C	~ -18	~ -9	Byfield *et al.* (1952)
78	$\pi^\pm$	Cu	$\sim -(35-45)$	~ -20	Williams *et al.* (1956 a, b)
80	π^+	Al	~ -20	$\sim -(10-25)$	Pevsner *et al.* (1955)
	π^-		$\sim -(30-40)$	Any value	
88	π^-	G5	$-(28 \pm 3)$	$-(32^{+20}_{-6})$	Present work

† Calculated from data in the paper.

The present analysis differs in two respects from others. Firstly obliquity has been taken into account in determining the angular distribution. Its effects are most important at large angles but these regions of the angular distribution have low statistical weight in the determination of k_1 by numerical integration. Secondly the real nuclear potential has been determined from the relativistic expression for k' (eqn. (2)). The values of the real potential expected from the calculations of Frank *et al.* (1956) at kinetic energies 60, 80 and 100 Mev are 20, 29, and 35 Mev respectively.

The analysis has been based on a square well potential of radius $r_0 A^{1/3}$ where r_0 has been assumed to be $1{\cdot}35\ 10^{-13}$ cm for consistency with other work from these laboratories. The weighted mean value from recent determinations is $r_0 = (1{\cdot}29 \pm 0{\cdot}01)\ 10^{-13}$ cm which would lead to even broader distributions than those computed; better agreement would be obtained for $r_0 > 1{\cdot}35 \times 10^{-13}$ cm.

ACKNOWLEDGMENTS

We wish to thank Professor G. D. Rochester, F.R.S. for his continued interest and advice. We are indebted to Professor J. M. Cassels and his staff for great help in carrying out an exposure to the meson beam of the Liverpool synchrotron. The work was carried out on Cooke M 4000 microscopes, two of which were kindly provided by a grant from the D.S.I.R. One of us (J.E.A.) is indebted to the D.S.I.R. for a studentship; (A.J.A.) to the I.C.I. for a Fellowship; (Y.L.J.) to the Atomic Energy Commission of the Republic of Korea, and (E.P.F.) to the Comision Nacional de Energia Atomica, Argentina for fellowship awards.

REFERENCES

ANDERSON, H. L., FERMI, E., LONG, A. E., MARTIN, R., and NAGLE, D. E., 1952, *Phys. Rev.*, **85,** 934.

BARKAS, W. H., DEUTSCH, R. W., GILBERT, F. C. and VIOLET, C. E., 1952, *Phys. Rev.*, **86,** 59.

BETHE and HOFFMANN, 1956, *Mesons and Fields*, Vol. II (New York: Row, Peterson and Co.).

BRUECKNER, K. A., SERBER, R., and WATSON, K. M., 1951, *Phys. Rev.*, **84,** 258.

BYFIELD, H., KESSLER, J., and LEDERMAN, L. M., 1952, *Phys. Rev.*, **86,** 17.

CRONIN, J. W., COOL, R., and ABASHIAN, A., 1957, *Phys. Rev.*, **107,** 1121.

FERNBACH, S., SERBER, R., and TAYLOR, T. B., 1949, *Phys. Rev.*, **75,** 1352.

FERRETTI, L., GESSAROLI, R., PUPPI, G., QUARENI, G., RANZI, A., STANTIC, S., and TOMASINI, A., 1956, *C.E.R.N. Symposium*, Vol. II, 308.

FESHBACH, H., and WEISSKOPF, V. F., 1949, *Phys. Rev.*, **76,** 1550.

FRANK, R. M., GAMMEL, J. L., and WATSON, K. M., 1956, *Phys. Rev.*, **101,** 891.

PEVSNER, A., RAINWATER, J., WILLIAMS, R. E., and LINDENBAUM, S. J., 1955, *Phys. Rev.*, **100,** 1419.

ROGERS, K. C., and LEDERMAN, L. M., 1957, *Phys. Rev.*, **105,** 247.

SHAPIRO, A. M., 1951, *Phys. Rev.*, **84,** 1063.

STERNHEIMER, R. M., 1956, *Phys. Rev.*, **101,** 384.

WILLIAMS, R. E., BAKER, W. F., and RAINWATER, J., 1956 a, *Phys. Rev.*, **104,** 1695.

WILLIAMS, R. E., RAINWATER, J., and PEVSNER, A., 1956 b, *Phys. Rev.*, **101,** 412.

Growth of Electron Space-charge and Radio Waves in Moving Ion Streams†

By R. Q. Twiss‡
Oxford and Cambridge University Club, London, S.W.1

[Received January 1, 1959]

Abstract

A criticism is given of a recent paper by Piddington with the same title. It is shown that his belief that the growing waves in a two-stream electron wave tube are really evanescent is untenable and that his own theory is effectively equivalent to the conventional one in which these growing waves are identified as being true amplified waves.

Piddington's conclusion that an initial disturbance in a two-stream medium will grow exponentially with time without oscillation is shown to be a consequence of highly idealized assumptions as to the nature of the medium and as to the initial and boundary conditions. In any practical case it is argued that double stream flow will build up oscillations at frequencies, in general around the plasma frequency, rather than produce charge separated blobs as in Piddington's theory. If temperature effects are allowed for it is shown that double stream flow does not occur in the corona in the case discussed by Piddington and reasons are also given for rejecting a theory of growing waves in shock fronts advanced by Sen.

Piddington's reasons for rejecting the existence at transverse space charge waves in a drifting ionized medium and for denying that growing evanescent waves can be excited by reflection are shown to be invalid. This removes Piddington's objection to an earlier theory of excess solar radio wave put forward by the writer, but it is agreed that this theory must now be rejected on other grounds.

§ 1. Introduction

Some years ago Piddington (1956 a, b) wrote a number of papers in which he attacked the accepted view that amplified growing waves could be excited in laboratory devices such as the two-stream electron wave tube and the travelling wave tube.

His criticism was primarily directed against the mathematical procedure adopted in the earlier papers on this subject, which did not go much further than proving that there were solutions for the longitudinal waves in a two stream electron wave tube of the general form

$$A \exp [\alpha(\omega)z + i(\omega t - k(\omega)z)]$$

where $\alpha > 0$ and $k(\omega)$ is real for a finite range of real values of ω.

As Piddington and others (Twiss 1951 b, Pierce and Walker 1956) have stressed, the existence of solutions of this type, does not by itself establish the existence of a true amplified 'growing' wave as opposed to an evanescent

---

† Communicated by the Author.
‡ On leave from Sydney University.

'growing' wave and this point is underlined, as Piddington has pointed out, by the fact that one of the solutions for the longitudinal space-charge waves in a thermal plasma is of the form

$$A \exp [\alpha(\omega)z + i\omega t]$$

for a finite range of real values of ω.

In this latter case it is clear from simple thermodynamic considerations that *amplified* 'growing' waves cannot exist so that these 'growing' waves must be evanescent and, indeed, they have some similarities to the 'growing' waves that can be excited by reflection in a waveguide below cut-off. However, it in no way follows, as Piddington seems to assume, that all 'growing' space-charge waves are evanescent just because some are, especially in view of the well-known experimental results with double stream amplifier tubes. Admittedly, Piddington attempted to explain the behaviour of the latter by a rather complex non-linear theory, but as Pierce and Walker (1956) pointed out, the predictions of this theory were incompatible with the experimental data. Furthermore, later analyses of the two stream amplifier have been published (Twiss 1951 a, 1952 a) in which the boundary and initial conditions were taken specifically into account which can immediately be applied to prove, firstly that real *amplified* 'growing' waves *can* arise in a two-beam tube and, secondly, that a complex propagation constant for a space-charge wave *is* proof of the possibility of amplification, as long as all the charge is moving in the same direction with respect to the point at which the input signal is applied. It is only when charge is moving in both directions, as in the thermal plasma, that special care in interpretation is required.

It was possibly for these reasons that Piddington's earlier criticisms do not seem to have excited much attention. However, he has recently (Piddington 1958) returned to the charge with a fresh paper which will be referred to hereafter as P.1. In the first four sections of this new paper Piddington reiterates his belief that the 'growing' waves in a two-stream electron wave tube are 'probably evanescent', but in § 6 he completely reverses himself and states explicitly that amplified spatially 'growing' waves *do* exist when a two-stream medium is excited by a sinusoidally varying input signal. Furthermore, the rate of amplification that he predicts is exactly that predicted by the standard procedure. Clearly there is some very serious confusion somewhere, and to help clear this up we shall give a fresh discussion of the two-stream amplifier in the light of the arguments developed in P.1.

§ 2. THE REALITY OF GROWING AMPLIFIED SPACE-CHARGE WAVES

Following Piddington, let us consider an ionized plasma consisting of two separate but interpenetrating streams in which the average electron charge is neutralized by streams of infinitely heavy ions. Then the dispersion equation for the longitudinal space-charge waves may be written

$$1 - \frac{{\omega_{01}}^2}{(\omega - u_1 k)^2} - \frac{{\omega_{02}}^2}{(\omega - u_2 k)^2} = 0. \quad . \quad . \quad . \quad . \quad . \quad . \quad (1)$$

where u_1, u_2 are the average velocities and ω_{01}, ω_{02} are the angular plasma frequencies of the two streams.

Piddington assumed that

$$\omega_{01}=\omega_{02} \qquad (2)$$

but we shall not make this restriction which, as we shall see, has led Piddington into serious errors of interpretation. Now for real values of k below a certain critical value of two the roots of eqn. (1) viewed as an equation for ω are complex. This implies, as Piddington *now* accepts, that the infinite double-stream medium is unstable to any initial spatial distributions of disturbance with wave numbers below the critical value, a fact first established by Bohm and Gross (1949 a, b). However, in the two-stream amplifier the interaction space is finite in extent, and the signal, at frequency ω, which is to be amplified, is applied, as velocity modulation, at the end of the tube at which the two streams both enter the interaction space. Under these conditions the amplifier is stable in the sense that the maximum disturbance, which occurs at the output end of the tube, is linearly proportional to the amplitude of the initial signal; at least as long as this latter in not so large that saturation effects can appear. For this case one will obviously not obtain the steady-state solution to the disturbance in the interaction space by solving for ω in terms of given k; on the contrary, since the frequency ω of the applied signal is known, one must solve the dispersion eqn. (1) for k for this value of ω. Only values of the propagation constants which satisfy this equation can apply to waves in the interaction space, and of these there are only four in the purely longitudinal mode for which the dispersion eqn. (1) is of the fourth degree. The steady-state amplitudes of these waves are determined by the initial density and velocity modulations on the two streams so that, as one would expect, the initial conditions give just four equations for the four unknown amplitudes. Of the four possible waves, two have complex propagation constants, for sufficiently small values of ω, and one of these two waves is the 'growing' wave which Piddington claims to be 'probably evanescent'. However, it is easy to show that this claim is wrong in the case, appropriate to the laboratory two-stream amplifier, in which the two streams enter the interaction space from the same end and have velocities of the same sign relative to the frame of reference in which the modulating signal is applied, since the associated longitudinal waves in this case are all forward waves in the sense that any modulation applied at the plane $z=d$ is convected away by the moving streams into the region $z>d$ and produces no disturbance in the region $z<d$ (Twiss 1951 a). None of the waves therefore and, in particular this includes the 'growing' wave, can be excited by reflection at the far end of the interaction space nor, as was shown in the paper just quoted, can the amplitudes of those waves depend on the boundary conditions at the far end of the tube. In no sense therefore can the 'growing' wave be termed 'evanescent' since the amplitude at the modulation plane is determined solely by the initial density and velocity modulations, and this amplitude will increase exponentially with distance

as one moves into the interaction space. Admittedly, it is conceivable that the 'growing' wave might always be excited with zero amplitude in nature if a certain linear relationship between the density and velocity modulation at the modulation plane were always satisfied identically. That this very implausible possibility is not in fact the case can be seen by considering the Gedank experiment in which two neutral uniform streams of gas are ionized at the modulation plane $z=d$ and enter the interaction space with zero density modulation but with arbitrary and independent velocity modulations; under these conditions it can be shown that the 'growing' wave is always excited with finite non-zero amplitude and, therefore, is indeed a true amplified wave. This argument cannot be applied as it stands to the case where some of the moving charge enters the interaction space from the far end so that the charge velocity with respect to the modulation plane is not all of the same sign, as in this case some of the waves will be 'backward' waves, the 'growing' waves may prove to be evanescent and a more detailed examination is needed to decide whether or not this is so.

In the two-stream amplifier the reality of space-charge wave amplification has been established without any explicit resource to a Laplace transform analysis except in so far as this is needed to prove that a stable steady-state solution exists. The fact that this has been shown to be the case (Twiss 1951 a) provides the justification for the argument, to which Piddington objects, that the 'instability' in the infinite two-stream medium excited by an arbitrary initial spatial disturbance, is physically an identical phenomenon to the amplification in the stable two-stream amplifier, the only difference between the two being the different initial conditions.

§ 3. The Major Inconsistency in Piddington's New Theory

In the previous section we have been concerned to disprove Piddington's claim that the spatially 'growing' waves in a two-stream electron wave amplifier are evanescent. A more detailed discussion does not seem justified in view of the fact that in § 6 of P.1 Piddington in effect, completely abandons the position which he had stoutly maintained, not only throughout his two earlier papers but also in the first four sections of P.1. Thus, in 'explaining' the two-stream amplifier, he argues that a sinusoidally varying input signal creates a series of identical equally spaced ion clouds in this medium moving with velocity U (where $U=(u_1+u_2)/2$ in the notation of the present paper) past the emitter. These drift along, each growing in time at the rate given by $\exp +\omega_i t$. In a time interval t a cloud moves a distance Ut and so shows an apparent *spatial* growth $\exp(\omega_i z/U)$. Piddington then goes on to apply a Galilean transformation with a velocity change $-U$ to the solution, in the case $u_1=-u_2$, for the infinite stream excited by an initial spatial distribution of disturbance and deduces that the solution in the two stream amplifier is of the form

$$A\exp\left[\frac{\omega_i x}{U}-ik_r(z-Ut)\right]. \quad \quad (3)$$

Of course, in general it is not possible to deduce the solution appropriate to one set of initial conditions (a sinusoidal time varying signal of frequency ω applied at a fixed point in space) by applying a Galilean or Lorentz transformation to the solution appropriate to a quite different set (an initial spatial sinusoidal distribution of disturbance). However, for the present, we are only concerned to point out that the expression given in (2), whether derived by a valid procedure or not, is exactly the same as that which would be obtained by the standard substitution procedure, which Piddington accused of interpreting 'evanescent' as amplified waves, if one puts $\omega = uk_r$ and $k = k_r - i\omega/U$ in eqn. (1) and solves for ω_i/U. Whether one says that the waves are really amplified or whether one says that they are really an instability which gives 'an apparent spatial growth' is simply a matter of taste, since physically the two descriptions are identical.

§ 4. AMPLIFIED SPACE-CHARGE WAVES IN NATURE AND THE LABORATORY

Piddington's reliance on the over-simplified model of two monochromatic streams of equal density and equal and opposite velocities has led him into a number of errors in his discussion of the phenomena which might arise when one or more fast streams of particles interact with a thermal plasma.

In the idealized case considered in P. 1 an initial sinusoidal disturbance of long enough wavelength builds up exponentially in time with no oscillation in the sense that the value of ω corresponding to this temporarily growing disturbance is purely imaginary. However, this picture of 'growing ion clouds' with exponentially increasing density is a most misleading one when applied to the actual conditions to be expected either in nature or in the laboratory. In the first place, the purely imaginary roots of ω only arise in the special case $\omega_{01} = \omega_{02} = \omega_0$ and $u_1 = -u_2$. If $\omega_1 \neq \omega_2$ then an arbitrary initial distribution of disturbance which is unstable will build up not exponentially, but in an oscillating manner whatever frame of reference the observer may be in. In the second place, there is no reason to assume that the appropriate initial conditions are those of an arbitrary spatial distribution of disturbance. Thus in the well-known experiments of Merrill and Webb (1939), in which a fast electron beam was injected into a thermal plasma from a hot cathode, it was found that oscillations were built up at about the plasma frequency in a narrow sheath a few millimetres from the cathode. This phenomenom can be explained by a model in which amplified space-charge waves and feed back effects both play a part (Twiss 1949), the appropriate initial condition being the modulation on the fast beam at the plasma boundary, but this bears no resemblance to Piddington's 'growing ion cloud' which would simply imply a phenomenom of exponentially increasing charge separation.

In the laboratory wave amplifier of course one always observes an oscillatory phenomenon and if amplified growing waves should arise in nature, say in the solar corona, one would expect them to occur predominantly at or near the plasma frequency of the background plasma.

However, it is still debatable whether suitable conditions for such growing waves ever do arise in the solar corona. Piddington suggests that they could be excited by clouds of ionized gas which have been seen to move in the corona with velocities up to 10^3 km/sec or even more. However, he has failed to allow fully for the effects of the corona temperature of 10^6 °K in which the r.m.s. electron thermal velocity is of the order of 6×10^4 km/sec so that there is no true double stream motion and, in such a case as shown by Bohm and Gross (1949), amplified growing waves will not be excited.

Sen (1954) has argued that growing amplified waves can arise in a magneto hydrodynamic shock front, but his proof of this relied simply on the fact that the propagation constants of the longitudinal waves could be complex for certain real values of ω. Unfortunately, this fact is not sufficient to establish the presence of amplification in his case in which particles were moving in both directions in the frame of reference in which the initial modulation was assumed to be applied. Indeed for amplified growing waves to arise in the ionized medium, it was shown by Bohm and Gross (1949) that the velocity distribution curve must be double humped. This is a necessary not sufficient condition and, in fact, the two peaks must be quite large and well defined. In the case considered by Sen, there is only one peak for the lower Mach number shocks, though he argued that amplification can take place even here, and although a second peak does develop at the higher Mach numbers, a detailed analysis shows that it is not well enough pronounced to lead to amplification.

§ 5. TRANSVERSE SPACE-CHARGE WAVES IN A DRIFTING MEDIUM

To complete this paper we shall criticize the discussion given in P. 1 of transverse waves in a drifting medium. If we consider the idealized case of an ionized gas at zero temperature drifting along a magnetic field, the dispersion equation for the purely transverse waves splits into two separate modes with opposite circular polarizations which may be written

$$k^2 - \frac{\omega^2}{c^2} - \frac{{\omega_0}^2\omega}{\omega - \omega_h - uk} = 0 \quad . \quad . \quad . \quad . \quad . \quad . \quad . \quad (4)$$

$$k^2 - \frac{\omega^2}{c^2} - \frac{{\omega_0}^2\omega}{\omega + \omega_h - uk} = 0 \quad . \quad . \quad . \quad . \quad . \quad . \quad (5)$$

where u is the drift velocity and where ω_h is the angular gyro frequency.

If we consider the dispersion equation for a particular mode as an equation for ω for given k, there are always three waves even when $u = 0$, the roots for ω being all real as long as k is real. For very large k the values for ω are such that:

$$\omega/k = +c, \ -c \text{ and } +u.$$

This solution is that appropriate to the steady-state solution in which the medium is excited by an initial spatial distribution of disturbance with three initial arbitrary conditions determined by the polarized transverse electric and magnetic field distributions and by the initial velocity distribution†. Viewed as an equation for k for real ω eqns. (3) are also of the third degree (except in the case $u=0$) as is to be expected, since there are still three arbitrary initial conditions when the external sinusoidal modulation is applied at a fixed point in space. Now when $u=0$ there are only two waves excited, which is again to be expected since there in no convection of the initial modulation away from the emitter, and therefore, no space-charge wave. However, this does not mean that this wave is spurious, as Piddington suggests, any more than are the longitudinal space charge waves in the drifting gas which obey the dispersion equation:

$$1-\frac{{\omega_0}^2}{(\omega-uk)^2}=0 \quad . \quad . \quad . \quad . \quad . \quad . \quad . \quad . \quad . \quad (6)$$

and which also have no solution of k for real ω when $u=0$. Furthermore, in the general case of N streams when the dispersion equation is of the form:

$$k^2-\frac{\omega^2}{c^2}-\sum_{s=1}^{N}\frac{{\omega_{0s}}^2\omega}{(\omega\pm\omega_{hs}-u_1k)}=0 \quad . \quad . \quad . \quad . \quad . \quad (7)$$

there are in general $N+2$ solutions for each mode and never less than $N+1$ even when the modulation is applied in a frame of reference at rest with respect to one of the beams so that in this case at least $N-1$ space charge waves are excited.

Piddington argued that the transverse space-charge waves were spurious on the grounds that the mere motion of an observer along an existing wave or waves cannot create another wave, and since there are only two waves in the frame of reference in which $u=0$, the third wave must be spurious. However, this argument completely misses the point; the wave is not created by moving the *observer* but by moving the *emitter* with respect to the medium, and this latter motion has a real physical significance which cannot be transformed away by any motion of the observer. Moreover, Piddington's argument that the third wave is really a field wave Doppler shifted by the observer's motion is quite unacceptable since at very high frequencies the medium can only have a negligible effect upon a field wave, the phase and group velocity of which must then be close to c. However, as $\omega\to\infty$ the propagation constant of the third wave $\to -\omega/u$ so that its phase and group velocity tend to u and it follows from this that it is indeed a space charge wave. Piddington's belief (1935) that only four waves can exist in a magneto ionic medium is therefore untenable. On the contrary, in a medium consisting of N streams it has been shown earlier (Twiss 1952 a) that a total of $4N+4$ waves can exist, a conclusion that agrees with that reached earlier by Bailey (1950) for the case $N=2$.

---

† The transverse waves have identically zero density modulation so that this does not provide a further initial condition.

§ 6. GROWING TRANSVERSE RADIO WAVES

A theory of excess sunspot radio noise given some years ago (Twiss 1952 b) relied upon the possibility of an exchange of energy between a transverse space-charge wave and the field waves at regions of discontinuity in the solar corona. Piddington's criticism that these transverse space-charge waves do not exist has been shown to be invalid, but despite this, the theory must now be rejected since it can be shown that such a transfer of energy can only take place when the drifting electrons are reflected or at least accelerated by an appreciable amount in a distance short compared with a space charge rather than with a field wavelength in the neighbourhood of the discontinuity, and this requirement is hopelessly improbable. It can also be shown for similar reasons, that the idealized boundary conditions needed to produce amplification in an evanescent region of the solar corona, as discussed elsewhere (Twiss 1951 b), are even harder to realize than was appreciated in this earlier discussion and this strengthens the conclusion reached there that this phenomenom can never occur in nature. However, this does not imply that the criticism given by Piddington in § 8 of P.1 is sound. The belief that the growing waves in Bailey's theory of sunspot noise (Bailey 1950) are really evanescent waves was put forward by the present writer (Twiss 1951 b) as well as by Piddington, but to maintain as does the latter that such 'growing' waves cannot be excited by reflection is quite another matter. The only argument put forward to support this view is the flat statement that 'standing' waves cannot be reflected. In this context Piddington appears to use the term standing wave to mean a wave with a purely imaginary propagation constant, and his assertion is clearly quite unfounded since it would imply *inter alia* that evanescent waves cannot be excited by reflection in a waveguide below cut off.

REFERENCES

BAILEY, V. A., 1950, *Phys. Rev.*, **78,** 428.

BOHM, D., and GROSS, E. P., 1949 a, *Phys. Rev.*, **75,** 1851; 1949 b, *Ibid.*, **75,** 1864.

MERRILL, H. J., and WEBB, H. W., 1939, *Phys. Rev.*, **55,** 1191.

PIDDINGTON, J. H., 1955, *Phil. Mag.*, **46,** 1037; 1956 a, *Aust. J. Phys.*, **9,** 31, 1956 b, *Phys. Rev.*, **101,** 9; 1958, *Phil. Mag.*, **3,** 1241.

PIERCE, J. R., and WALKER, L. R., 1956, *Phys. Rev.*, **104,** 306.

TWISS, R. Q., 1949, *Proceedings of Conference on Dynamics of Ionized Media* (Massey); 1951 a, *Proc. Phys. Soc. Lond.* B, **64,** 654; 1951 b, *Phys. Rev.* **84,** 448; 1952 b, *Nature, Lond.*, **169,** 185; 1952 a, *Phys. Rev.*, **88,** 1392.

SEN, H. K., 1954, *Aust. J. Phys.*, **7,** 30.

EDITORIAL NOTE

Growth of Electric Space-charge and Radio Waves in Moving Ion Streams

The paper on this subject by R. Q. Twiss which appears on a previous page, criticizes an earlier paper in this Journal by J. H. Piddington. The paper was therefore submitted to Piddington in the hope of securing some agreement between them on their conclusions. But the authors have not found it possible to accept each other's views. Acting on the advice of an independent referee, the paper by Twiss has been published.

Subsequent to its receipt, another paper was received from V. A. Bailey of the University of Sydney ; this was also critical of Piddington's views and in defence of his own. In particular Bailey claims that Piddington has based his arguments on a negation of Einstein's principle of special relativity and quotes statements from Piddington's earlier papers as refuting his present standpoint.

But owing to an accumulation of papers awaiting publication, the Editorial Board cannot allot space for a polemic in this subject. Readers who are interested are therefore invited to form their opinion from papers already published, the relevant references to which are those quoted by Twiss, together with the following :

Bailey, V. A., 1948, *Aust. J. sci. Res.* A, **1,** 351; 1957, *Phys. Rev.*, **106,** 1356.
Dungey, 1951, *Nature, Lond.*, **167,** 1029.
Piddington, J. H., 1955, *Nature, Lond.*, **176,** 875; 1956, *Phys. Rev.*, **101,** 14.
Sturrock, P. A., 1958, *Phys., Rev.*, **112,** 1488.

Editor

CORRESPONDENCE

On a Feature of Galactic Radio Emission

By Hugh M. Johnson
Mount Stromlo Observatory, Canberra

[Received February 10, 1959]

A conspicuous excess of galactic radio radiation appears to be concentrated like a minor Milky Way along most of the perimeter of a small circle about 70° from a pole near the galactic coordinates $l = 70°$, $b = +10°$. The only published explanations of this excess are those of Mrs. Tunmer (1958) and of the writer (1957). Mrs. Tunmer raises three major objections to her own idea and satisfactorily answers at least two of them. But the writer believes that she has not shown that the direction of the 'local spiral arm' (or rather its mean magnetic field) coincides with the polar axis of the excess. The $+10°$ latitude of the pole of the excess, and the 20° level of the excess above the great circle parallel to it, are not so serious as the discrepancy between the 70° longitude of the pole of the excess and the direction of the mean magnetic field in the galactic plane. Within a few hundred parsecs of the sun the direction of the mean magnetic field is most directly determined from the polarization of starlight interpreted on the theory of Davis and Greenstein (1951). Hiltner (1956) has thus shown that the mean magnetic field is directed toward $l = 12°$ (Aquila) in the northern hemisphere. The writer (1957) has further shown that the observable function varies rather smoothly along the *entire* galactic equator so that the field extends toward $l = 12° + 180° = 192°$ (Monoceros). There is now an unacceptable discrepancy of $70° - 12° = 58°$ between the observed direction of the mean magnetic field near the sun and the direction required of it by Mrs. Tunmer.

It is of interest that the polarization measures of Hiltner and others make the magnetic field and the OB-star 'arms' of Morgan *et al.* (1953) parallel, while these arms differ in direction from that of the line tangent to the 21 cm neutral hydrogen 'arm' which passes near the sun. The latter is a nearly circular arc centred on the nucleus of the Galaxy at $l = 328°$, so that its line of direction is about $l = 328° \pm 90°$ (toward Cygnus and Vela). At present the structural relations between hot stars, neutral hydrogen, and magnetic fields in the Galaxy are far from clear, and the *spiral* nature of the structure near the sun has not been proved.

References

Davis, L., and Greenstein, J. L., 1951, *Astrophys. J.*, **114**, 206.
Hiltner, W. A., 1956, *Astrophys. J. Suppl.*, **2**, 389.
Johnson, H. M., 1957, *Pub. astro. Soc. Pacif.*, **69**, 130.
Morgan, W. W., Whitford, A. E., and Code, A. D., 1953, *Astrophys. J.*, **118**, 318.
Tunmer, H., 1958, *Phil. Mag.*, **3**, 370.

Dislocation Structures Observed in High-purity Recrystallized Aluminium by X-ray Diffraction

By A. R. Lang
Division of Engineering and Applied Physics, Harvard University, Cambridge 38, Massachusetts, U.S.A.†
and G. Meyrick
H. H. Wills Physics Laboratory, University of Bristol

[Received February 23, 1959]

The x-ray diffraction method of observing dislocations within crystals (Lang 1958) allows examination of sections up to several millimetres in thickness in the case of light elements. Hence the dislocation density found this way should be typical of the material in bulk. We wish to report preliminary results of a survey of crystals of especially pure aluminium grown in this laboratory. X-ray examination indicates a quite low dislocation density, in the range of 10^4 to 10^5 lines per cm^3 within sub-grains. A variety of interesting dislocation configurations has been observed, and from the quality of dislocation contrast some general conclusions can be drawn about the perfection of the crystals.

The starting material, 99·999% pure Al, was zone-refined with twenty passes. Portions taken from the purest region of the ingot were cold-rolled into strips approximately 5 cm by 1 cm by 2 mm, After etching and washing, these were annealed overnight in air at 495°c. During the anneal they rested on a bed of alumina powder. The strips were then given a 2% extension in a Hounsfield tensometer, re-annealed overnight at 495°c and electropolished. The resulting grains averaged about 1 cm^2 in area.

Figure 1 (*a*) and (*b*) (Pl. 92) shows a stereo-pair of x-ray diffraction micrographs taken by the method of 'projection topographs' (Lang 1959) using AgKα radiation and the 111 and $\bar{1}\bar{1}\bar{1}$ reflections. These figures are photomicrographic prints from the original x-ray images, hence dislocations appear light on a dark background. The field covered is about 700 by 950 microns in area. The particular region shown has the shape of a blunted wedge, about 20 μ thick at the sub-grain limit in the upper right and increasing to about 100 μ in the lower left. The near surface of the wedge is the surface of the specimen, the far surface is a sub-grain boundary. Figure 2 provides a key to some of the features which are, of course, more clearly seen on the original x-ray images. The sub-grain boundary outcrops at the specimen surface along the line A: a fair amount of extra x-ray reflecting power is irregularly distributed on this boundary and can be seen as a sheet dipping into the crystal when the micrographs are viewed stereoscopically. Quite frequently observed are irregular helical dislocations B. Their pitch varies widely, 50 μ being about an average value.

---

† On leave at H. H. Wills Physics Laboratory, University of Bristol.

Isolated loops are seen at C, and D appears to be a distorted figure-of-eight loop. The three features E are believed to be smaller loops. (The present resolution of the x-ray method does not resolve loops as such when their diameter is 5 μ or less.) A single dislocation leaving and returning to the low-angle boundary is seen at F. Features of interest which are fairly frequently observed are indicated at G. As far as they can be resolved, they appear to be mainly lines of regularly spaced loops of diameter and spacing in the range 10 to 15 μ, but regular helices, figures-of-eight, and multiple figures-of-eight also can be seen. There is a close resemblance to the features observed in silver chloride crystals by Jones and Mitchell (1958) and Parasnis and Mitchell (1959).

Fig. 2

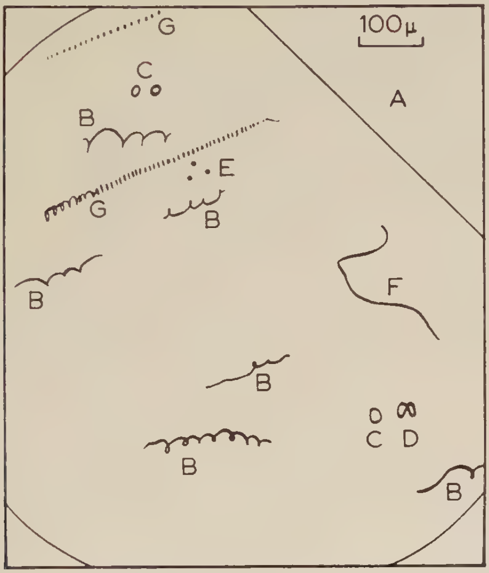

Key to dislocation features in x-ray topographs.

By comparison with silicon, germanium and good quality halide crystals, the dislocation contrast is very poor. Some type of lattice imperfection is present other than the dislocations seen in the figures. The x-ray evidence does not rule out the presence of large numbers of dislocation loops of 1 μ diameter or less, which could not be seen individually. However, we believe the principal imperfection to be small variations in lattice parameter caused by irregularly distributed impurities. In nearly perfect crystals local variations from the mean lattice parameter of the order of 1 part in 10^6 cause a recognizable increase in x-ray reflecting power. Very noticeable in the x-ray topographs of aluminium are diffuse sheets and lenticles of increased reflectivity. Some of these appear to be associated with concentrations of slip lines prior to recrystallization.

ACKNOWLEDGMENTS

One of the authors (A. R. Lang) wishes to thank the U.S. Office of Naval Research for support, while the other (G. Meyrick) is grateful to the D.S.I.R. for a maintenance grant. The experiments were carried out on diffraction instruments constructed under Contract Nonr–1866(39). The x-ray source was a Microfocus Unit made by Messrs. Hilger and Watts Ltd., whose help with the equipment we gratefully acknowledge. We also wish to thank Professor F. C. Frank, F.R.S., for his interest and helpful discussion during the course of the work.

REFERENCES

JONES, D. A., and MITCHELL, J. W., 1958, *Phil. Mag.*, **3,** 1.
LANG, A. R., 1958, *J. appl. Phys.*, **29,** 597 ; 1959, *Acta cryst.* (in the press).
PARASNIS, A. S., and MITCHELL, J. W., 1959, *Phil. Mag.*, **4,** 171.

The Strain Dependence of the Residual Resistivity of Potassium

By Z. S. BASINSKI, J. S. DUGDALE and D. GUGAN
Division of Pure Physics, National Research Council, Ottawa, Canada

[Received April 7, 1959]

DURING an investigation of the effect of the martensitic transformation on the electrical resistivity of lithium and sodium (Gugan and Dugdale 1958) we have strained wires of these metals at low temperatures in order to enhance the proportion of the low temperature phase. For comparison, similar experiments were made on potassium which is known *not* to change its crystal structure, even under strain, down to 4°K. Our results on the change of electrical resistivity of lithium and sodium agree well with those of Hull and Rosenberg (1959) but our results for potassium are quite different. We find, using two entirely different apparatuses, that the resistivity change in potassium at 4°K as a function of strain is about the same as that in sodium. Figure 1 shows the results of an experiment in which we achieved a strain of more than 15% before the wire broke. We believe that the reason why Hull and Rosenberg did not observe any resistivity change is that they were not able in their resistance-measuring experiments to achieve strains of more than 3–4%.

A spurious apparent increase in resistivity could arise if the wire were not uniformly deformed. Examination of the wire during the experiment showed no non-uniformity and, after breaking, the only region of non-uniformity was in the region where the wire broke. The wire we used was initially about 5 cm long and 0·1 cm in diameter. The chucks at each end enclose the wire for about 0·5 cm and since this part of the wire is covered with oil which cannot easily be removed, there is an uncertainty as to how much of this part of the wire is strained. We have assumed that all the straining takes place in the free central portion of the wire; this gives the minimum change of resistivity with strain consistent with the experimental data.

Figure 2 shows the stress–strain curve measured at the same time on the same specimen. If we interpret this by analogy with the behaviour of other body-centred cubic metals and in the light of the resistivity–strain curve shown below, we reach rather different conclusions from those of Hull and Rosenberg. They regarded the initial steep rise in the stress–strain curve at 4·2°K as due to some mechanism of rapid hardening. We believe, on the other hand, that it should be regarded rather as a slight departure from truly elastic behaviour which results from minor rearrangements of dislocations and not from their profuse multiplication. Such a profuse multiplication would be expected to produce a marked increase in resistivity within the first 1% of strain and this is not observed.

From the data of Hull and Rosenberg it can be seen that the flow stress in potassium increases rapidly with falling temperature. By analogy with the behaviour of iron (Basinski and Christian 1959) which is also body-centred cubic in structure, we think that this rapid change of flow stress with temperature is probably due to the large Peierls–Nabarro stress inherent in this lattice. At low temperatures, where thermal fluctuations are small, large-scale plastic flow can take place only after the applied stress has reached values higher than this Peierls–Nabarro stress. The amount of true strain hardening in potassium observed at 4·2°K could then be regarded as being comparatively small, as in other b.c.c. metals. An estimate of the strain dependence of the resistivity using this hypothesis is indicated in fig. 1, and its shape is seen to accord well with that found experimentally. In making this estimate we have assumed that the Peierls–Nabarro stress has the value shown in fig. 2 and that the flow stress increases as the square root of the dislocation density (cf. Blewitt *et al.* 1955).

The similarity between the resistivity–strain curves of potassium and sodium at 4·2°K suggests that stacking faults, which are thought to be present only in the h.c.p. phase of sodium, are *not* the dominant source of electron scattering in sodium. This idea is supported by the observed shape of the resistivity–strain curve for sodium. In this metal, the strain-induced transformation from b.c.c. to the highly faulted h.c.p. phase takes place most markedly at small strains† and so the number of stacking faults increases most rapidly in this region. The presence of stacking faults should be reflected in the resistivity if they scatter electrons strongly but a steep rise in resistivity at small strains is not in fact observed (Hull and Rosenberg 1959). Another piece of evidence comes from temperature-cycling experiments on sodium at low temperatures (Dugdale and Gugan 1959). In these, the proportion of the h.c.p. phase formed spontaneously on cooling to 4°K was diminished by

---

† Straining experiments on sodium at 20·4°K (Dugdale and Gugan 1959) show that the ideal resistivity diminishes most rapidly at low strains and this implies that the transformation is occurring most rapidly here.

Fig. 1

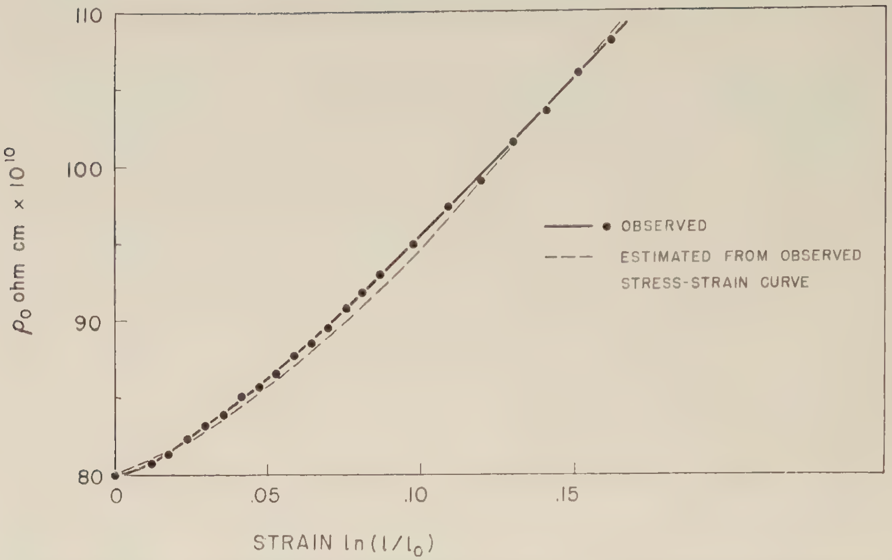

The resistivity of potassium versus strain at 4·2°K. The ratio of the resistivity of the sample at 4·2°K to that at 0°C was $1{\cdot}3\times10^{-3}$.

Fig. 2

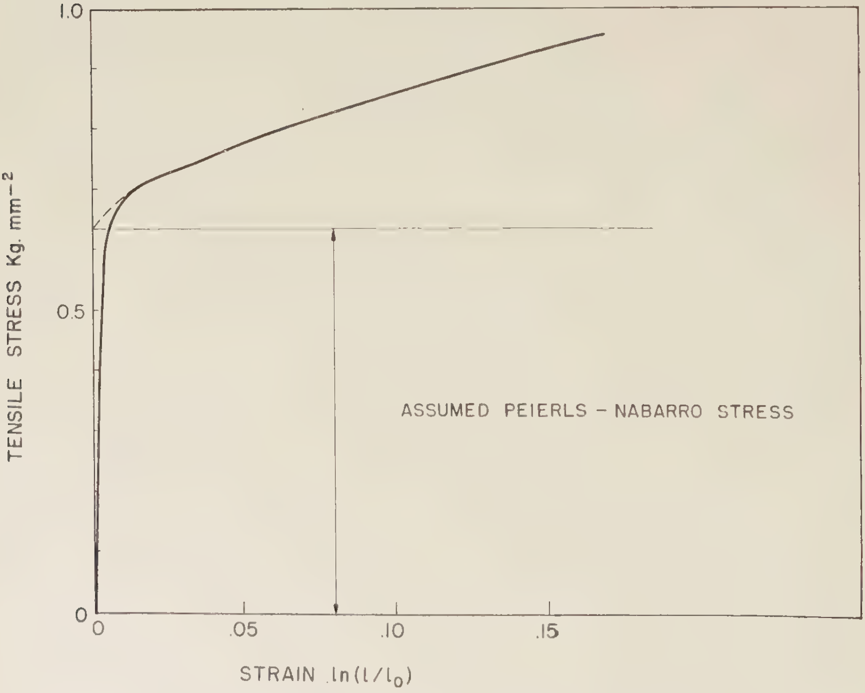

The stress–strain curve for potassium at 4·2°K.

suitable temperature cycling. The residual resistivity was, however, not diminished as might be expected if the scattering of electrons by stacking faults were the dominant process.

ACKNOWLEDGMENTS

We are grateful to Dr. Rosenberg for allowing us to see his results before publication. We are indebted to Dr. A. V. Gold for his help with the resistivity measurements using a sensitive galvanometer amplifier.

REFERENCES

BASINSKI, Z. S., and CHRISTIAN, J. W., 1959 (to be published).

BLEWITT, T. H., COLTMAN, R. R., and REDMAN, J. K., 1955 *Report of the Conference on Defects in Crystalline Solids* (London: The Physical Society), p. 369.

DUGDALE, J. S., and GUGAN, D., 1959 (to be published).

GUGAN, D., and DUGDALE, J. S., 1958, *Canad. J. Phys.*, **36**, 1348.

HULL, D., and ROSENBERG, H. M., 1959, *Phil. Mag.*, **4**, 315.

CORRIGENDUM

A Possible Determination of the Activation Energy for Self-Diffusion in Aluminium, by T. FEDERIGHI, 1959, *Phil. Mag.*, **4**, 502.

In the computation of τ_0 in the equation

$$\tau = \tau_0 \exp (Q/KT) \qquad (2)$$

by the values of τ reported in the table, I made a numerical error, giving $\tau_0 = 2{\cdot}6 \times 10^{-8}\,\mathrm{sec}^{-1}$. The right value is $\tau_0 = 2{\cdot}6 \times 10^{-12}\,\mathrm{sec}^{-1}$. I am indebted to Dr. J. Silcox and Dr. M. J. Whelan for pointing out this error.

REVIEWS OF BOOKS

Free Radicals: as studied by electron spin resonance. By D. J. E. Ingram. (London: Butterworths, 1958.) [Pp. 274.] 50*s.*

This book provides an introduction to electron spin resonance (electron paramagnetic resonance) as applied primarily to the study of free radicals of organic molecules. Some account is also given of inorganic radicals, but work on the uncoupled electrons in the inner *d* and *f* orbitals of transition element or rare earth compounds is specifically excluded; the field of semiconductors is only touched on.

An introductory section relates the electron spin resonance method to others that are used for studying free radicals. It is followed by three chapters which outline the basic physical theory and experimental techniques, and the theory of hyperfine interaction between the magnetic moment of the spinning electron and magnetic nuclei within the free radical. The last five chapters deal with actual spectra obtained from stable free radicals, radicals produced by irradiation, polymerization or pyrolysis, inorganic radicals, biradicals and the triplet state, and free radicals in biological and medical systems.

The book as a whole provides a very interesting survey of all aspects of the subject, and will be primarily of use to the chemist, physicist, or biologist who is interested in the possibilities of this new and rapidly expanding technique. It does not aim to give detailed accounts of either the experimental techniques or the theory of the spectra. Indeed to the reviewer some parts of these chapters did not seem to be very clearly written, possibly because the author was in some haste to produce an up-to-date book without delay. The half of the book that deals with experimental results is, on the other hand, distinguished by an excellent choice of spectra for discussion with the result that all the main points are brought out clearly and well.

The book fills an important gap in the literature, and can be highly recommended as a stimulating account of electron spin resonance. N. S.

The Neutrino. By J. S. Allen. (Princeton University Press; London: Oxford University Press, 1959.) [Pp. 168.] 36*s.*

If ever in physics there was an ugly duckling that grew into a swan it surely is the neutrino. An *ad hoc* hypothesis thirty years ago, it is now a fully established particle (complete with anti-particle) with a say in cosmology and supreme defiance of parity. While we are still shocked by Pauli's untimely death, it is good to think that he lived to see his brain child rise to such glory.

Of what we know about the neutrino, much has been found by studying the nuclear recoil in beta decay, and J. S. Allen has done much in this difficult line of work. But his book deals impartially, clearly, and readably with all our sources of information, including the shapes of beta spectra, double beta decay, the detection of free neutrinos, and meson decays. Experimental arrangements are fully described, with discussion of possible errors. Theoretical formulae are given without derivation. A list of references is found after each chapter; this is somewhat inconvenient in particular as there is no author index. The breakdown of parity came as the book was practically complete, but a great effort was made to report progress up to the last moment, including the two-component theory and the V-A-interaction. O. R. F.

Liquid Helium. By Professor K. R. ATKINS. (Cambridge: University Press, 1959.) [Pp. 312.] 60*s*.

THIS is the first sizeable book to be devoted solely to the liquids of helium, and it could hardly have appeared at a more useful or appropriate time. Appropriate because last year was the fiftieth anniversary of the first liquefaction of helium, the superfluid properties began to be noticed a quarter of a century ago, and ^{3}He was first liquefied about an eighth of a century ago. Useful because, although there have always been a small band of devotees of the liquid, during the last few years an intensive and widespread experimental and theoretical assault has been made on the phenomenological fortress of liquid helium, in which the author of the book has played no small part, and it would appear that the fortress has to a considerable degree capitulated.

In describing the present picture of the liquid, Professor Atkins has admirably followed what one likes to think is the best Cambridge tradition, in which the emphasis is always kept firmly fixed on clear and succint statements of the relevant physical ideas. This is naturally always important but it is particularly so here because these two liquids, which exist over such an apparently restricted temperature interval, cover between them probably a wider range of physical concepts than do any other two substances in nature, extending from the hydrodynamics of an ideal classical fluid (the only known example) through thermodynamics and what might be called quantum thermo-hydrodynamics, through the two varieties of quantum statistical mechanics and some of the finer details of nuclear structure, not omitting magnetism, and all of this fundamentally because they are composed of very nearly the simplest possible atoms.

For students of liquid helium and other low temperature phenomena the book will be essential, undergraduates will certainly gain benefit from it, but apart from all this the style is so clear and pleasant that many physicists and other scientists will find it almost in the category of ' bedside ' reading, in the best sense of course.

J. F. A.

Conduction of Heat in Solids. Second Edition. By H. S. CARSLAW and J. C. JAEGER. (Oxford: Clarendon Press, 1959). [Pp. viii+510.] 84*s*.

PROFESSOR JAEGER has made many additions in the second edition of this well-known book, first published thirteen years ago, but he has not changed the general plan or methods. He has aimed to make as complete as possible the account of known exact solutions of problems of heat flow. All of the most important boundary value problems are presented in adequate detail, with solutions by classical methods except that the Laplace transform with respect to the time variable is very frequently used as a first step. Subsidiary problems of great variety and scope are outlined, and the chief results quoted, in a uniform notation. The list of references exceeds 700 titles.

New in this edition are applications to geophysics and to industry, and discussions of heat flow in anisotropic or moving media. Professor Jaeger has added two short survey chapters on Integral Transforms and Numerical Methods.

In addition to its great value as an almost exhaustive reference book, this forms a first-rate introduction to classical methods of solution of boundary value problems. The physical concepts are elementary and the interpretation of the mathematics is straight-forward even where the formulae are complicated. Many of the 63 figures exhibit the meaning of such formulae graphically and enable the reader to get a clear grasp of the main characteristics of the heat flow. The clarity of exposition is such that the book could be read by an undergraduate working alone. Professor Jaeger is to be congratulated on the skill with which he has preserved this character of the text in bringing the book up to date.

E. R. L.

Classical Mechanics. By J. W. Leech. (London: Methuen & Co.) Monographs on Physical Subjects. [Pp. 149.] 12*s.* 6*d.*

The transition from classical mechanics to either quantum or relativistic mechanics is made most readily from the expression of classical mechanics in the analytical form which leads to the equations of Lagrange and Hamilton. Dr. Leech describes classical mechanics with this in mind, in a treatment intended for undergraduates in their final year and for first-year graduates. He begins with Newton's laws for the motion of a particle, and after a discussion of the equation of virtual work and d'Alembert's principle, Lagrange's equations are derived, for conservative and non-conservative unconstrained systems, and for systems with holonomic constraints, giving examples of their use. He gives the warning in the introduction that the analytical formulations of dynamics, in common with vector methods, do not usually simplify the working out of particular problems, their advantage being that they often make it considerably easier to put a physical problem into mathematical terms.

I think the author is a little too eager in his support of the analytical method when he suggests that the centrifugal and centripetal terms arising from the use of rotating frames of reference introduce conceptual complications in the vectorial approach not present in the analytical. The extra terms arise in the vectorial equations as a consequence of the relation between the time derivatives of a vector calculated in inertial and rotating frames, and of the fact that Newton's laws only apply in an inertial frame.

In Chapter V he introduces the Hamiltonian function and Hamilton's equations. By describing the motion of a sleeping top using a rotating frame he shows that the Hamiltonian may not be the total energy, and that both may be distinct constants of the motion. A word or two on the calculus of variations leads to the equivalence of the dynamical equations to Hamilton's principle, and to the principle of least action. This is followed by a concise exposition of canonical transformations, the Hamilton–Jacobi equation, and Poisson brackets, and from the infinitesimal contact transformation a brief indication is given of the analogy of dynamics with wave optics, and an indication is given of the transition to Heisenberg's representation of quantum mechanics. On page 93 the symbols ' W ' and ' X ' should be interchanged in the second member of the right-hand side of the equation on line 17, and in the third and fourth members on line 18. The result is correctly given. In Chapter IX the transition to a continuous system is illustrated by the limiting case of a chain of particles connected by elastic springs, and the energy and field momentum densities are discussed. In the next chapter, concerned with the special theory of relativity, the motion of a particle under no forces, and of a charged particle in the electromagnetic field are treated, first by the extension of Newton's laws, and then by the much more elegant covariant formulation. The last chapter is an introduction to field theory.

This is a straightforward and stimulating introduction to analytical dynamics, which may well bring some to the more extensive treatises on the subject (there is a short bibliography), as well as providing an excellent introduction to relativistic mechanics and preparation for quantum mechanics and field theory.

P. J. M.

Optical Properties of Semiconductors. By T. S. Moss. (London: Butterworths, 1959.) [Pp. 279.] 50*s.*

This is another of a valuable series of monographs on semiconductors. It falls into two parts; the first eight chapters deal with the general principles of optical effects, including absorption processes, photoelectric and magneto

optical effects, and the emission of radiation from semiconductors ; the remainder is a review of the observational results, element by element, and compound by compound. The treatment is very straightforward and clear, and eminently suitable for experimental research workers in this field. There is no attempt to derive the more fundamental formulae, but a number of macroscopic phenomena are deduced in a form convenient for practical application. The survey of the data will be extremely useful for reference, especially as it covers such a wide range outside the heavenly twins, silicon and germanium.
J. M. Z.

Introduction to the Physics of Many-Body Systems. By D. Ter Haar. (New York: Interscience Publishers Ltd., 1958.) [Pp. 127.] 30*s*.

Dr. Ter Haar makes an ambitious attempt in this book to introduce the reader to the most recent methods for studying many-body systems. He includes in the first part of the book methods used in atomic theory, nuclear theory and solids. The second part of the book is concerned with collective motion with particular reference to sound waves in gases and solids, plasma oscillations in metals, nuclear rotational motion, and liquid helium.

The book will probably be most useful as a limited guide to research workers who specialize in one of the fields covered and require an outline of other aspects of the many-body problem. Perhaps it should be emphasized that the book is primarily concerned with mathematical methods in different physical systems and not with the physics of these systems as its title might suggest. Unfortunately the methods are described uncritically, and some have developed so rapidly during the past two years that their presentation in the book is already out of date.
R. J. E.

Nonlinear Problems in Random Theory. By Norbert Wiener. (New York: Technology Press of M.I.T. and J. Wiley & Sons, 1959.) [Pp. x+132.] 36*s*.

This series of fifteen lectures on non-linear random processes is permeated with the author's wide outlook, and includes comment on frequency modulation, brain waves (literally), quantum theory, coding and statistical mechanics. The basic mechanical tool is an orthogonal development of non-linear functionals of Brownian motion, used at this stage as a purely theoretical framework. The value of this technique is well illustrated in lectures 10 and 11, where it is transformed into experimental apparatus for determining the characteristics of non-linear electrical networks. In spite of its dependence on abstract mathematical analysis, the book's informality of style should help to make it reasonably intelligible to many who are not professional mathematicians. A few minor criticisms† are not intended to deter readers from studying a stimulating book.
M. S. B.

---

† (i) It is not always made too clear (*a*) where the orthogonal functional expansions are indispensable, (*b*) where the Brownian motion moves over from a mathematical artifice to a physical assumption. Thus formula (5·24) for the first example of frequency modulation is not only to be anticipated, but is readily generalized to explicit functionals of 'additive' inputs for which the 'shot' density is not high enough for the process to be normal. Formula (7·22) for 'quadratic frequency-modulation', while not so generalizable, is clearly independent of the orthogonality technique (at least if interpreted in relation to actual Brownian motion).

(ii) The relation of Brownian motion to other random 'distributions' (in the sense of Schwartz), such as additive processes of 'point' processes, might have been raised. Point processes are avoided in the last lectures on statistical mechanics by a deliberate omission of a gas's 'granularity', but the discussion seems in consequence rather dubious and sketchy.

(iii) The existence of particular probabilities with a similar structure to probabilities in quantum theory is demonstrated, but no suggestion is made as to why these *particular* probabilities should be relevant.

Finite Difference Equations. By H. Levy and F. Lessman. (London: Pitman, 1959.) [Pp. viii + 278.] 37*s*. 6*d*.

As the authors remark, books on Finite Difference Equations are not common in English, the works of George Boole and L. M. Milne-Thomson are outstanding—most other work is confined to a chapter or two in larger works, but the treatment of linear equations in Fort's *Finite Differences* is worth mention.

A new book on the subject is thus of interest, and may be expected to contain a fair amount of new material. There is, in fact, in the present work some interesting new material that will repay study.

The first two chapters are elementary, dealing with Elementary Difference Operations and with Interpolation and Extrapolation. This suggests that it should be useful to students and novices in the subject. It is with regret, therefore, that one must warn the reader of an almost complete disregard of mathematical rigour which is so widespread that only an expert can read the book in safety. The lack of rigour applies not only to proofs, where it might be pardonable, but also to statements of theorems. This culminates in the disastrous Theorems 1 and 2 on pp. 86 and 87, both of which are thoroughly false; Theorem 1 is not even true, *as stated*, for linear equations, as the example $y_{n+2}=y_n$, $y_0=y_2=1$, readily shows. Example 4, p. 88 provides another counter example to Theorem 1, with uncountably many solutions.

Page 83 provides further mis-statements and false implications concerning primes and there are numerous other examples, of which the most widespread are (*a*) tacit assumptions of continuity, and (*b*) the assumption that n linear algebraic equations in n unknowns have a unique solution.

To sum up, the book is interesting, with interesting graphical and series approaches to solutions of difference equations, and a good deal more, but it has many errors, serious and trivial. It is safe only for the expert or sceptic to read.

J. C. P. M.

[*The Editors do not hold themselves responsible for the views expressed by their correspondents.*]

Fig. 1

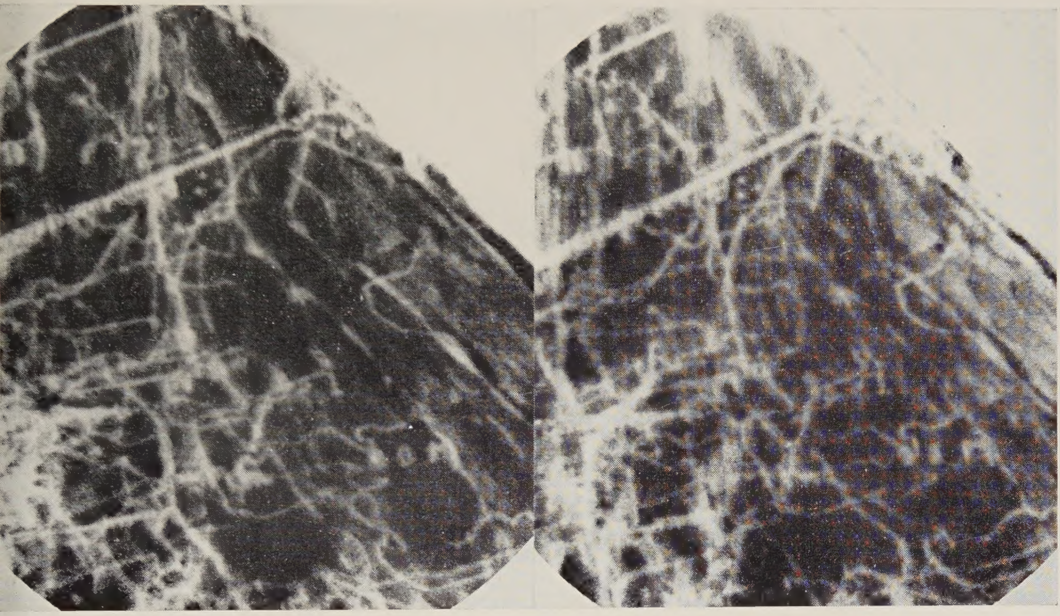

(*a*) (*b*)

Stereo-pair of x-ray projection topographs of aluminium.